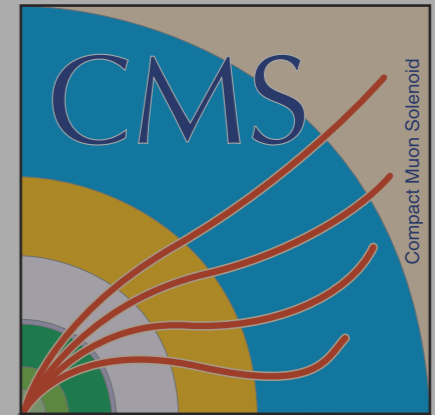


# Diffractive cross sections and hard diffraction at the LHC

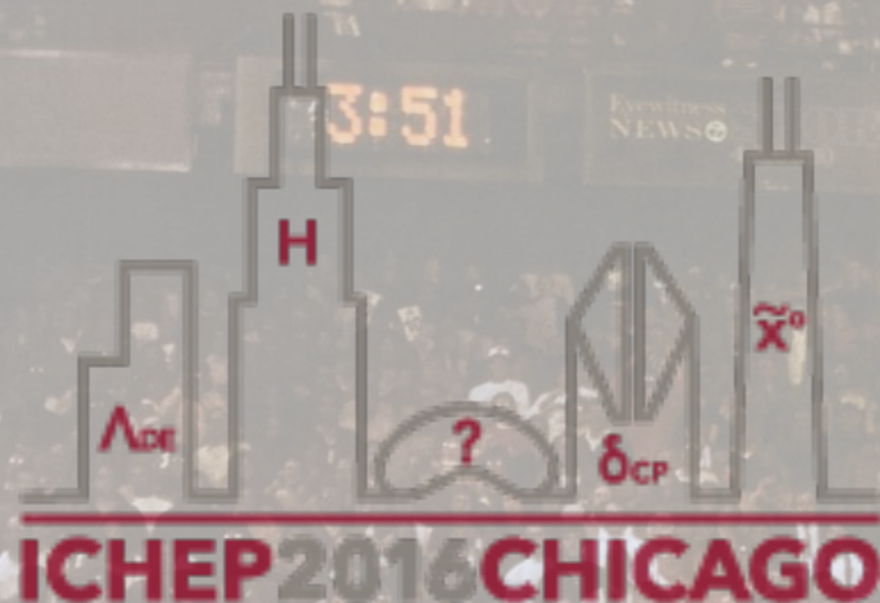


A. Vilela Pereira on behalf of the ATLAS, CMS  
and TOTEM Collaborations  
Universidade do Estado do Rio de Janeiro



**ATLAS**  
EXPERIMENT

<http://atlas.ch>



38th International Conference on High Energy Physics - Chicago  
August 3 - 10, 2016



gettyimages®  
NBA Photos

1436678

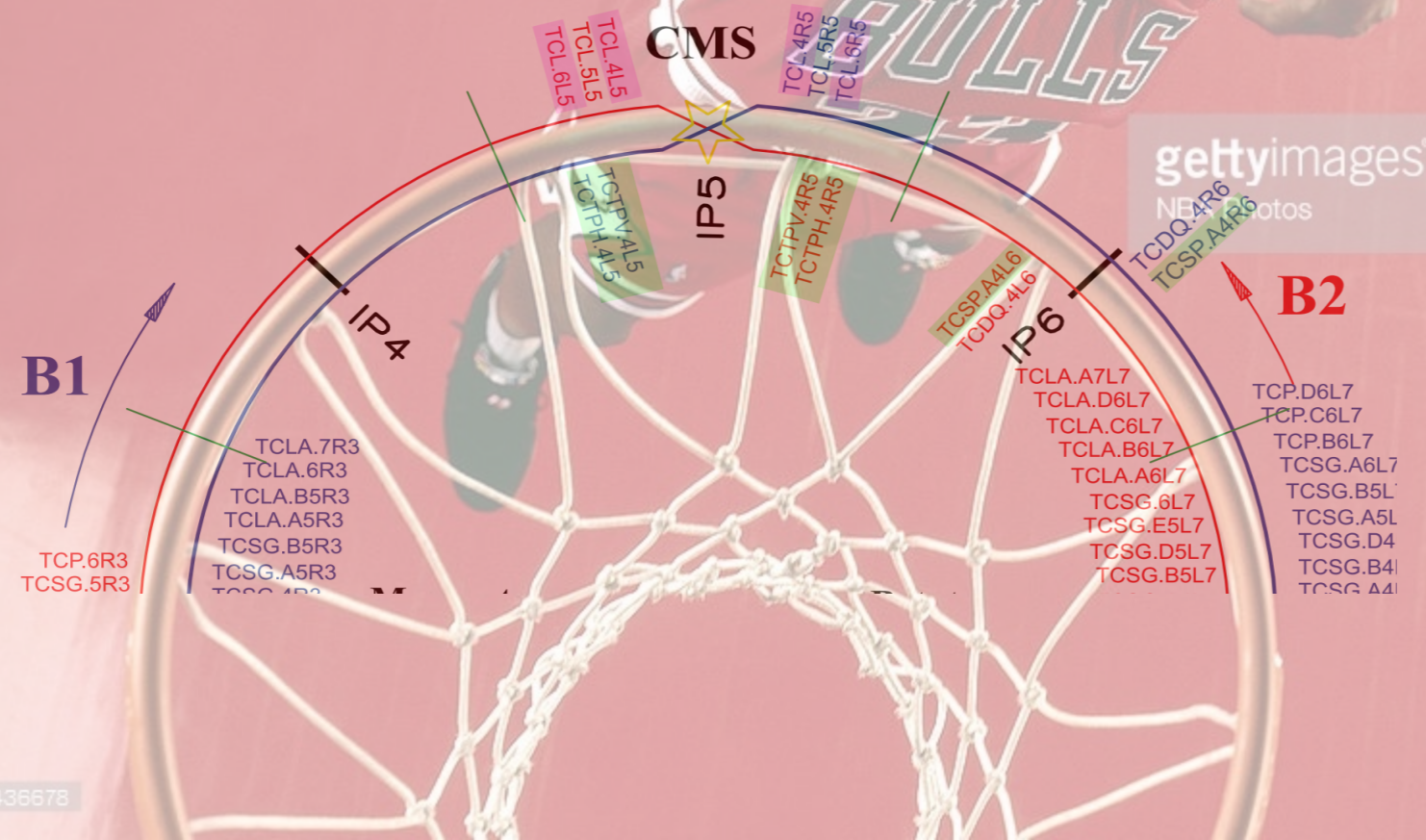
# Outline

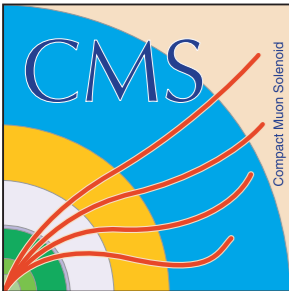
Total, inelastic & diffractive cross section measurements at the LHC

Hard diffraction

High- $\beta^*$ /Low pile-up running with proton tagging

CT-PPS and AFP: proton spectrometers at high-luminosity

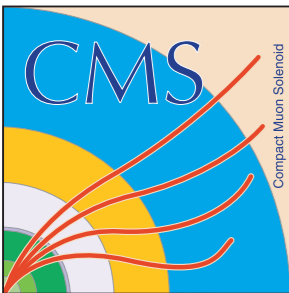




# ATLAS, CMS & TOTEM @ LHC

Large Hadron Collider  
27 km circumference





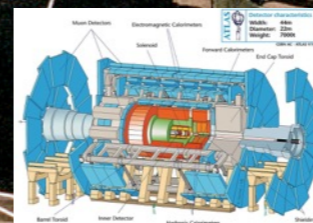
# ATLAS, CMS & TOTEM @ LHC

Large Hadron Collider  
27 km circumference



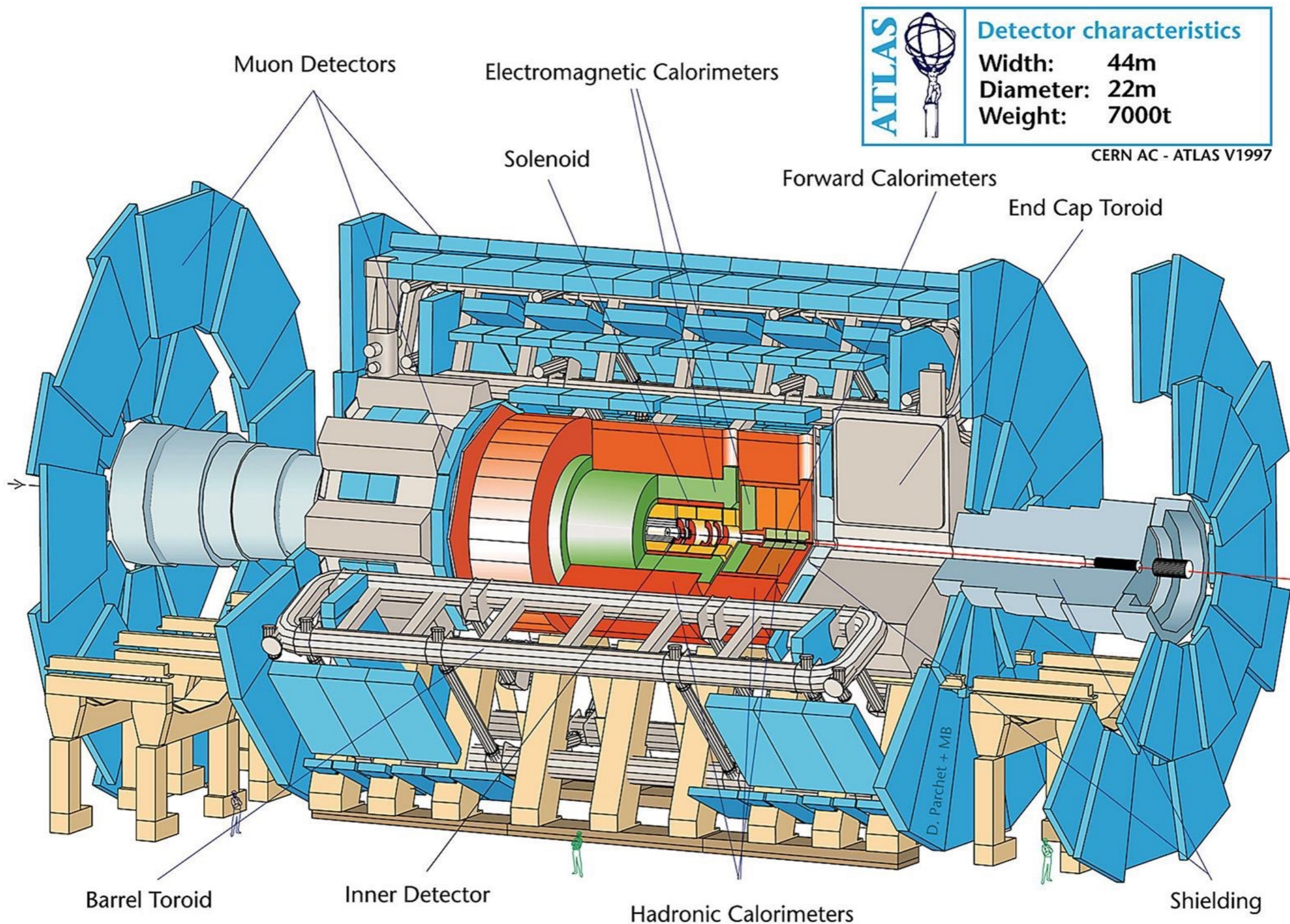
LHCb

ATLAS

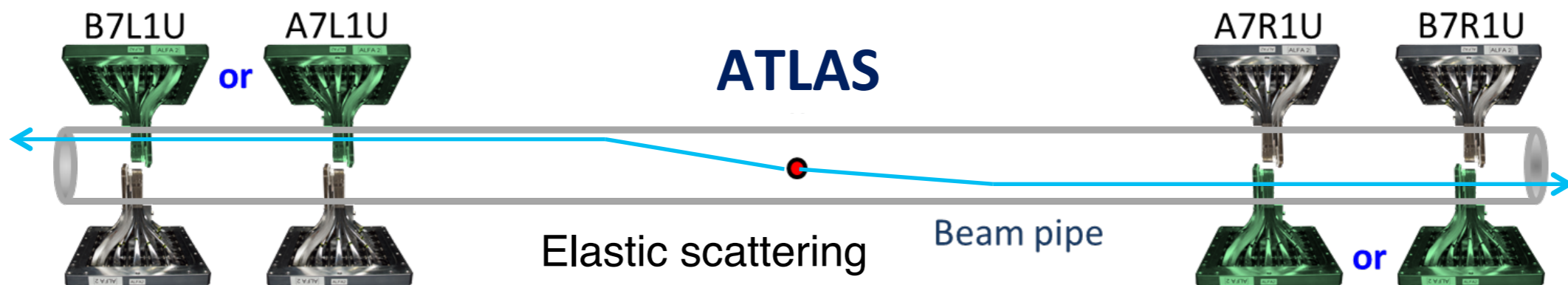


ALICE

# The ATLAS detector



# ATLAS - ALFA

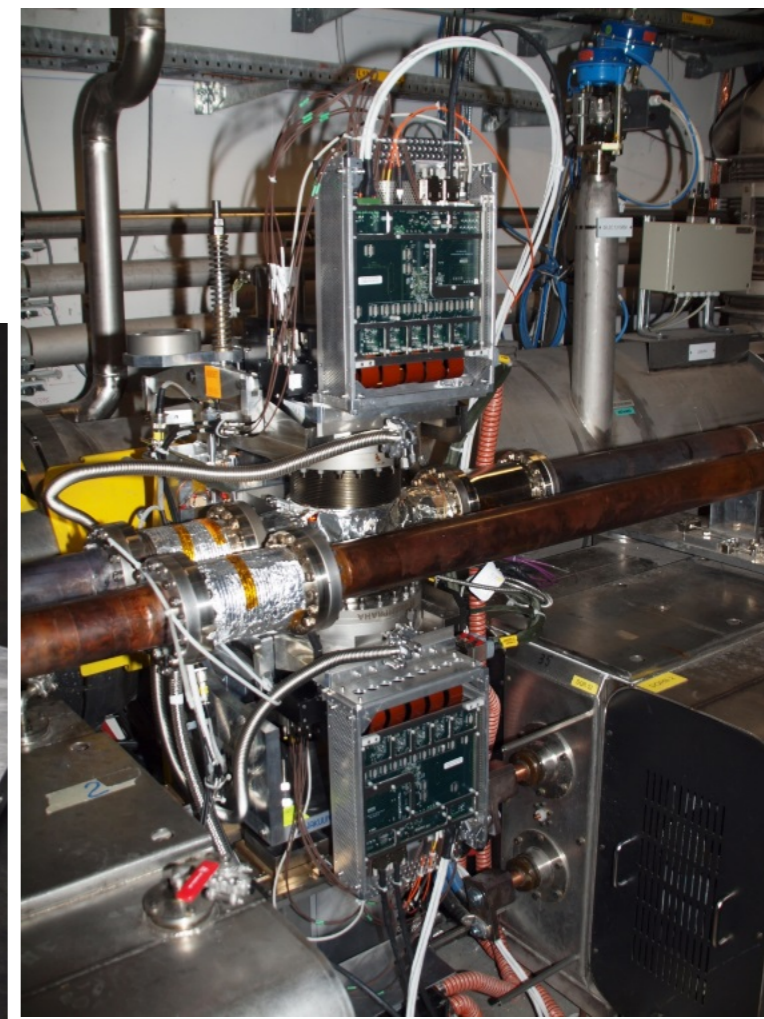
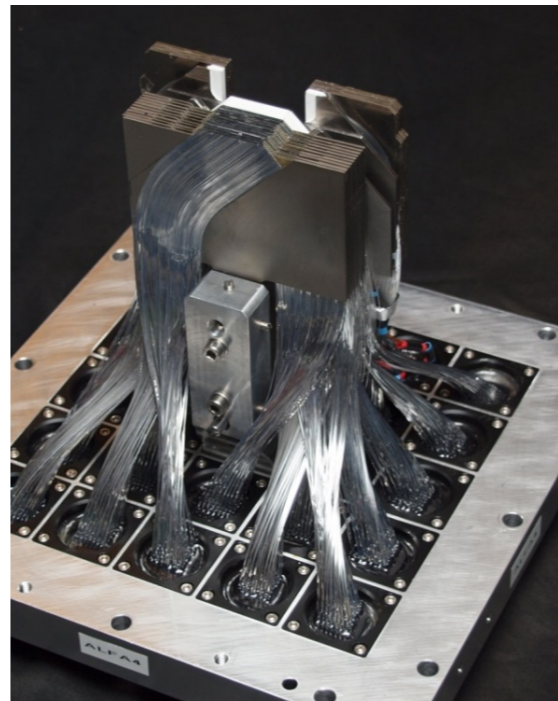


Roman Pot (RP) (vertical) stations at  
~ 240 m from ATLAS IP.

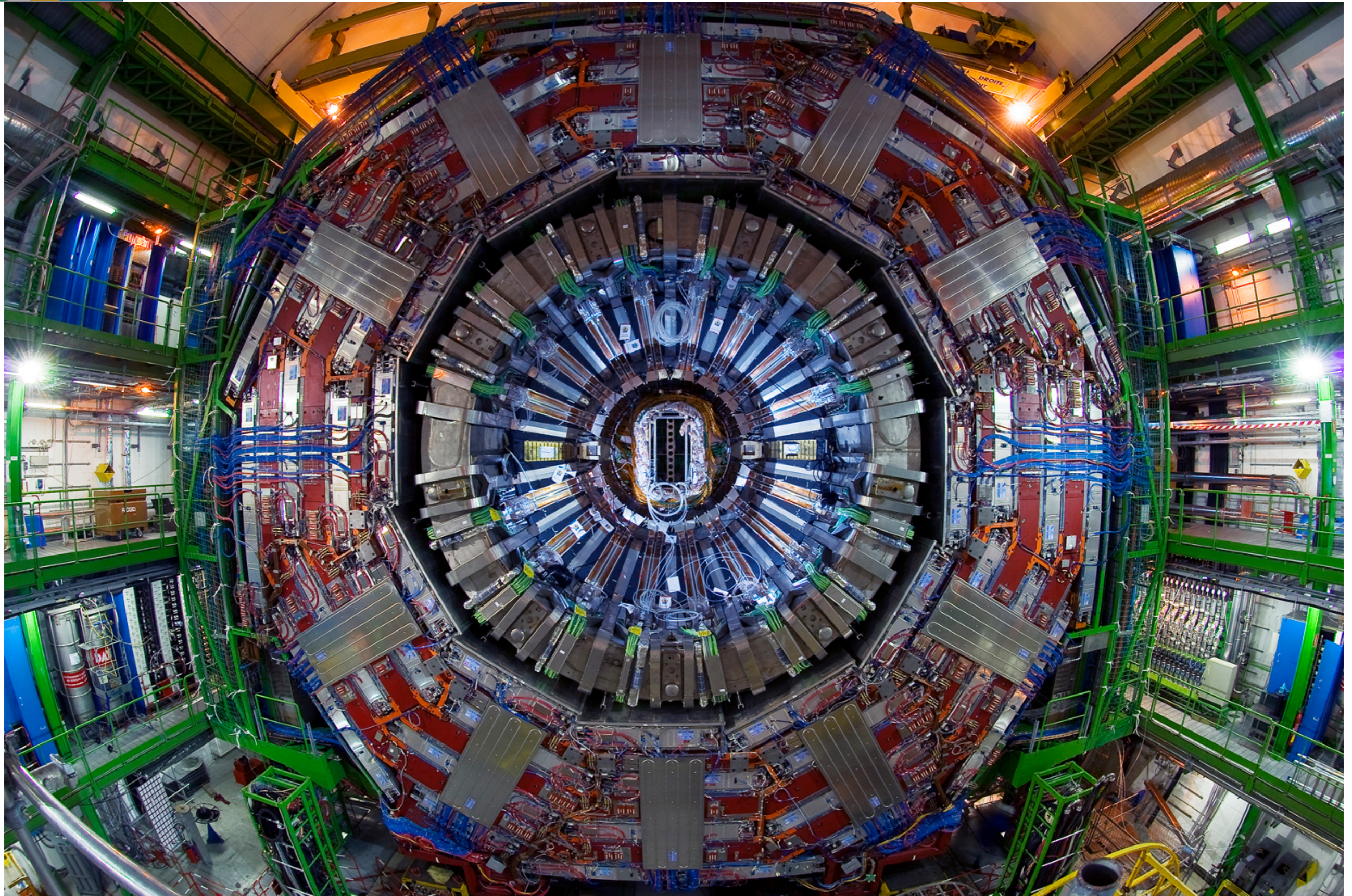
8 fiber detectors (2 x 10 layers; 0.5  
mm fibers; resolution ~ 35  $\mu$ m).

Fully integrated in ATLAS DAQ.

Material taken from P.Fassnacht  
Forward Physics Working Group  
workshop - March 2016



# The CMS detector



# The CMS detector

## CMS Detector

Pixels  
 Tracker  
 ECAL  
 HCAL  
 Solenoid  
 Steel Yoke  
 Muons

**SILICON TRACKER**  
 Pixels ( $100 \times 150 \mu\text{m}^2$ )  
 $\sim 1\text{m}^2$  66M channels  
 Microstrips ( $50\text{-}100\mu\text{m}$ )  
 $\sim 210\text{m}^2$  9.6M channels

**CRYSTAL ELECTROMAGNETIC CALORIMETER (ECAL)**  
 76k scintillating  $\text{PbWO}_4$  crystals

**PRESHOWER**  
 Silicon strips  
 $\sim 16\text{m}^2$  137k channels

**CASTOR CALORIMETER**  
 Tungsten + quartz plates

**FORWARD CALORIMETER**  
 Steel + quartz fibres

**MUON CHAMBERS**  
 Barrel: 250 Drift Tube & 500 Resistive Plate Chambers  
 Endcaps: 450 Cathode Strip & 400 Resistive Plate Chambers

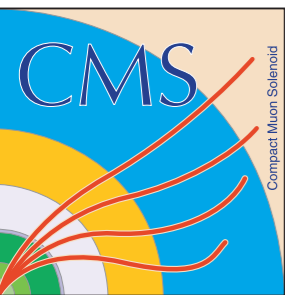
**HADRON CALORIMETER (HCAL)**  
 Brass + plastic scintillator

**SUPERCONDUCTING SOLENOID**  
 Niobium-titanium coil  
 carrying  $\sim 18000\text{ A}$

**STEEL RETURN YOKE**  
 $\sim 13000$  tonnes

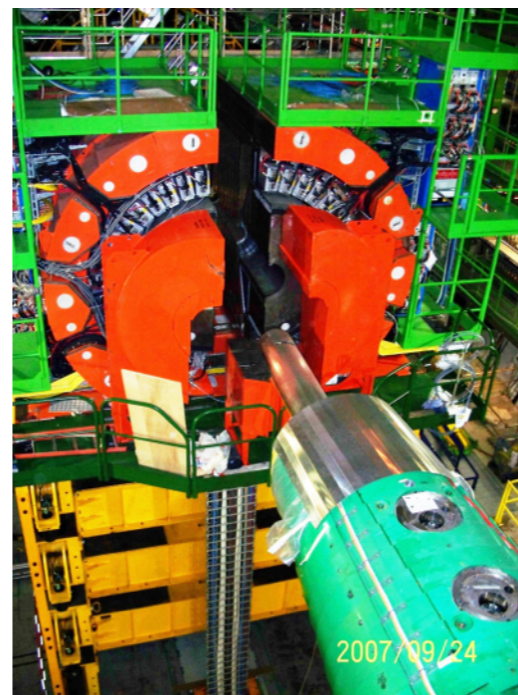
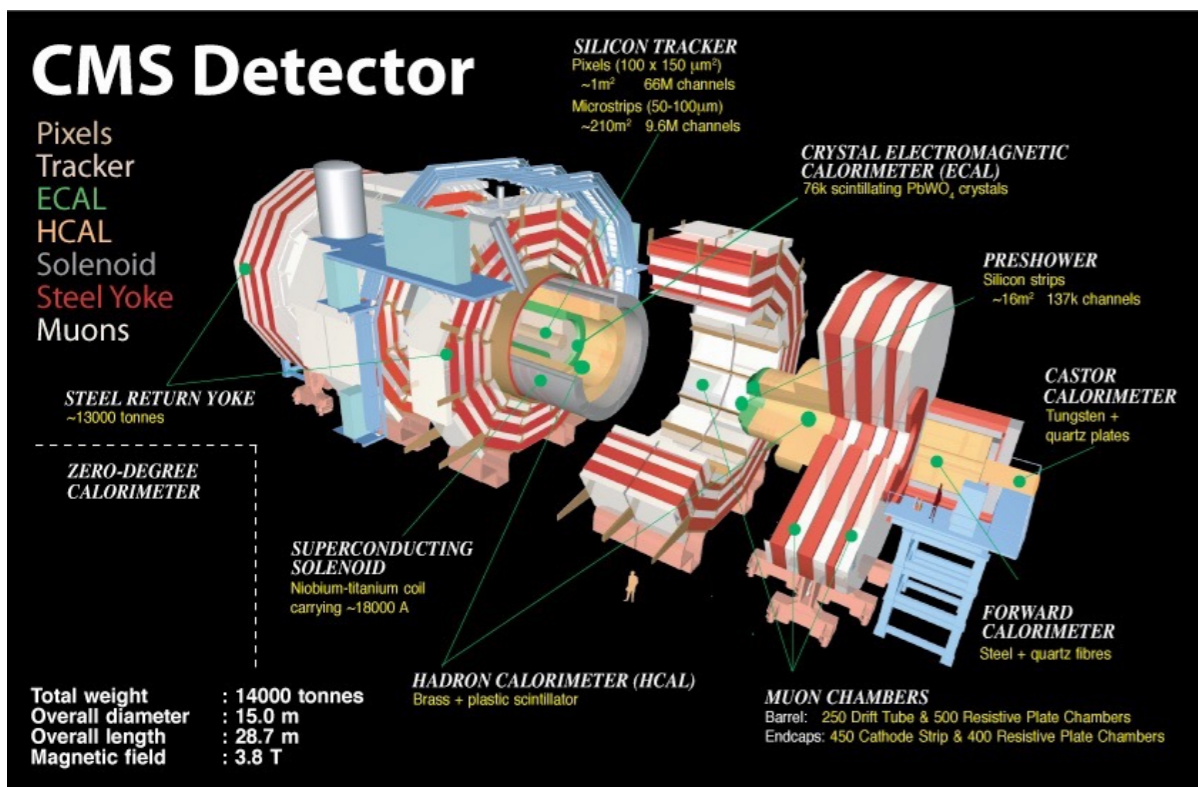
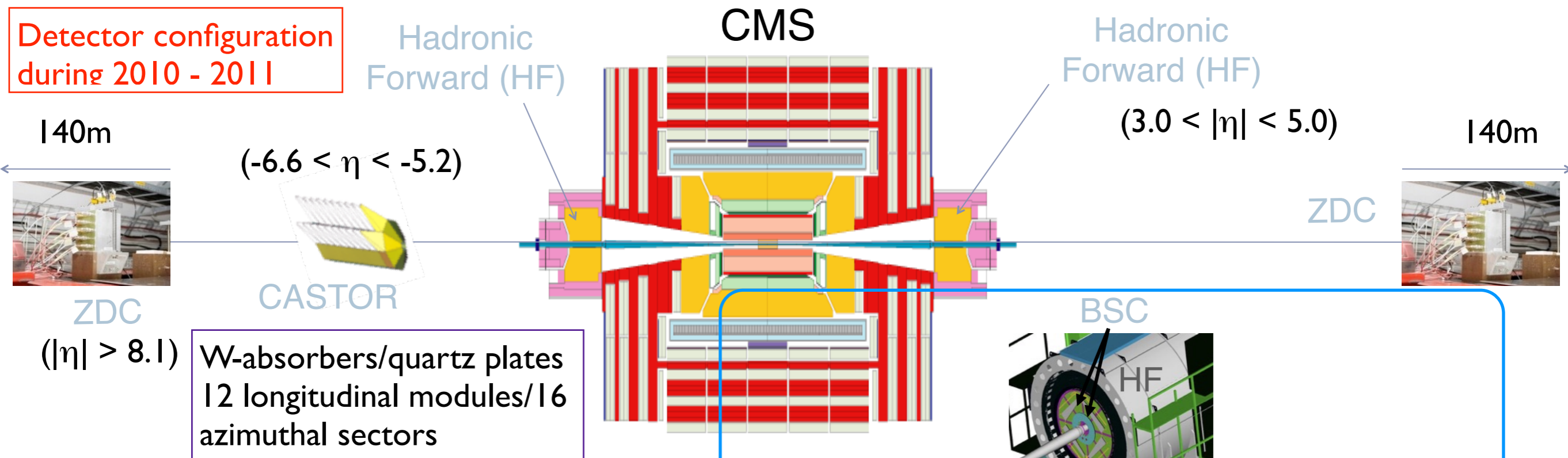
**ZERO-DEGREE CALORIMETER**

Total weight : 14000 tonnes  
 Overall diameter : 15.0 m  
 Overall length : 28.7 m  
 Magnetic field : 3.8 T



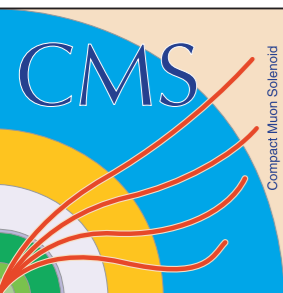
# Forward detectors @ CMS

Detector configuration during 2010 - 2011



Hadron Forward:  
@11.2m from interaction point  
Rapidity coverage:  $3 < |\eta| < 5$   
Steel absorbers/quartz fibers (Long+short fibers)  
0.175x0.175 η/φ segmentation

Acceptance limited to  $|\eta| < 4.9$  at analysis level



# Forward detectors @ CMS

Detector configuration during 2010 - 2011

Hadronic Forward (HFC)

Analogous forward detector instrumentation, at large pseudorapidity, present as well in ATLAS, in particular:

Forward Calorimeter (FCal): Liquid argon sampling calorimeter ( $3.1 < |\eta| < 4.9$ ).

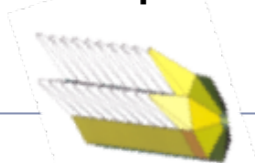
Minimum-bias trigger scintillators (MBTS):

In front of each endcap calorimeter. Inner and outer octagonal rings w/ 8 and 4 counters respectively ( $2.07 < |\eta| < 3.86$ ).

LUCID: Forward Cherenkov detector ( $5.6 < |\eta| < 5.9$ ).

140m

$(-6.6 < \eta < -5.2)$

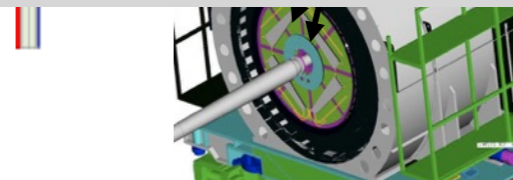
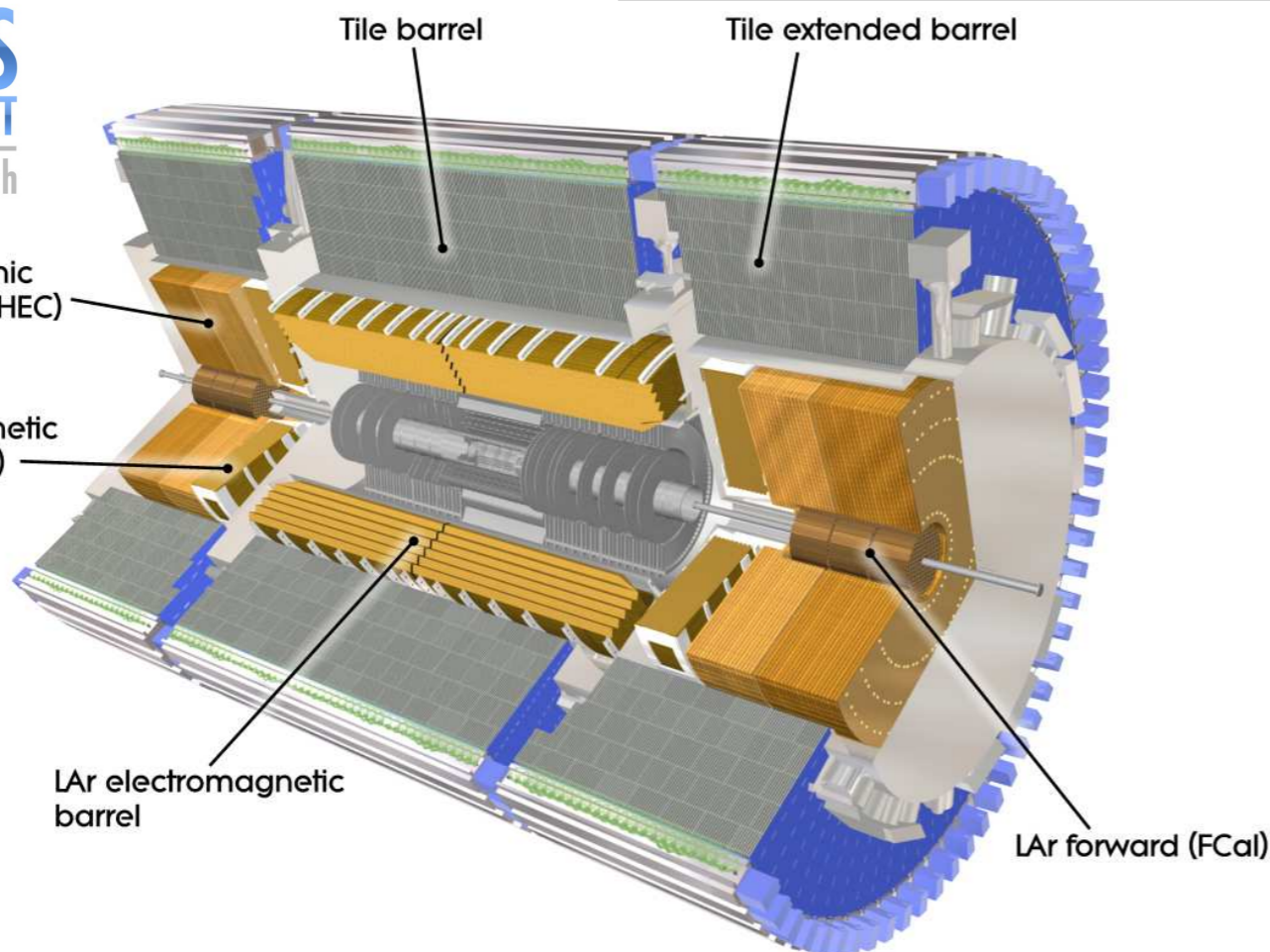


CASTOR

ZDC

$(|\eta| > 8.1)$

W-absorbers/quartz plate



Hadron Forward:

@ 11.2m from interaction point

Rapidity coverage:  $3 < |\eta| < 5$

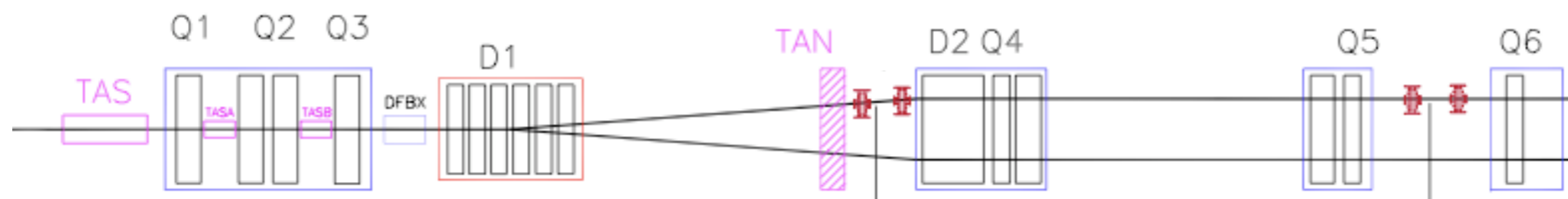
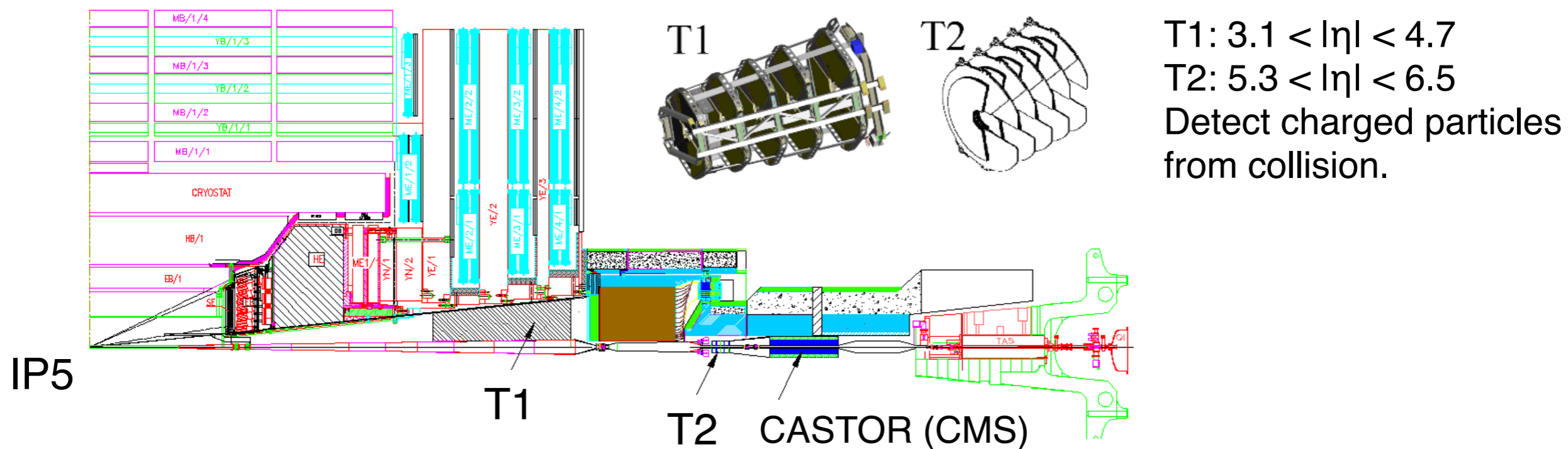
Steel absorbers/quartz fibers (Long+short fibers)

0.175x0.175  $\eta/\phi$  segmentation

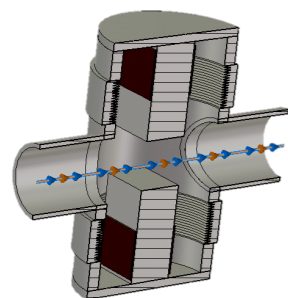
Acceptance limited to  $|\eta| < 4.9$  at analysis level



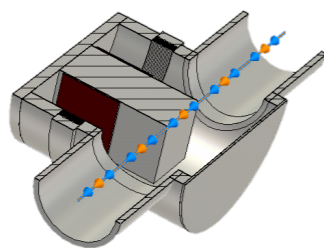
# The TOTEM detectors



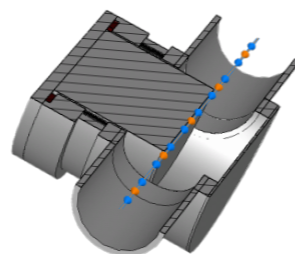
Roman Pots (RPs) ~ 220 m  
Detect outgoing protons at very small angles  
(elastic, diffractive and photon-induced processes).



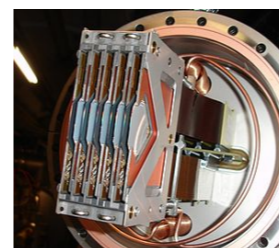
Vertical RPs



Horizontal RPs



Cylindrical RPs  
(w/ CT-PPS)



Material taken from N. Minafra - Low-x 2016

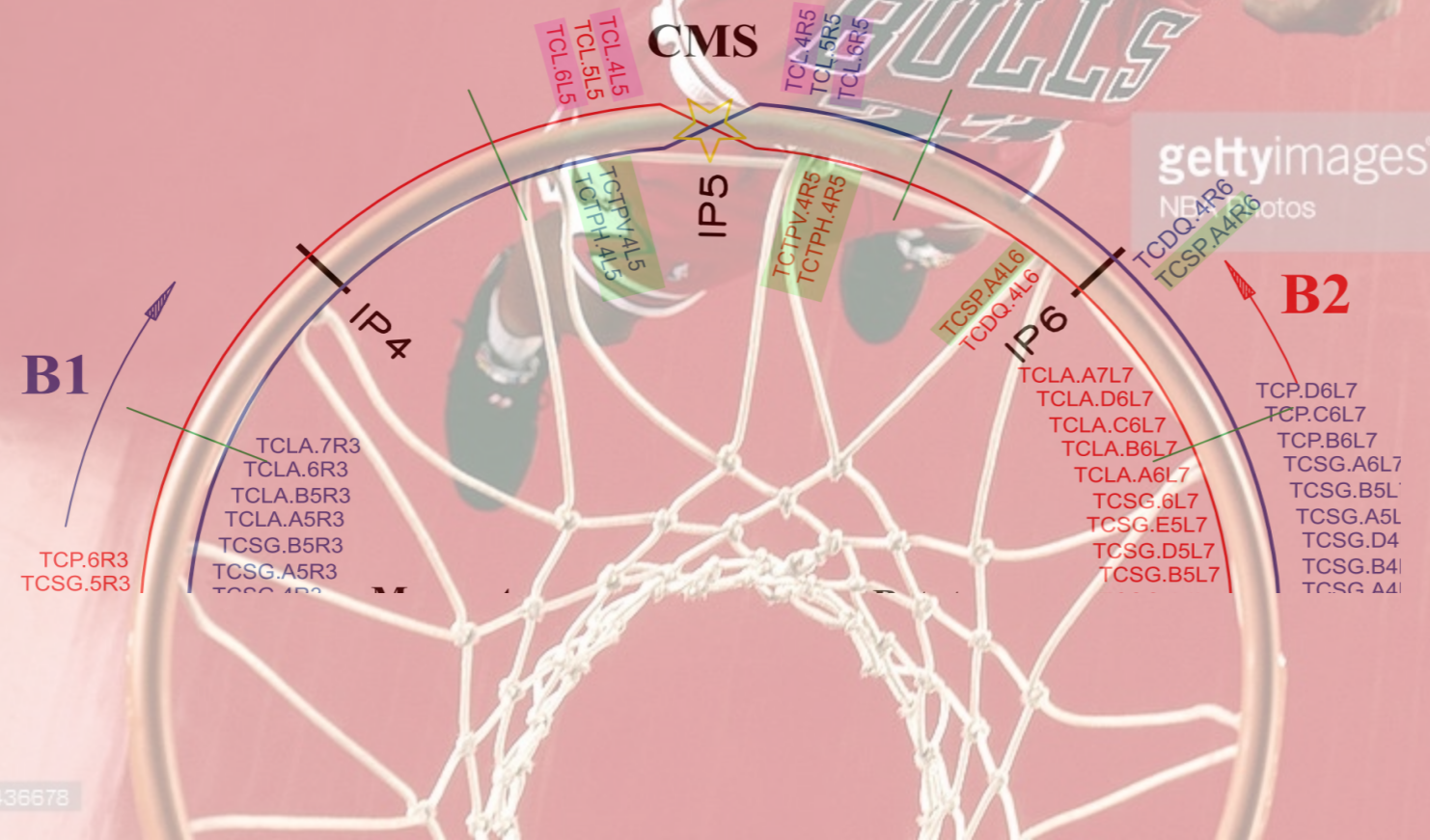
# Outline

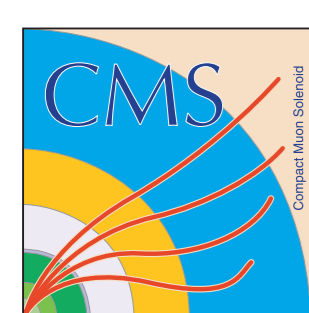
Total, inelastic & diffractive cross section measurements at the LHC

Hard diffraction

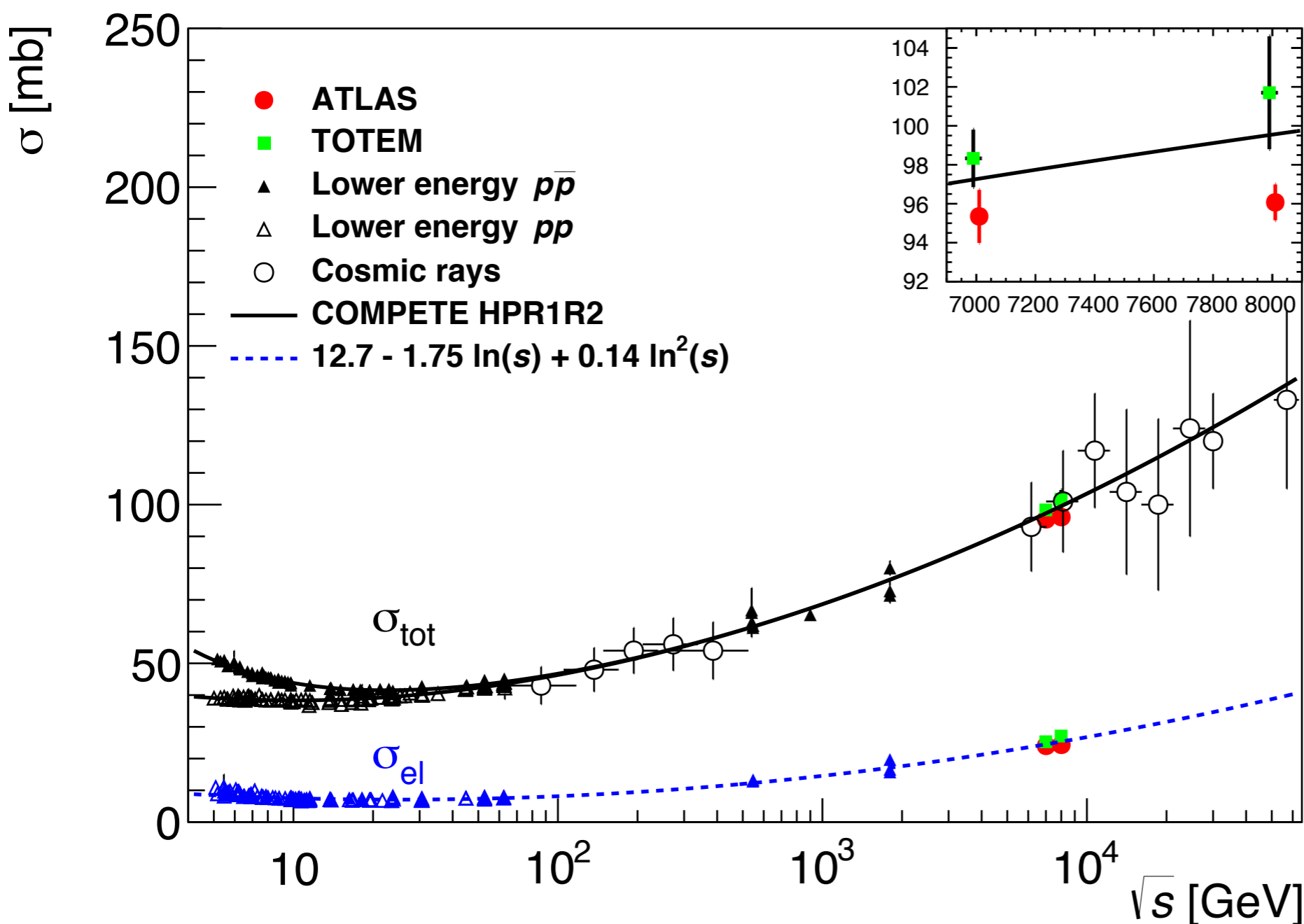
High- $\beta^*$ /Low pile-up running with proton tagging

CT-PPS and AFP: proton spectrometers at high-luminosity





# The total and (in)elastic cross sections



Luminosity dependent:

$$\sigma_{\text{tot}}^2 = \frac{16\pi}{1 + q^2} \frac{1}{\mathcal{L}} \left. \frac{dN_{\text{el}}}{dt} \right|_0$$

Luminosity independent:

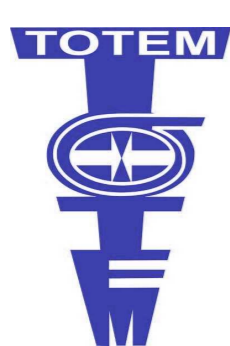
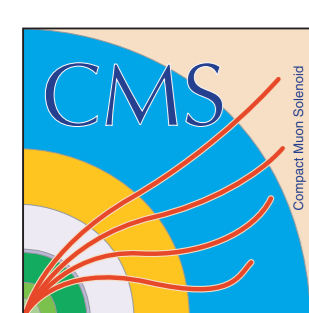
$$\sigma_{\text{tot}} = \frac{16\pi}{1 + q^2} \frac{dN_{\text{el}}/dt|_0}{N_{\text{el}} + N_{\text{inel}}}$$

$\rho$ -independent:

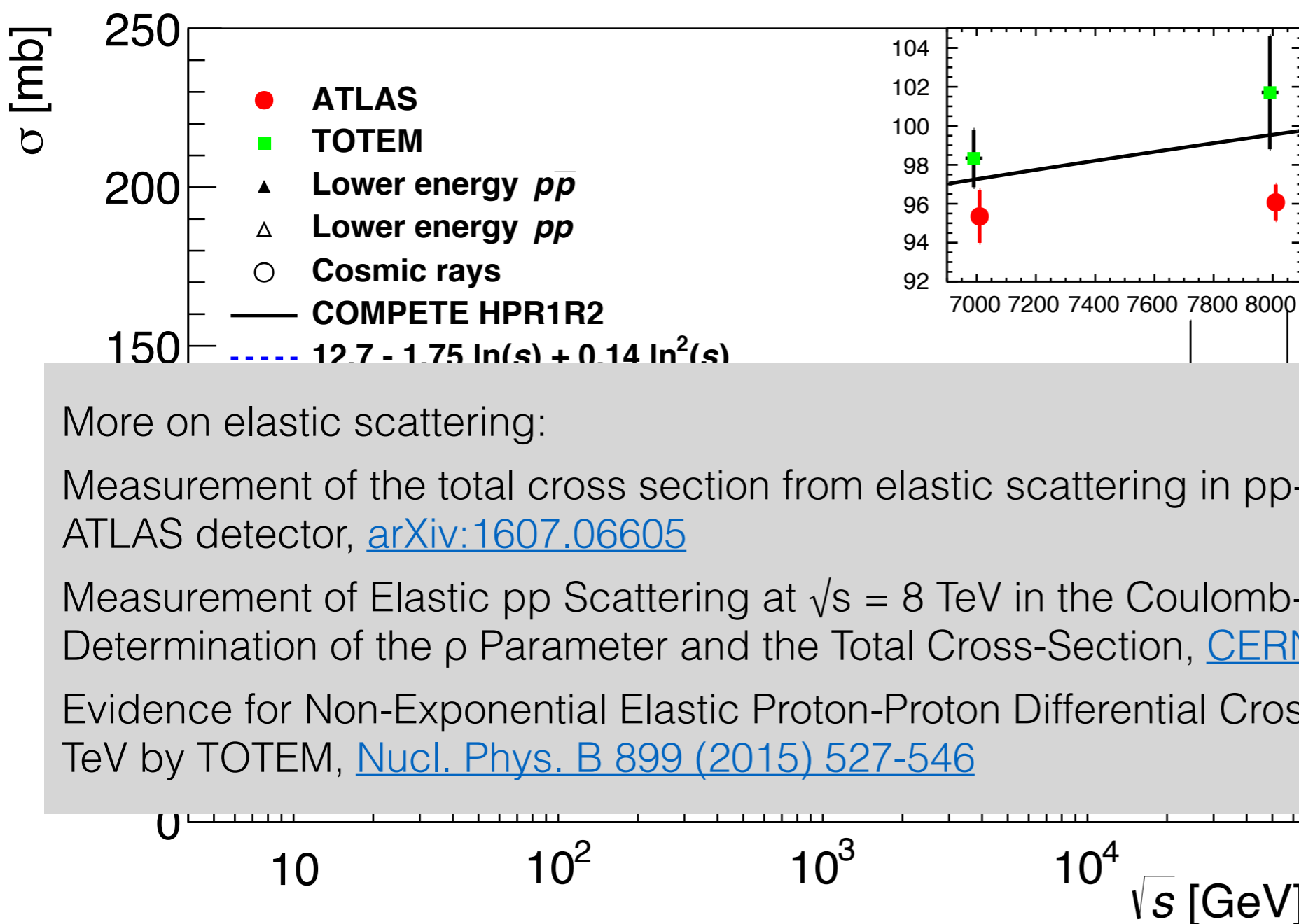
$$\sigma_{\text{tot}} = \frac{1}{\mathcal{L}} (N_{\text{el}} + N_{\text{inel}})$$

[ATLAS STDM-2015-22](#)  
[arXiv:1607.06605](#)

TOTEM:  
[EPL 96\(2011\) 21002](#)  
[EPL 101\(2013\) 21002](#)  
[EPL 101\(2013\) 21004](#)  
[PRL 111 \(2013\) 012001](#)



# The total and (in)elastic cross sections



Luminosity dependent:

$$\sigma_{\text{tot}}^2 = \frac{16\pi}{1 + q^2} \frac{1}{\mathcal{L}} \left. \frac{dN_{\text{el}}}{dt} \right|_0$$

Luminosity independent:

More on elastic scattering:

Measurement of the total cross section from elastic scattering in pp-collisions at  $\sqrt{s}=8$  TeV with the ATLAS detector, [arXiv:1607.06605](https://arxiv.org/abs/1607.06605)

Measurement of Elastic pp Scattering at  $\sqrt{s} = 8$  TeV in the Coulomb-Nuclear Interference Region – Determination of the  $\rho$  Parameter and the Total Cross-Section, [CERN-PH-EP-2015-325](https://arxiv.org/abs/1505.03251)

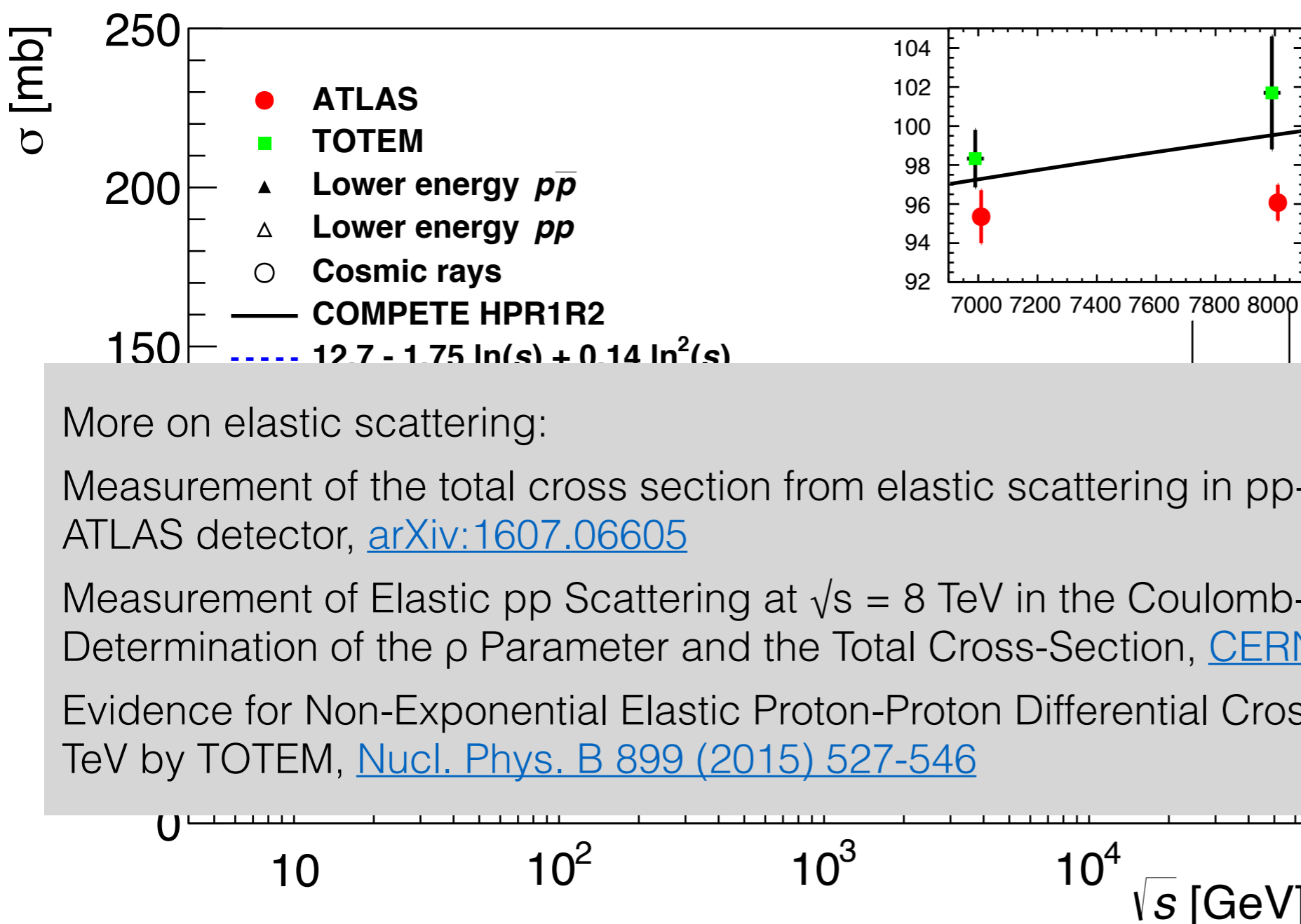
Evidence for Non-Exponential Elastic Proton-Proton Differential Cross-Section at Low  $|t|$  and  $\sqrt{s} = 8$  TeV by TOTEM, [Nucl. Phys. B 899 \(2015\) 527-546](https://arxiv.org/abs/1505.03251)

[ATLAS STDM-2015-22](https://arxiv.org/abs/1607.06605)  
[arXiv:1607.06605](https://arxiv.org/abs/1607.06605)

**TOTEM:**  
[EPL 96\(2011\) 21002](https://arxiv.org/abs/1105.3544)  
[EPL 101\(2013\) 21002](https://arxiv.org/abs/1305.3544)  
[EPL 101\(2013\) 21004](https://arxiv.org/abs/1305.3544)  
[PRL 111 \(2013\) 012001](https://arxiv.org/abs/1305.3544)



# The total and (in)elastic cross sections



Luminosity dependent:

$$\sigma_{\text{tot}}^2 = \frac{16\pi}{1 + q^2} \frac{1}{\mathcal{L}} \left. \frac{dN_{\text{el}}}{dt} \right|_0$$

Luminosity independent:

More on elastic scattering:

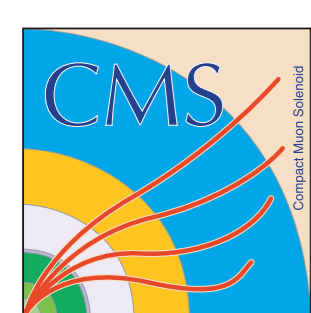
Measurement of the total cross section from elastic scattering in pp-collisions at  $\sqrt{s}=8$  TeV with the ATLAS detector, [arXiv:1607.06605](https://arxiv.org/abs/1607.06605)

Measurement of Elastic pp Scattering at  $\sqrt{s} = 8$  TeV in the Coulomb-Nuclear Interference Region – Determination of the  $\rho$  Parameter and the Total Cross-Section, [CERN-PH-EP-2015-325](https://arxiv.org/abs/1505.03285)

Evidence for Non-Exponential Elastic Proton-Proton Differential Cross-Section at Low  $|t|$  and  $\sqrt{s} = 8$  TeV by TOTEM, [Nucl. Phys. B 899 \(2015\) 527-546](https://arxiv.org/abs/1505.03285)

See talk later today on “Total, elastic and inelastic pp cross sections at the LHC” by Tomas Sykora.

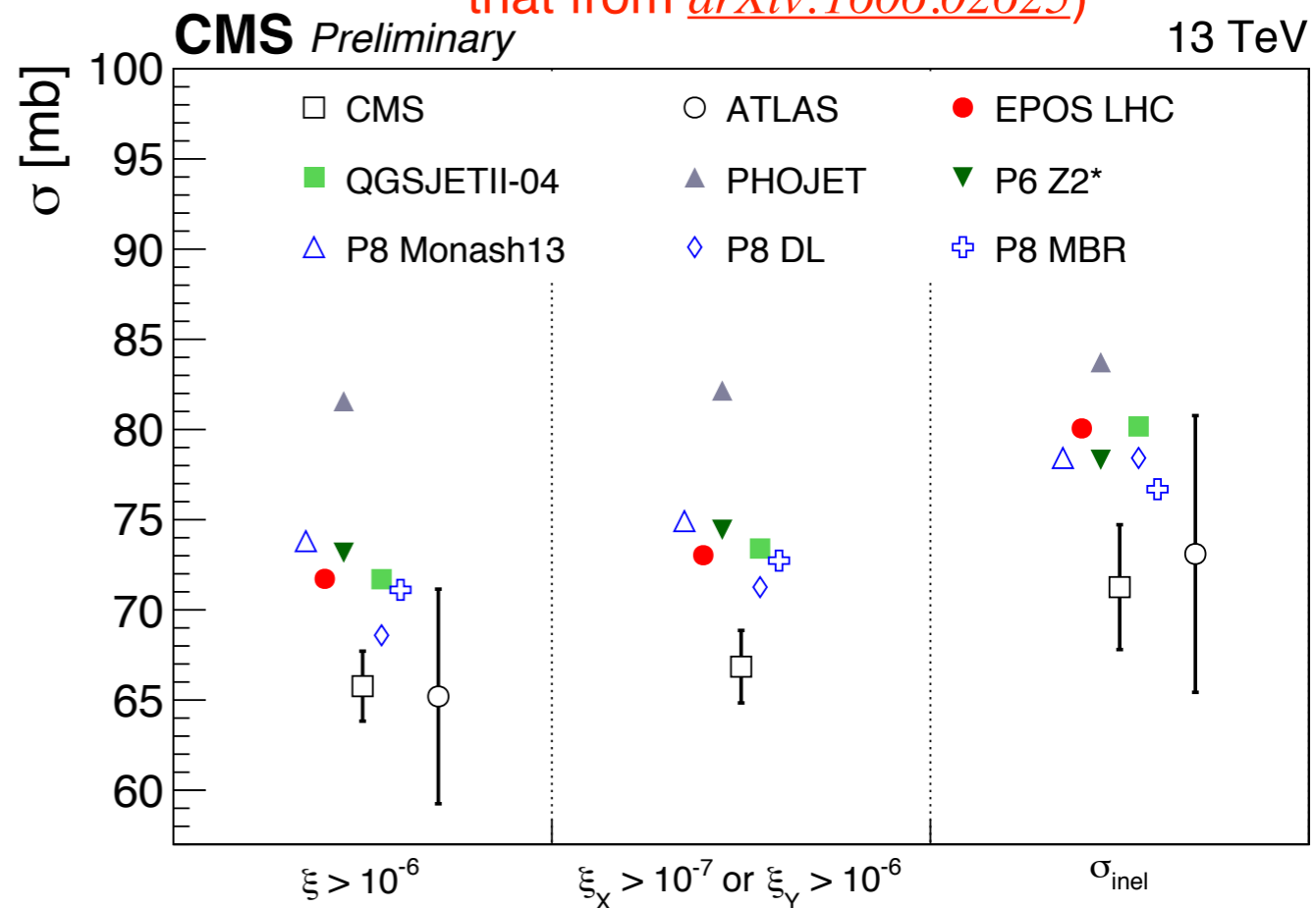
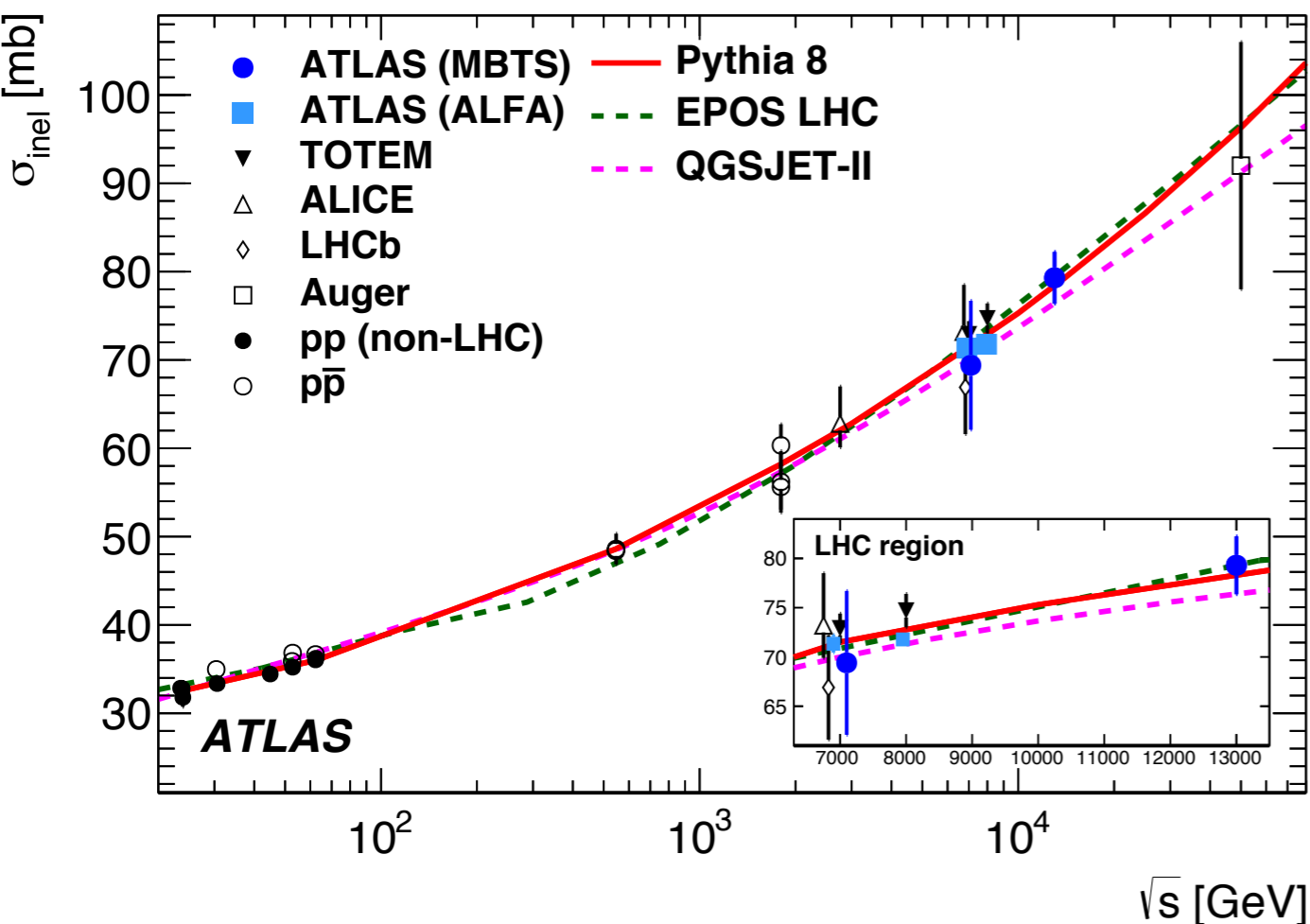
**TOTEM:**  
[EPL 96\(2011\) 21002](https://arxiv.org/abs/1011.4092)  
[EPL 101\(2013\) 21002](https://arxiv.org/abs/1303.3251)  
[EPL 101\(2013\) 21004](https://arxiv.org/abs/1303.3251)  
[PRL 111 \(2013\) 012001](https://arxiv.org/abs/1303.3251)



# The inelastic cross section at 13 TeV



Preliminary ATLAS result (instead of that from [arXiv:1606.02625](https://arxiv.org/abs/1606.02625))

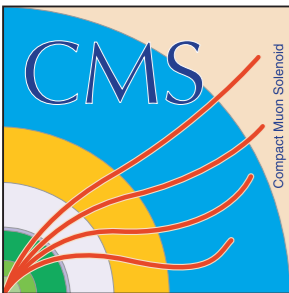


[ATLAS STD-2015-05](#)  
[arXiv:1606.02625](https://arxiv.org/abs/1606.02625)

[CMS FSQ-15-005](#)

Higher detector acceptance by using CASTOR

See talk later today on “Total, elastic and inelastic pp cross sections at the LHC” by Tomas Sykora.

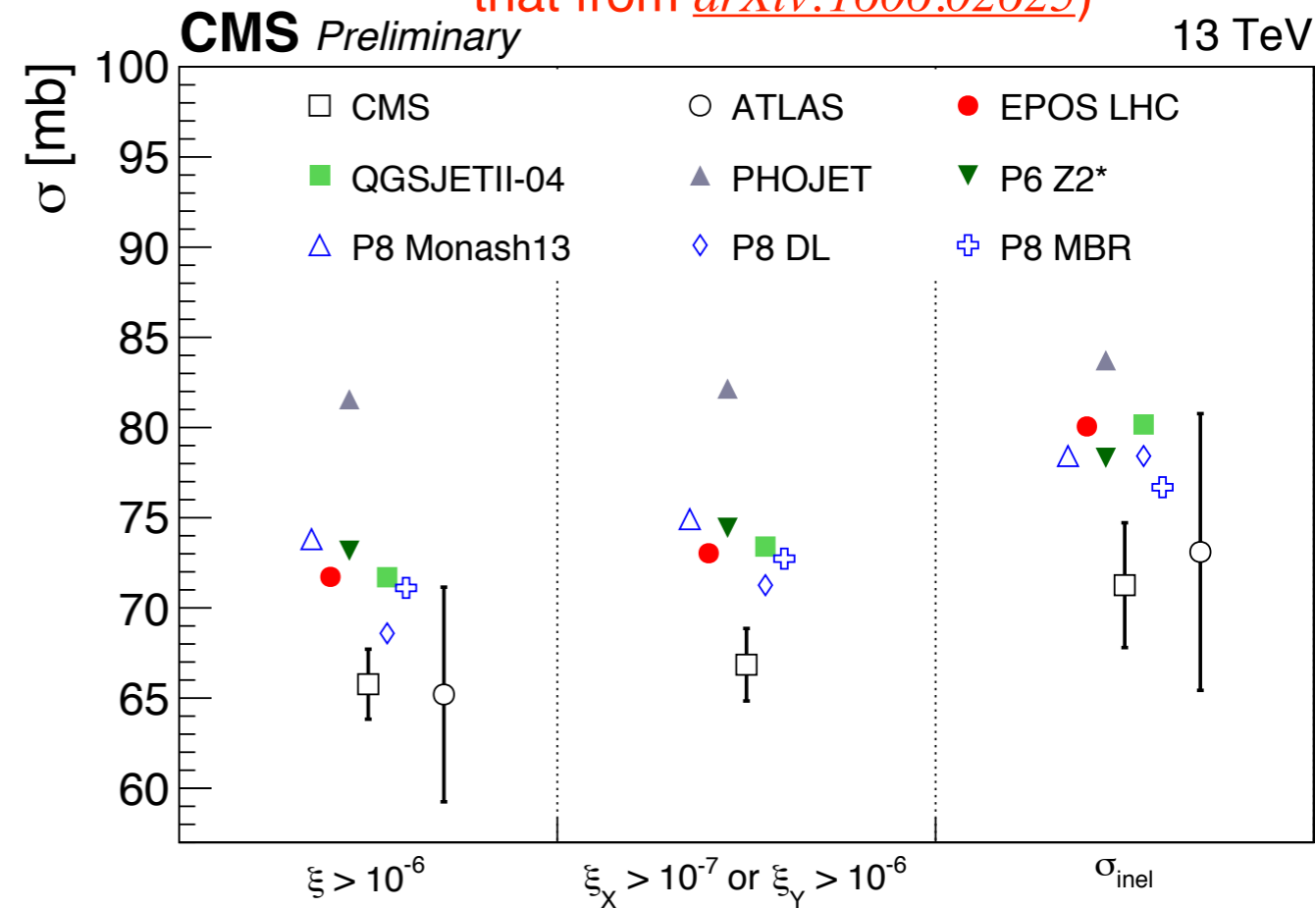
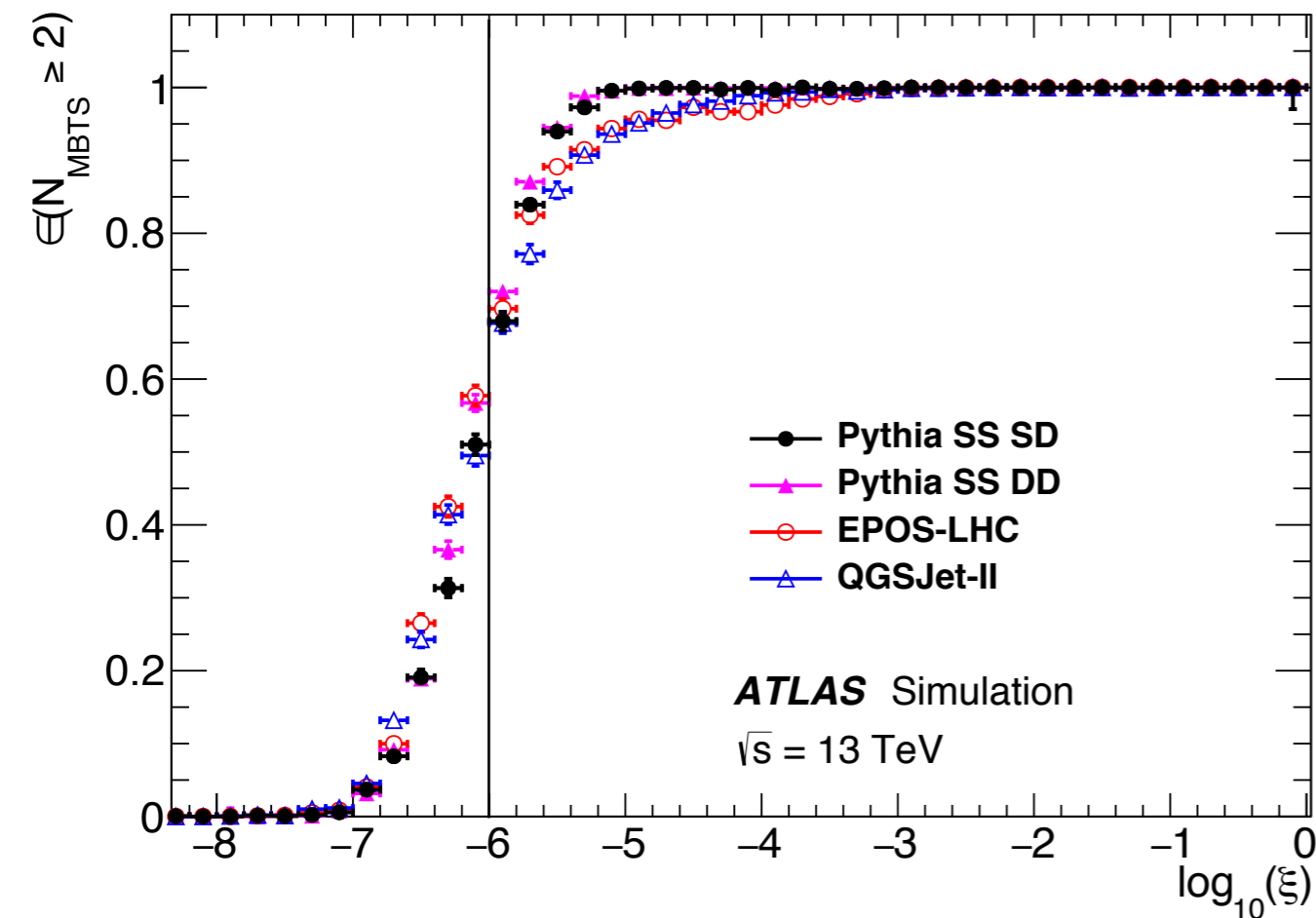


# The inelastic cross section at 13 TeV



Model-dependent extrapolations to  $\xi < 10^{-6}$  region

Preliminary ATLAS result (instead of that from [arXiv:1606.02625](http://arxiv.org/abs/1606.02625))



[ATLAS STDM-2015-05](http://atlas.stdm-2015-05)

[arXiv:1606.02625](http://arxiv.org/abs/1606.02625)

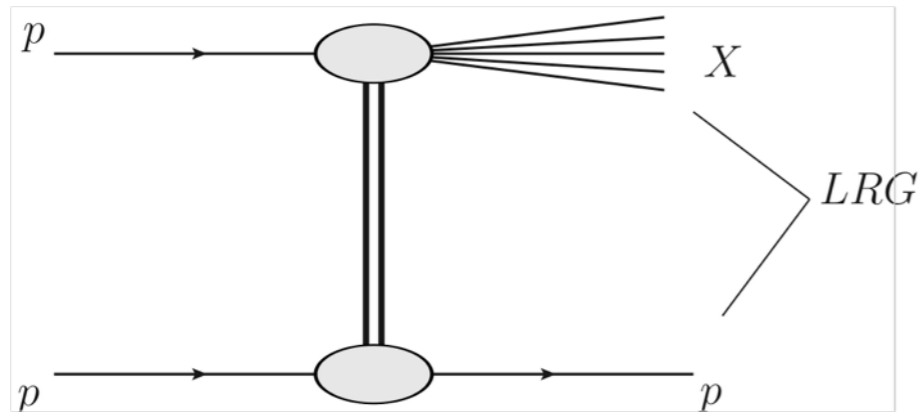
[CMS FSQ-15-005](http://cms.fsq-15-005)

Higher detector acceptance by using CASTOR

See talk later today on "Total, elastic and inelastic pp cross sections at the LHC" by Tomas Sykora.

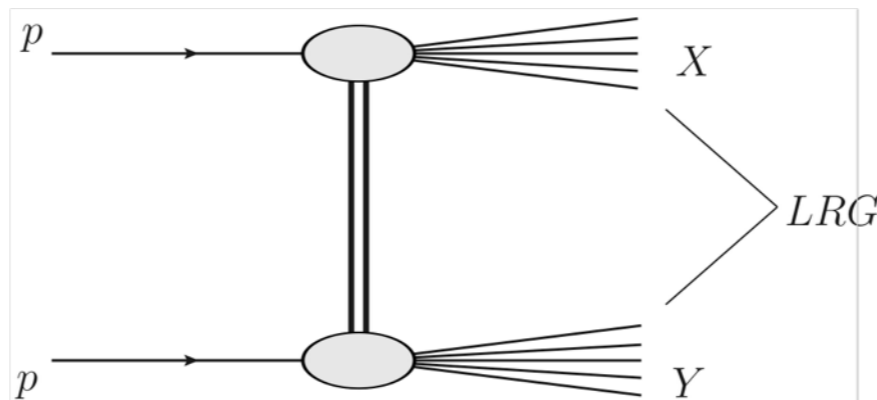
# Diffractive dissociation processes

Single-diffractive dissociation (SD):

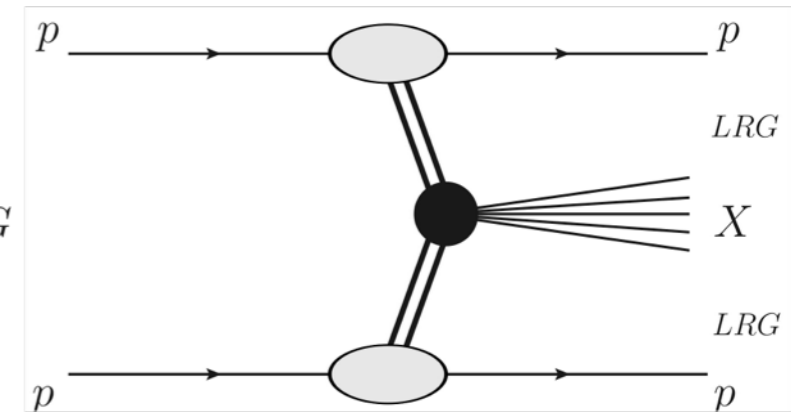


$$t = (p - p')^2; \xi = (M_X)^2/s$$

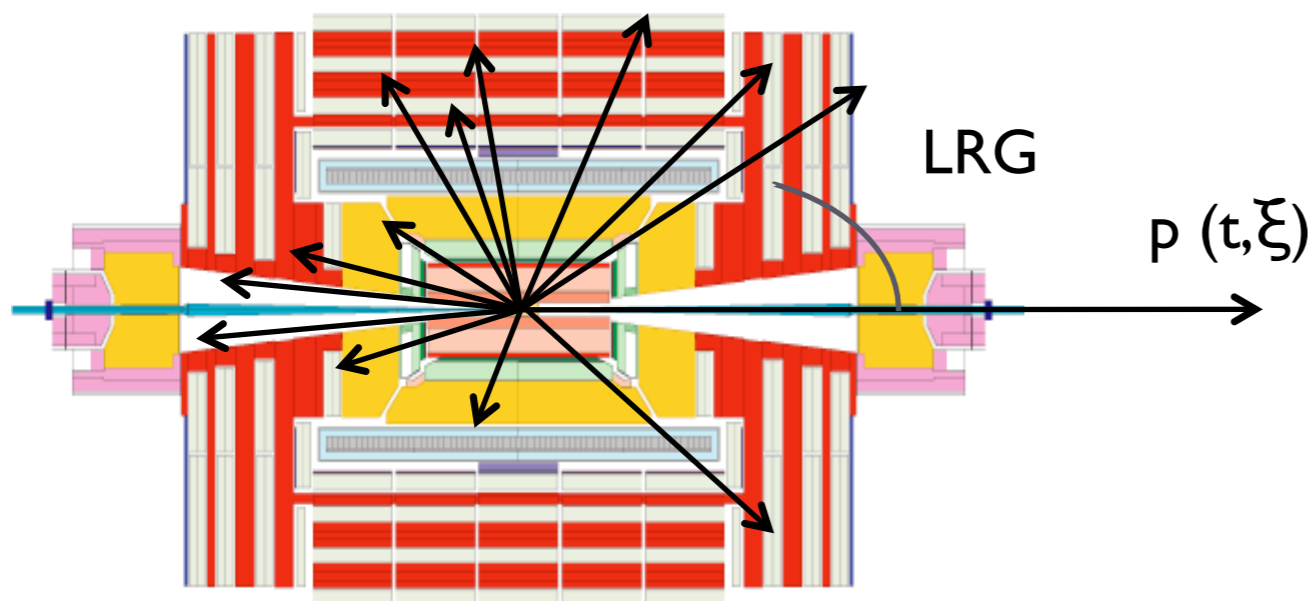
Double-diffractive dissociation (DD):



Central-diffractive dissociation (CD):



Sketch of single-diffractive event:



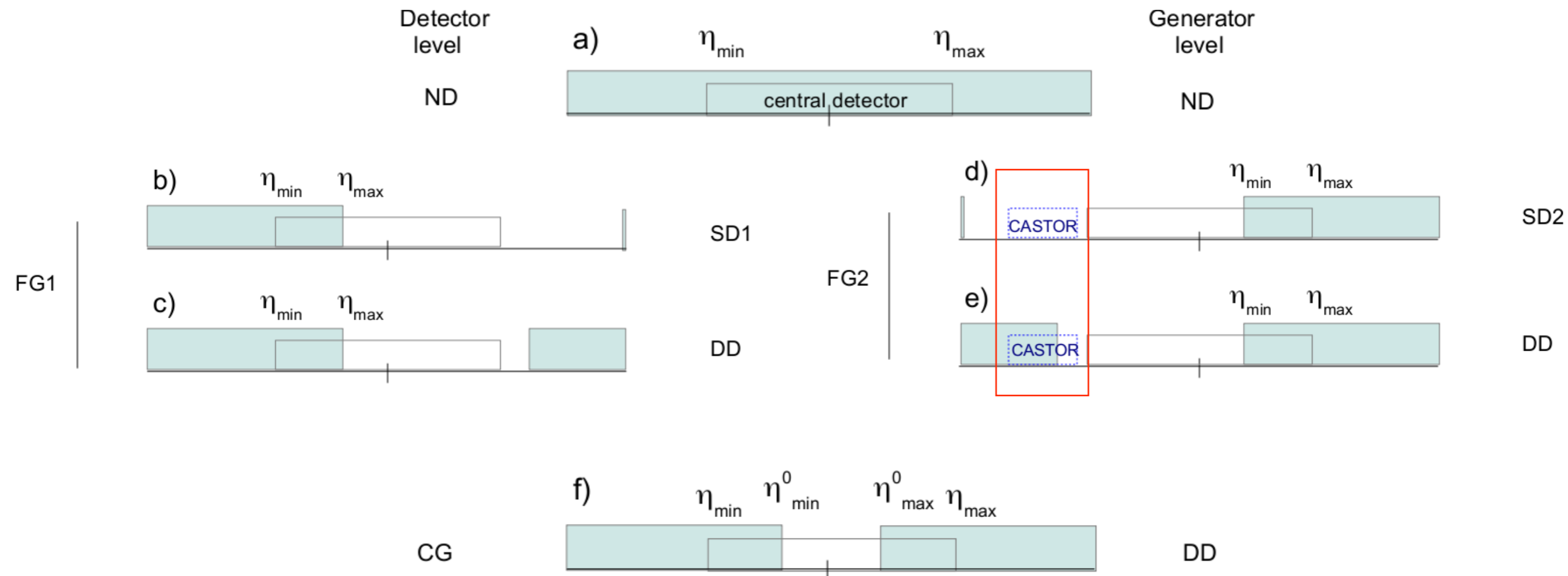
LRG: Large Rapidity Gap

Diffractive dissociation corresponds to a considerable fraction of the pp inelastic cross section.

Soft diffraction in general model dependent.

Defining and constraining diffractive component important ingredient in the tuning of MC generators at the LHC.

# Diffractive topologies at detector level



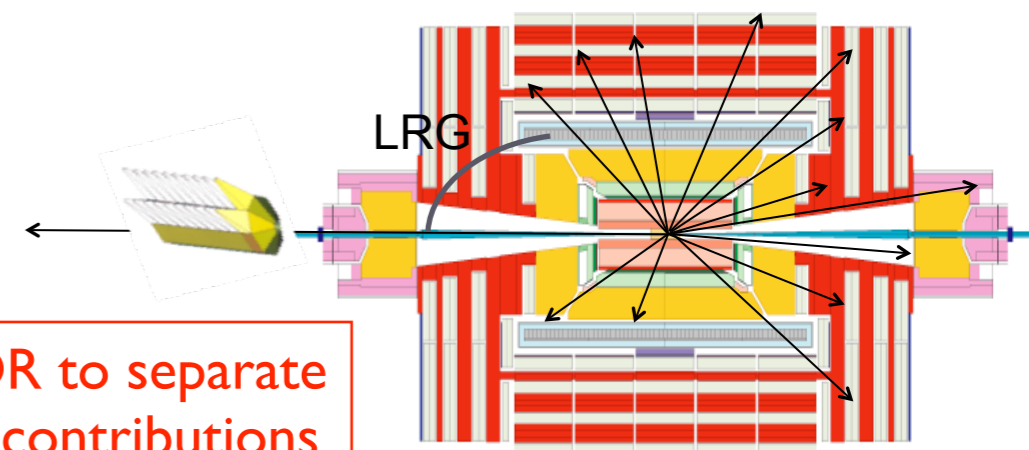
Look at highest/lowest  $\eta$  of particles reconstructed in detector ( $\eta_{\max}/\eta_{\min}$ ) for forward gaps (SD/DD)

Look at closest-to-zero positive/negative  $\eta$  of particles in detector ( $\eta_{\max}^0/\eta_{\min}^0$ ) for central gaps (DD)

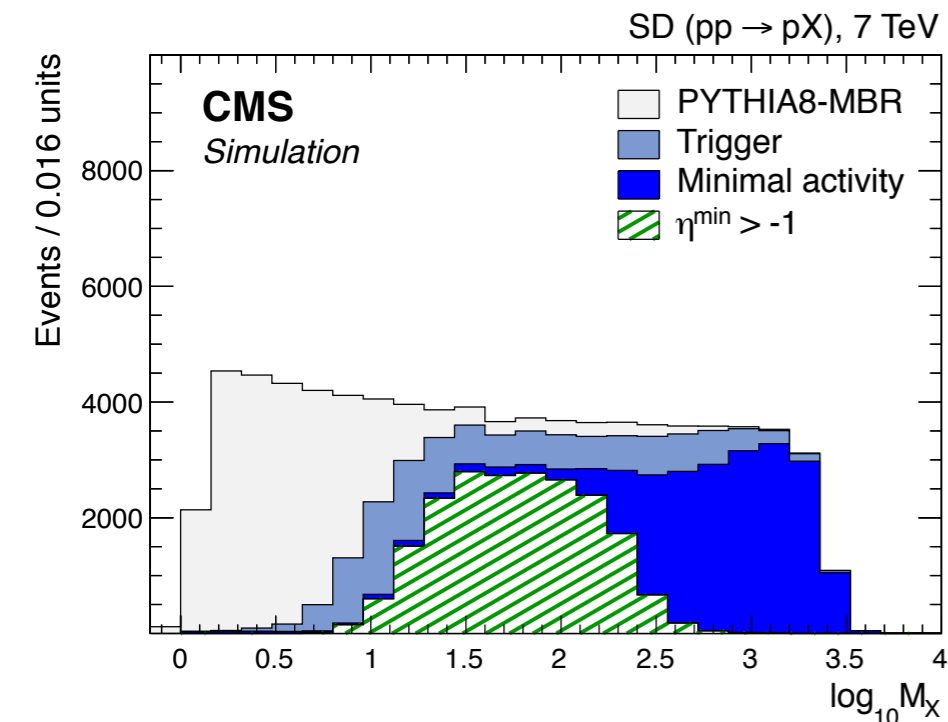
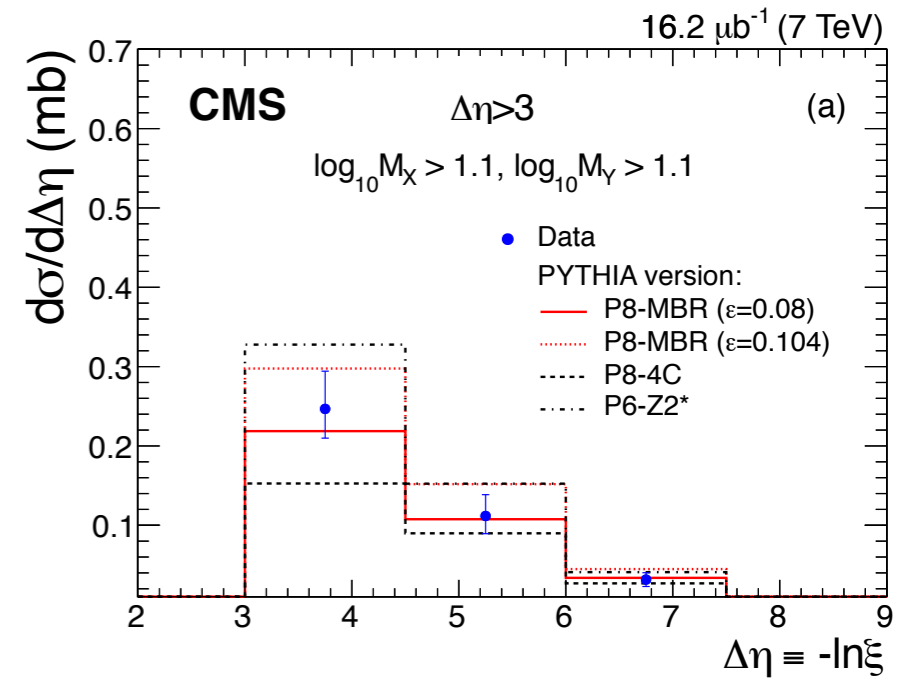
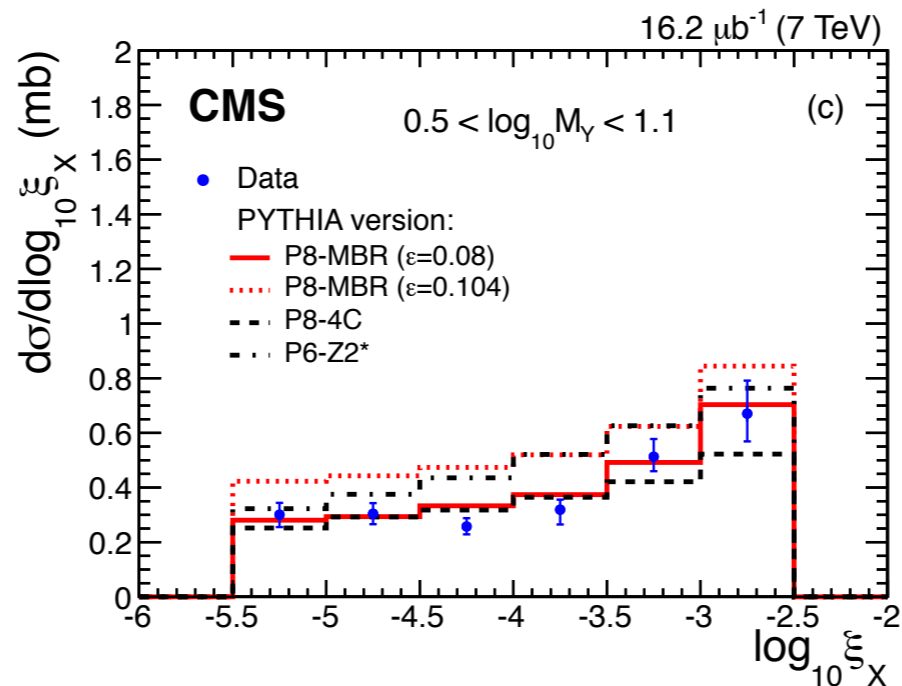
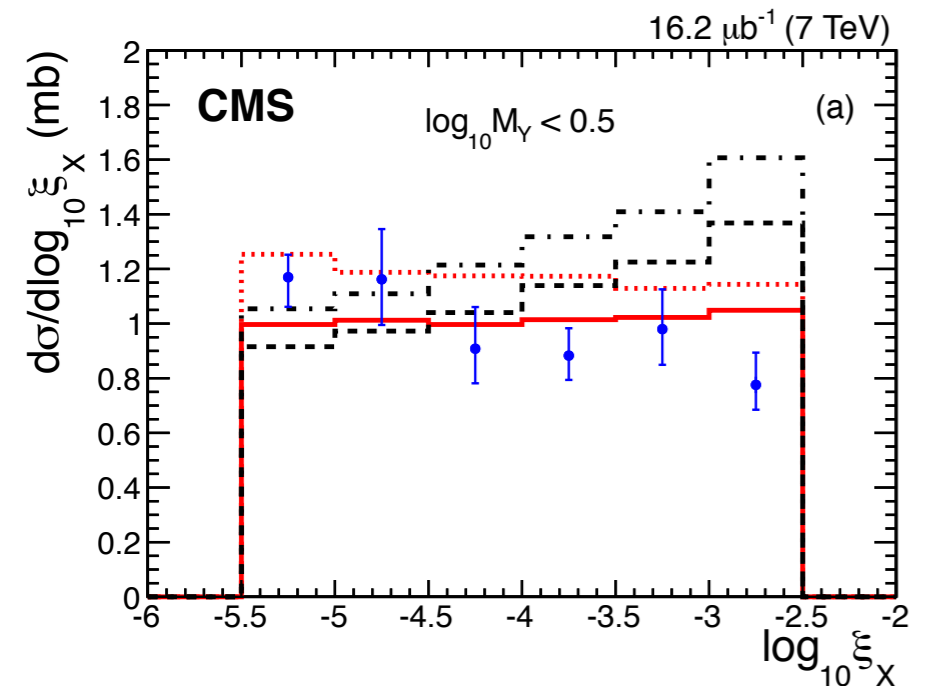
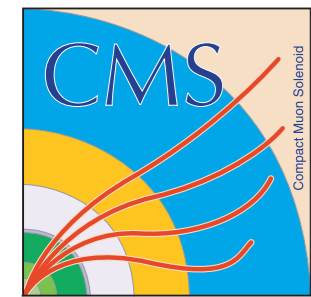
[CMS FSQ-12-005](#)

[Phys. Rev. D 92 \(2015\) 012003](#)

Use CASTOR to separate SD and DD contributions



# Diffractive cross sections



Results compared to predictions from PYTHIA6, PYTHIA8 (Tune 4C), PYTHIA8-MBR (+ other models)

$$\sigma_{\text{vis}}^{\text{SD}} = 4.06 \pm 0.04 \text{ (stat.) } {}^{+0.69}_{-0.63} \text{ (syst.) mb} \\ (-5.5 < \log_{10} \xi_{X,Y} < -2.5)$$

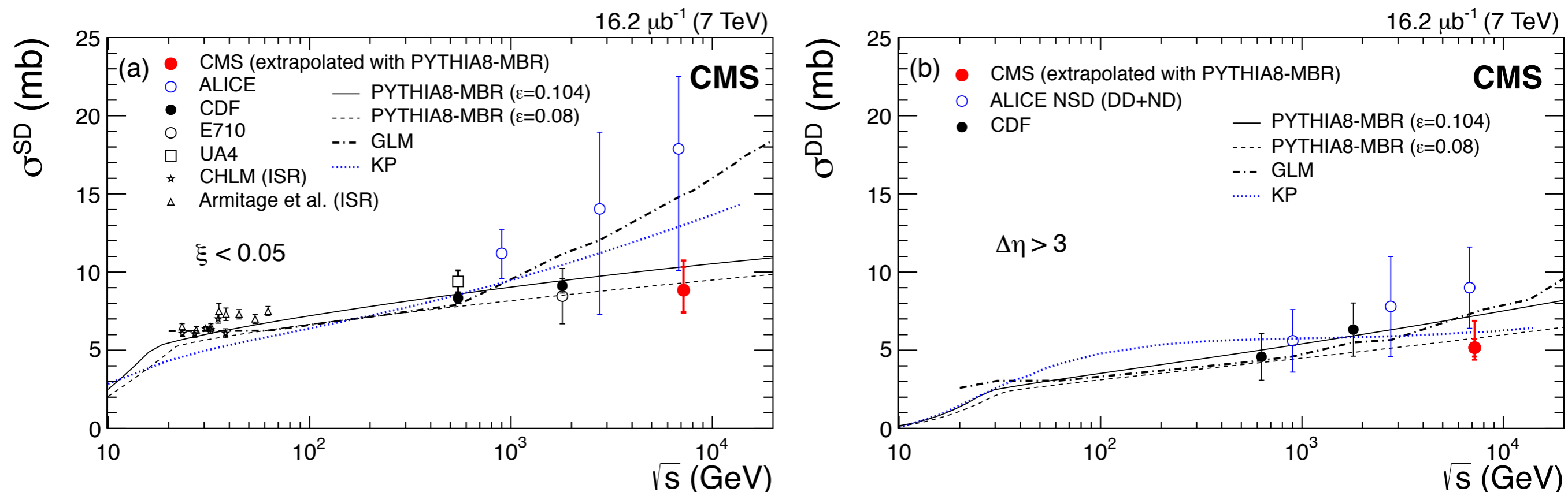
$$\sigma_{\text{vis}}^{\text{DD}} = 2.69 \pm 0.04 \text{ (stat.) } {}^{+0.29}_{-0.30} \text{ (syst.) mb} \\ (-5.5 < \log_{10} \xi_{X,Y} < -2.5 ; 0.5 < \log_{10} M_{Y,X} < 1.1 ; \\ \oplus \log_{10} M_X > 1.1 ; \log_{10} M_Y > 1.1 ; \Delta\eta > 3)$$

[CMS FSQ-12-005](#)

[Phys. Rev. D 92 \(2015\) 012003](#)



# Diffractive cross sections



$$\sigma^{\text{SD}} (\xi < 0.05) = 8.84 \pm 0.08 \text{ (stat.) } {}^{+1.49}_{-1.38} \text{ (syst.) } {}^{+1.17}_{-0.37} \text{ (extrap.) mb}$$

$$\sigma^{\text{DD}} (\Delta\eta > 3) = 5.17 \pm 0.08 \text{ (stat.) } {}^{+0.55}_{-0.57} \text{ (syst.) } {}^{+1.62}_{-0.51} \text{ (extrap.) mb}$$

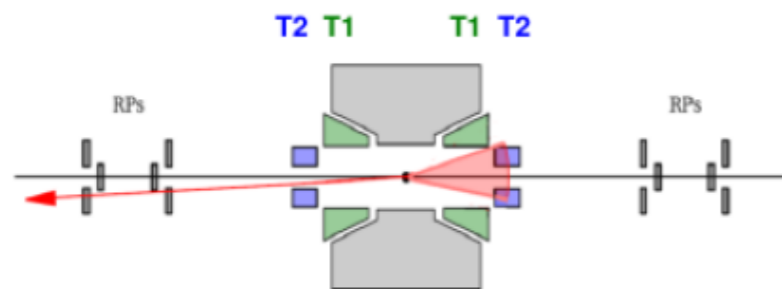
Extrapolated cross sections

[CMS FSQ-12-005](#)

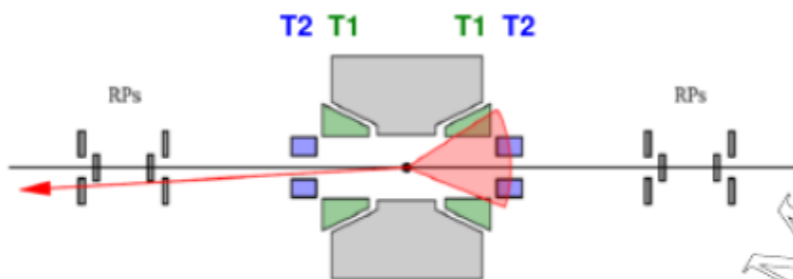
[Phys. Rev. D 92 \(2015\) 012003](#)

# Diffractive cross sections (TOTEM)

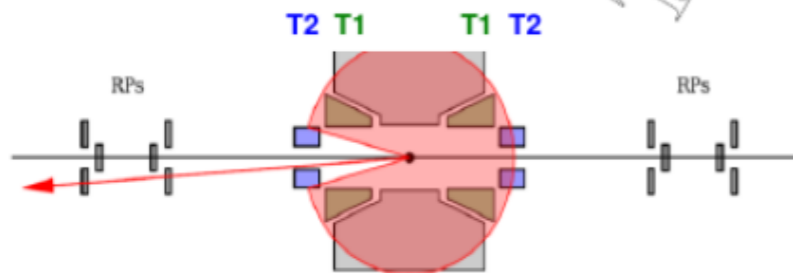
**Low mass**  
 $M_{\text{diff}} = 3.4 - 8 \text{ GeV}$



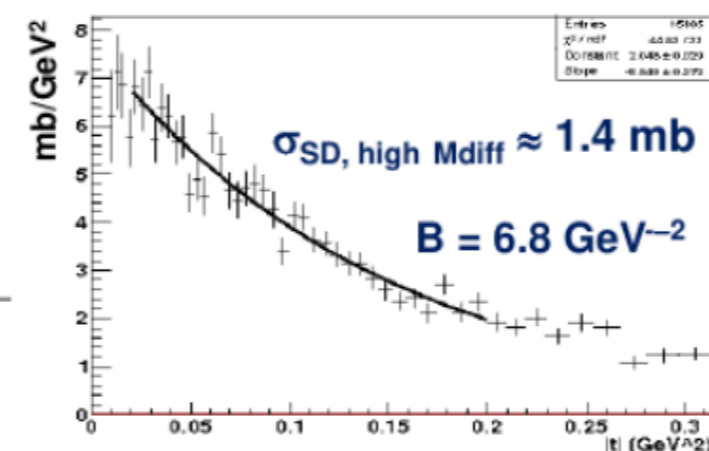
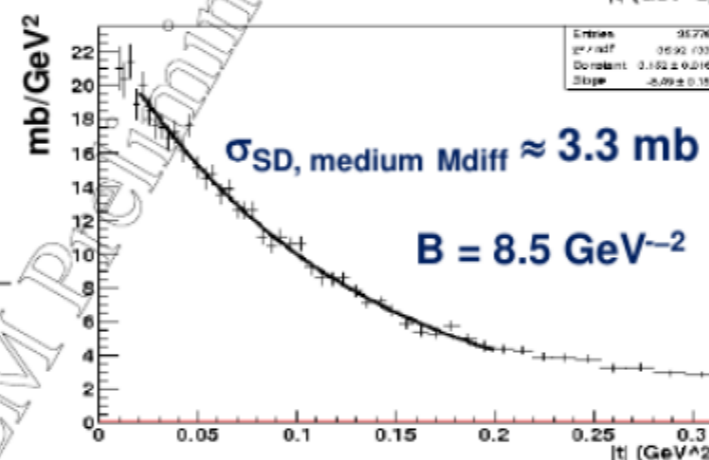
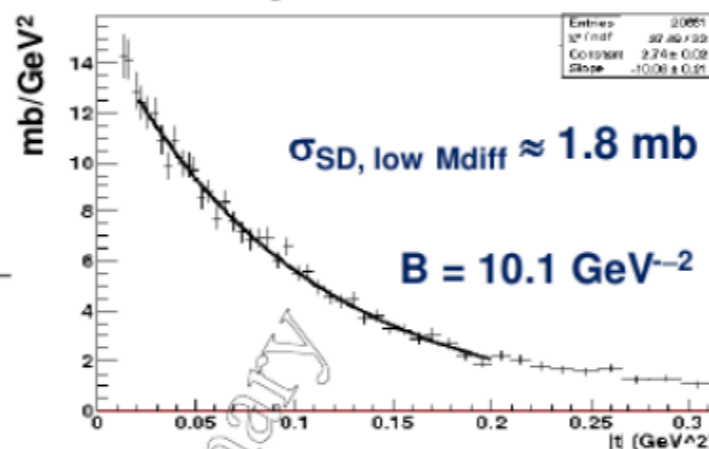
**Medium mass**  
 $M_{\text{diff}} = 8 - 350 \text{ GeV}$



**High mass**  
 $M_{\text{diff}} = 0.35 - 1.1 \text{ TeV}$



$$d\sigma/dt \sim A \cdot e^{-Bt}$$

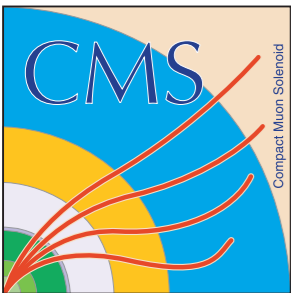


$$\sigma^{\text{SD}} = 6.5 \pm 1.3 \text{ mb}$$

$(3.4 \text{ GeV} < M_{\text{diff}} < 1.1 \text{ TeV})$

TOTEM Preliminary

Material taken from N. Minafra - Low-x 2016



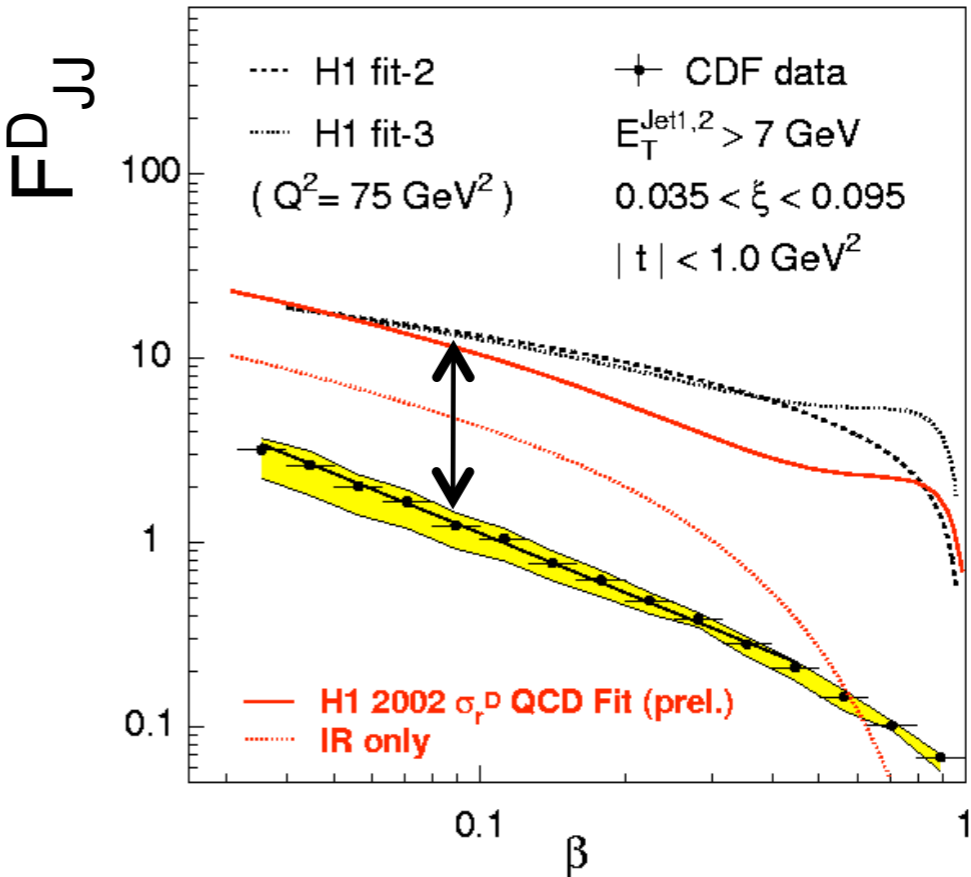
# Probing hard diffraction

Diffractive events where a hard scale is present: high- $p_T$  jets, W/Z's, ...

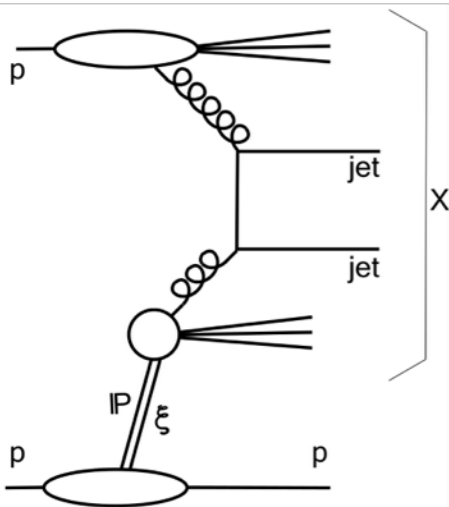
HERA/Tevatron: Breaking of QCD factorization in hadron-hadron collisions.

Smaller cross sections than expected based on diffractive PDFs (dPDFs) convolved with partonic cross sections.

Soft interactions between spectator partons from incoming protons quantified by “rapidity gap survival probability” ( $\langle S^2 \rangle$ ), roughly independent of the hard process.



CDF Collaboration,  
Phys. Rev. Lett. 84, 5043 (2000)



$$\xi = \frac{M_X^2}{s}$$

$$\frac{d^2\sigma}{d\xi dt} = \sum \int dx_1 dx_2 \left[ f(\xi, t) f_{IP}(x_1, \mu) \right] \left[ f_p(x_2, \mu) \right] \hat{\sigma}$$

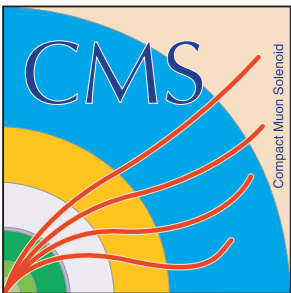
dPDF parameterisation:  
Pomeron (and Reggeon) flux  $\otimes$  pdf

Partonic cross section

proton PDF

$$f(\xi, t) = \frac{e^{Bt}}{\xi^{2\alpha_{IP}(t)-1}}$$

Implemented in “hard-diffractive” MC’s, e.g. POMPYT, POMWIG, FPMC; also PYTHIA8, HERWIG++ etc.



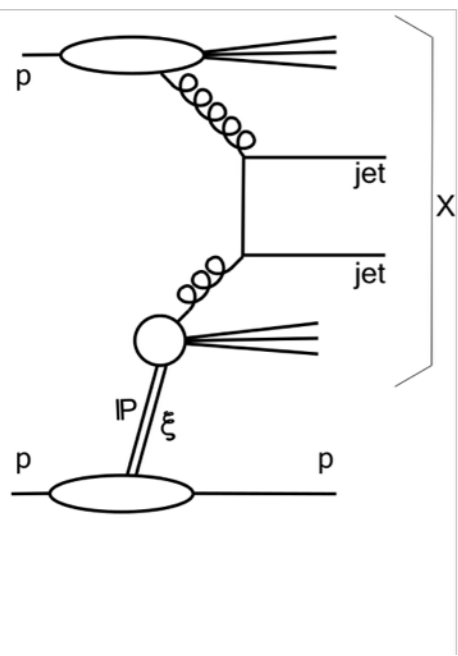
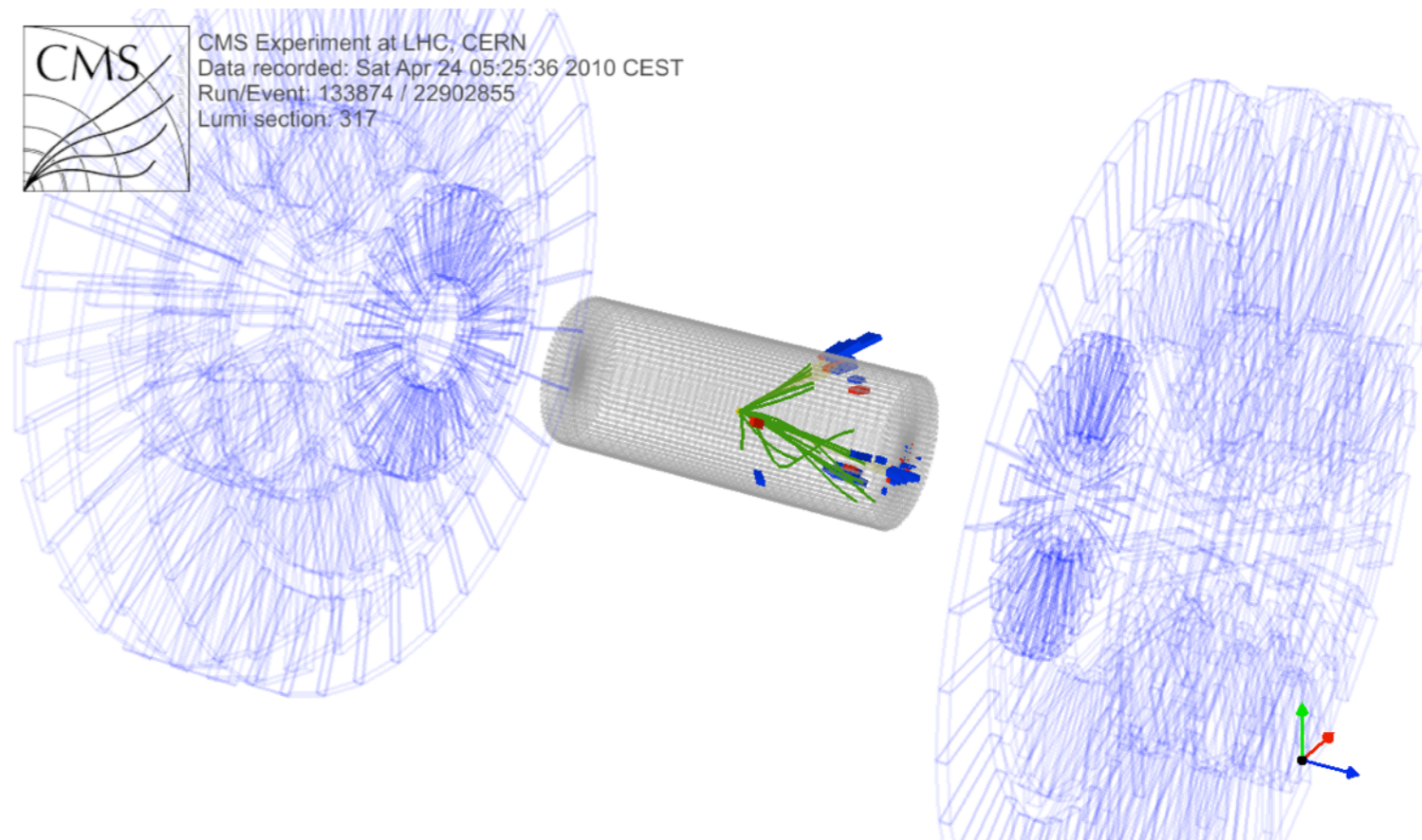
# Probing hard diffraction

Diffractive events where a hard scale is present: high- $p_T$  jets, W/Z's, ...

HERA/Tevatron: Breaking of QCD factorization in hadron-hadron collisions.

Smaller cross sections than expected based on diffractive PDFs (dPDFs) convolved with partonic cross sections.

Soft interactions between spectator partons from incoming protons quantified by “rapidity gap survival probability” ( $\langle S^2 \rangle$ ), roughly independent of the hard process.



$$\xi = \frac{M_X^2}{s}$$

$$\frac{d^2\sigma}{d\xi dt} = \sum \int dx_1 dx_2 \left[ f(\xi, t) f_{IP}(x_1, \mu) \right] \left[ f_p(x_2, \mu) \right] \left[ \hat{\sigma} \right]$$

$f(\xi, t) = \frac{e^{Bt}}{\xi^{2\alpha_{IP}(t)-1}}$

dPDF parameterisation:  
Pomeron (and Reggeon) flux  $\otimes$  pdf

Partonic cross section

proton PDF

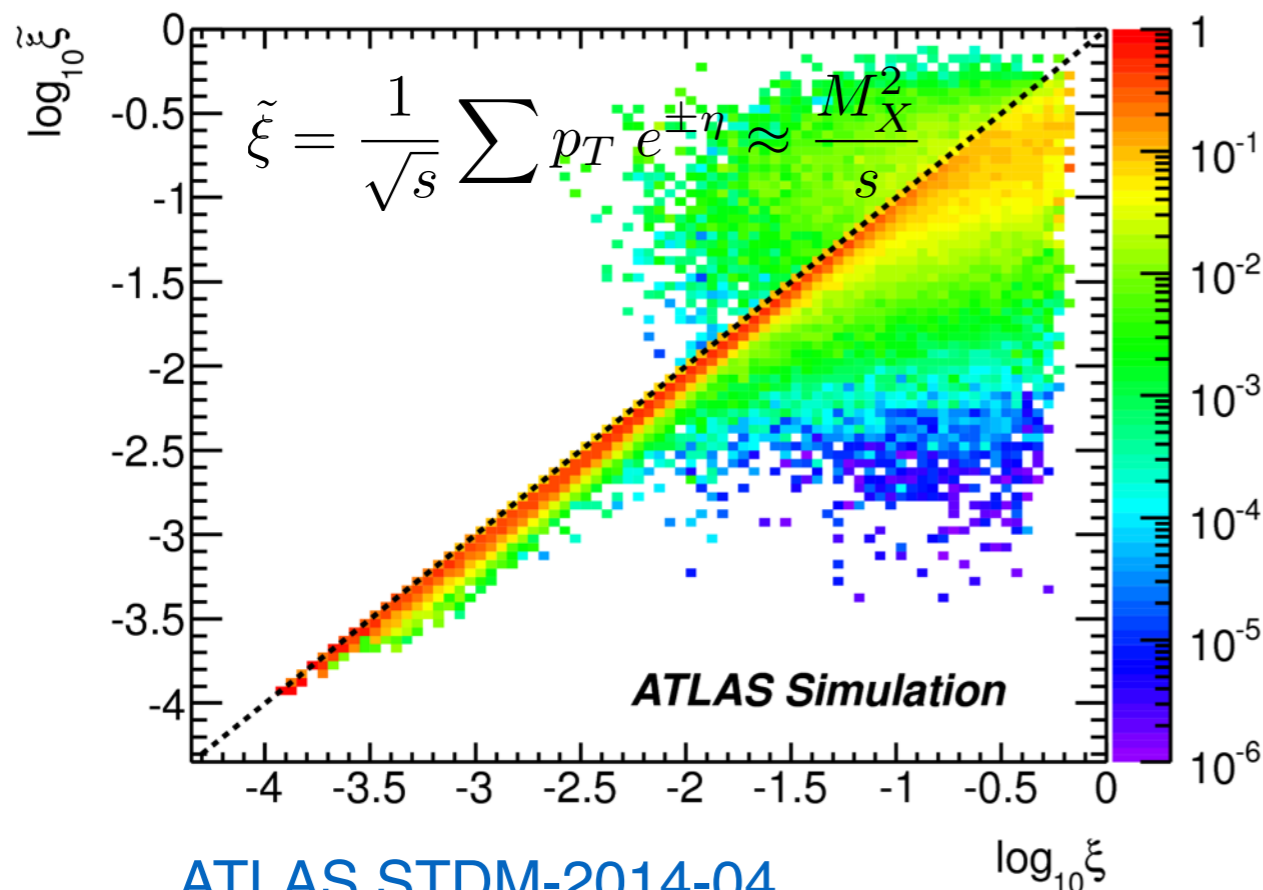
Implemented in “hard-diffractive” MC’s, e.g. POMPYT, POMWIG, FPMC; also PYTHIA8, HERWIG++ etc.

# Evidence of hard diffraction

Diffractive component is enhanced with respect to the non-diffractive (ND) in the low- $\xi$  and high  $\Delta\eta^F$  (size of forward gap) region.

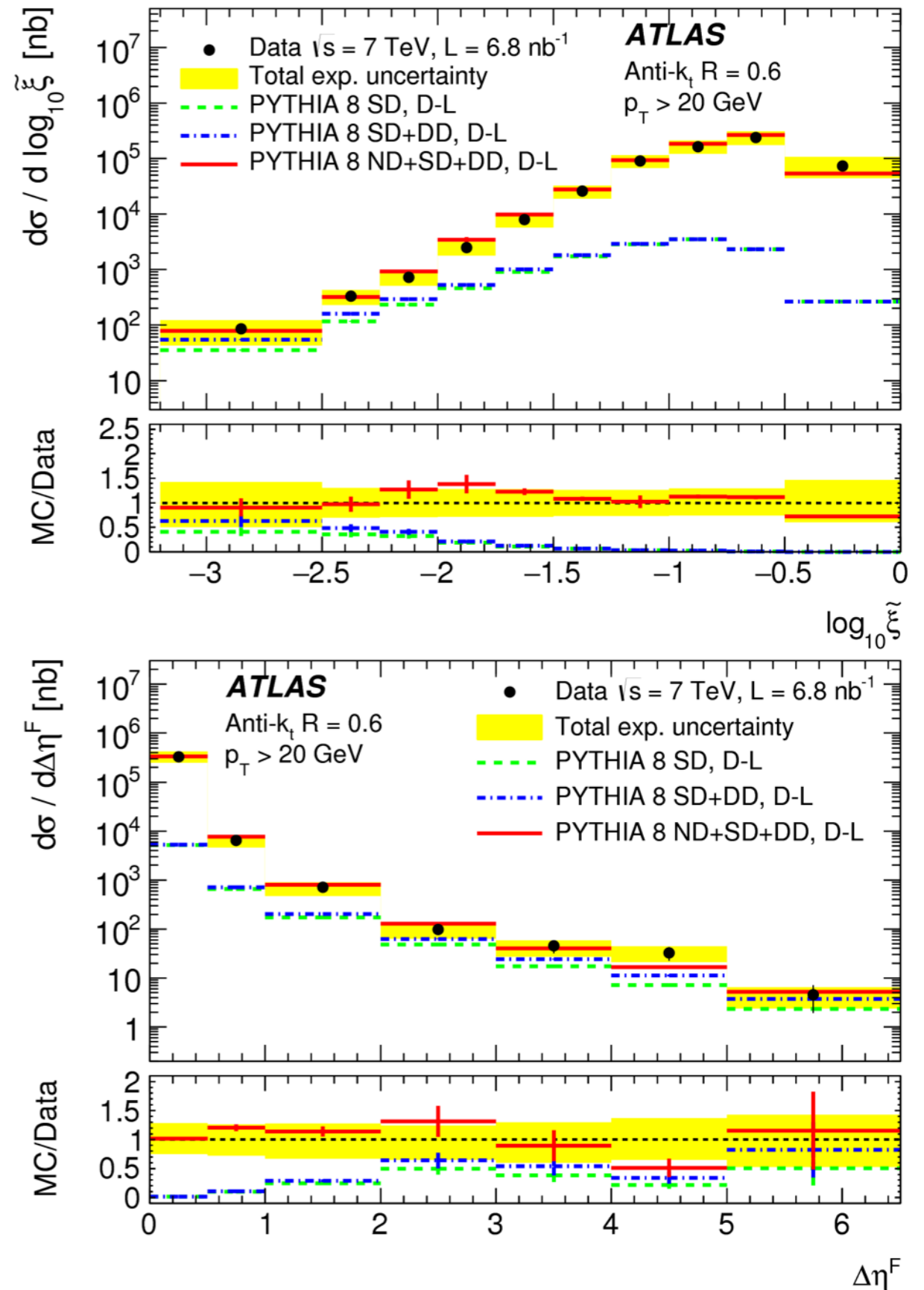
Information from central ATLAS apparatus (sum over all particles in event).

High ND contribution in diffractive kinematic region.

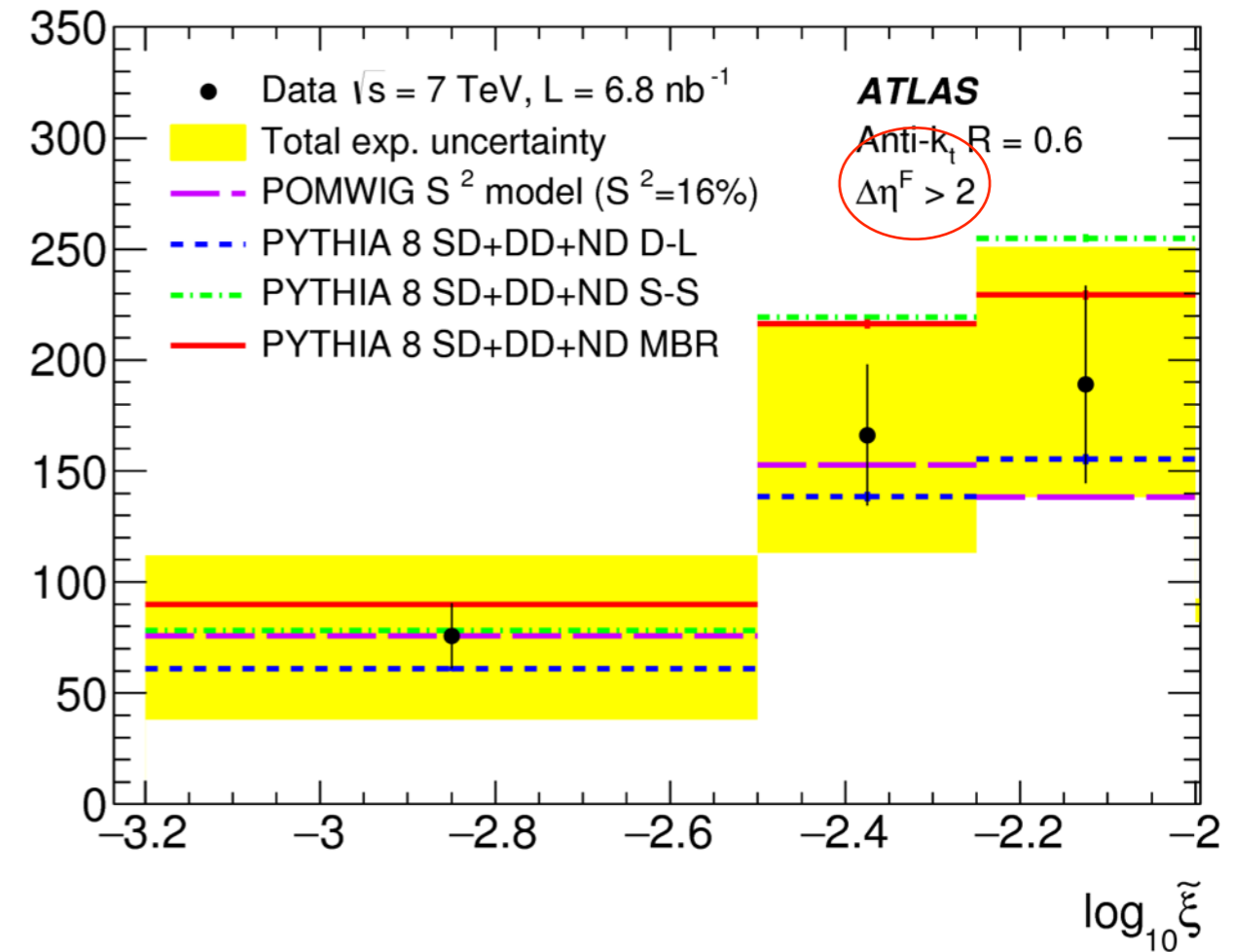
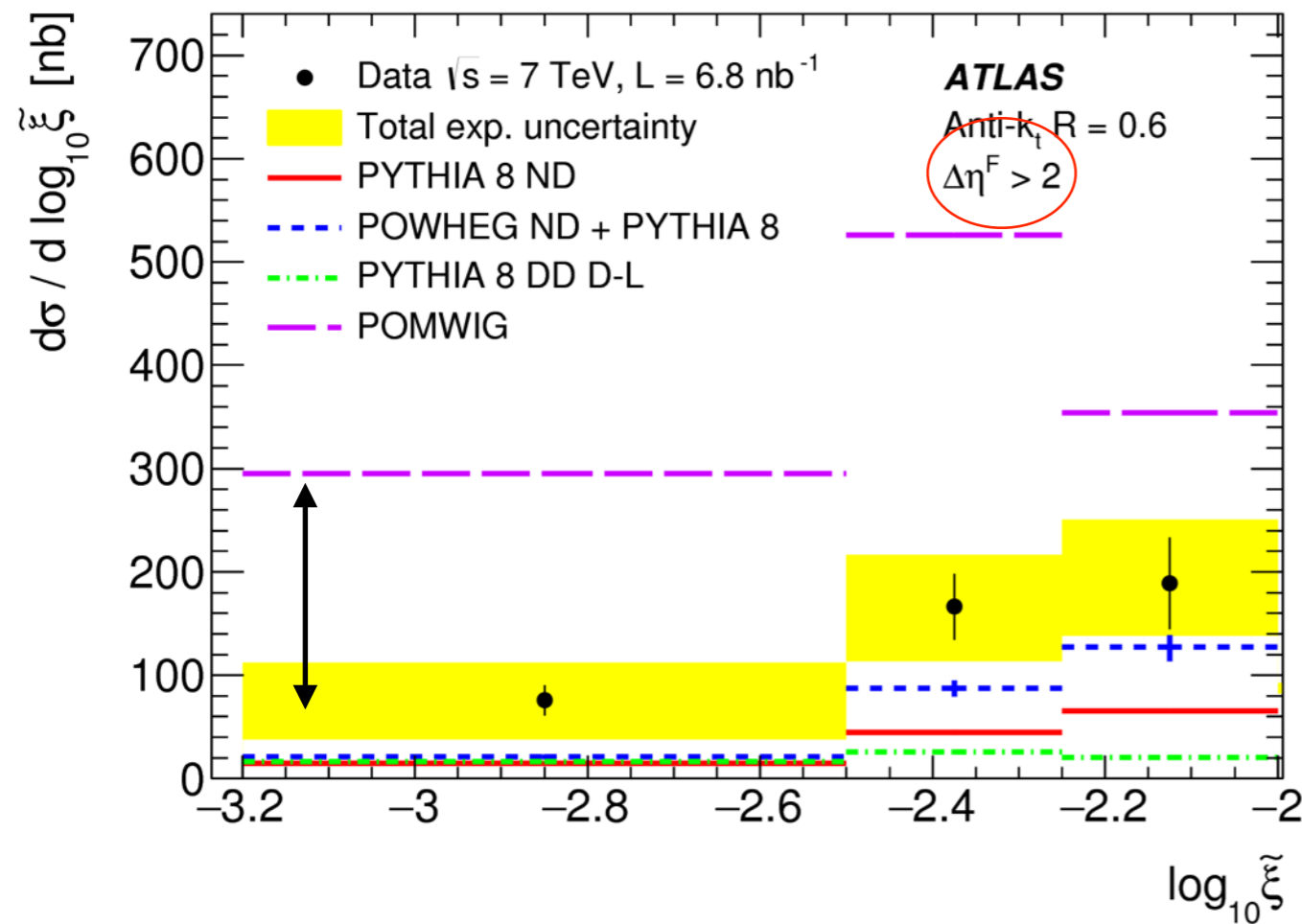


[ATLAS STDM-2014-04](#)

[doi:10.1016/j.physletb.2016.01.028](https://doi.org/10.1016/j.physletb.2016.01.028)



# Evidence of hard diffraction

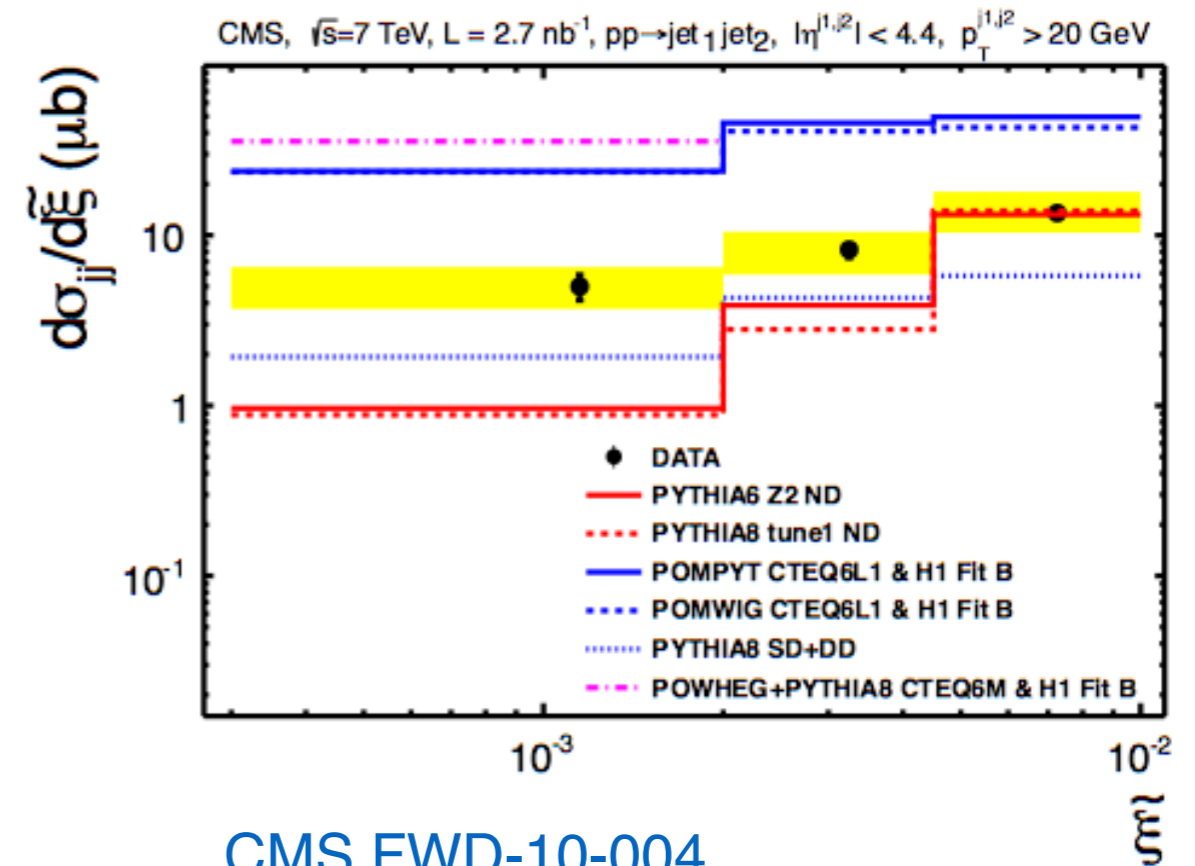
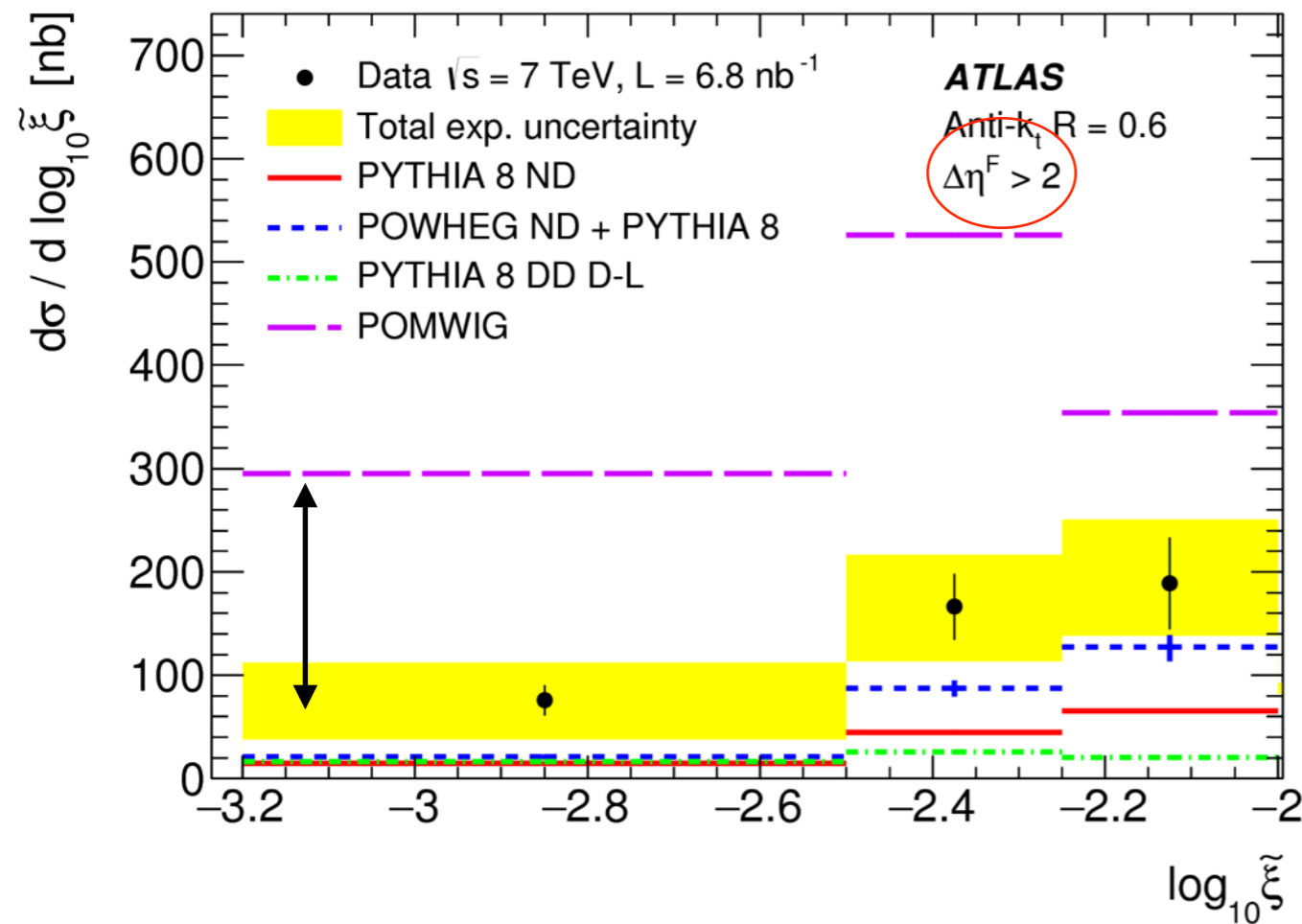


Requiring forward gap ( $\Delta\eta^F > 2$ ), excess is seen at low  $\xi$ .

MC-based extraction of gap survival probability.

$$S^2 = 0.16 \pm 0.04 \text{ (stat.)} \pm 0.08 \text{ (syst.)}$$

# Evidence of hard diffraction



[CMS FWD-10-004](#)

[Phys. Rev. D 87 \(2013\) 012006](#)

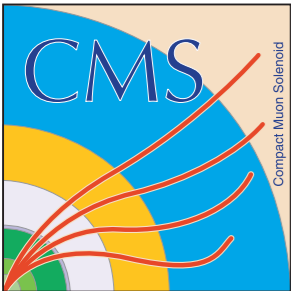
Requiring forward gap ( $\Delta\eta^F > 2$ ), excess is seen at low  $\xi$ .

MC-based extraction of gap survival probability.

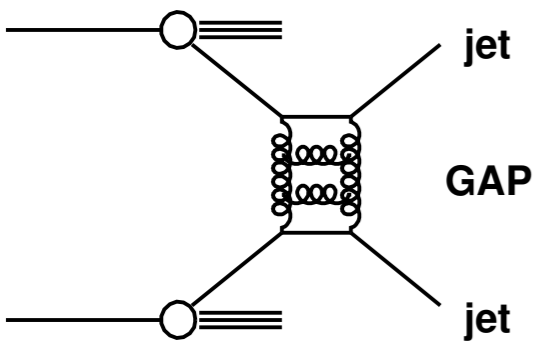
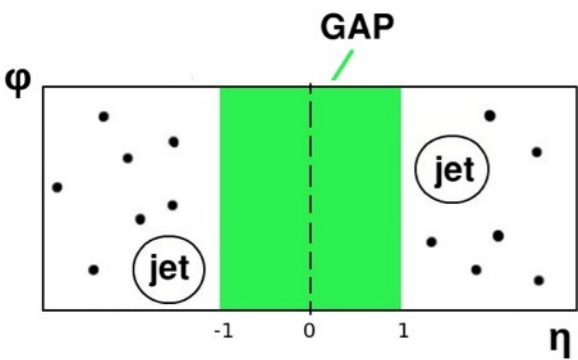
$$S^2 = 0.16 \pm 0.04 \text{ (stat.)} \pm 0.08 \text{ (syst.)}$$

$$S^2_{\text{data/MC}} = 0.12 \pm 0.05 \text{ (LO MC)}$$

$$S^2_{\text{data/MC}} = 0.08 \pm 0.04 \text{ (NLO MC)}$$



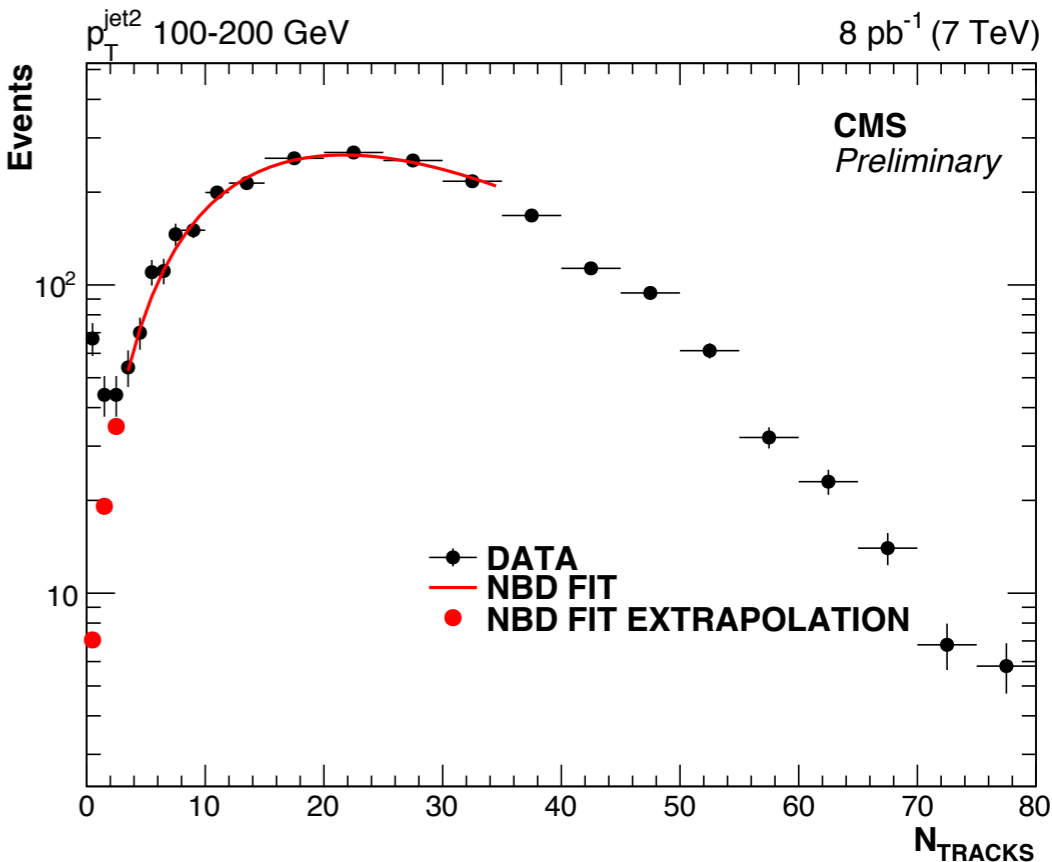
# Production of jets separated by a large rapidity gap



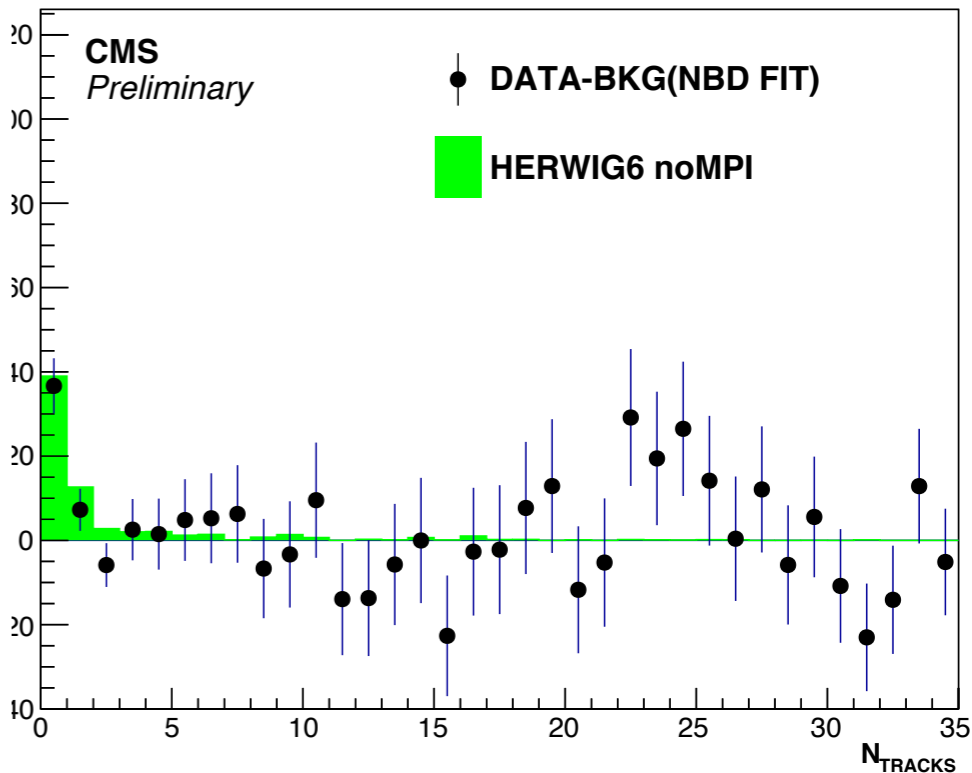
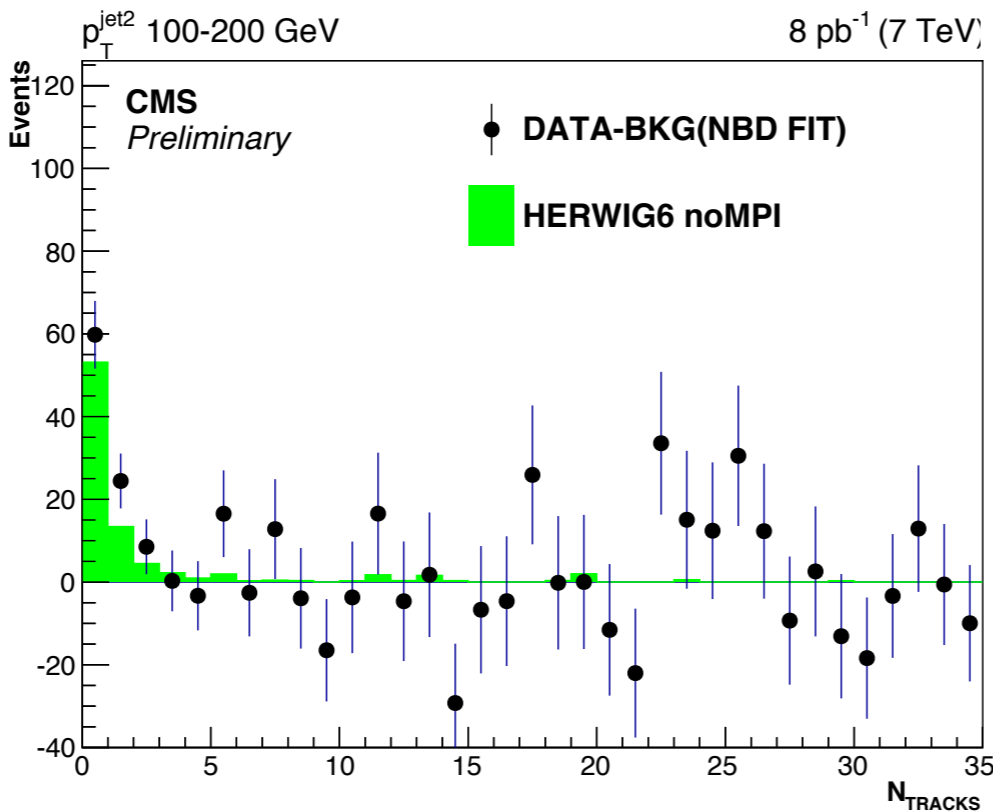
Events with two jets separated by a large rapidity gap.

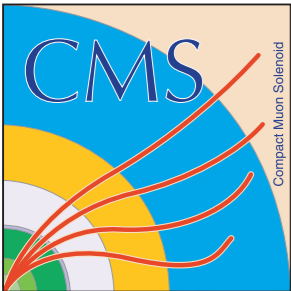
Color-singlet exchange; sensitive to BFKL dynamics and rapidity gap survival probability.

HERWIG6: hard color-singlet exchange (LL Mueller-Tang model) + UE.

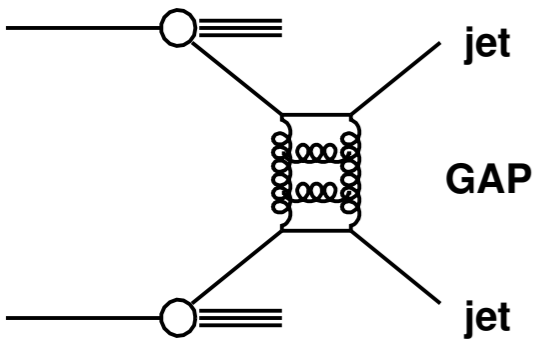
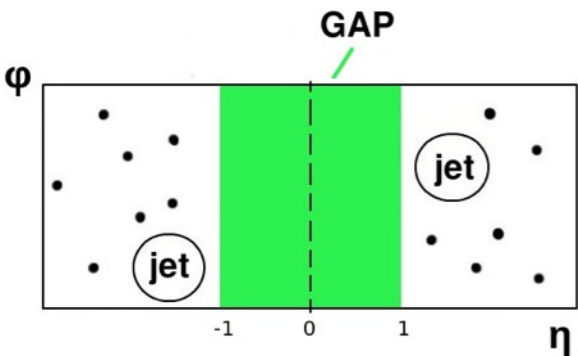


CMS FSQ-12-001





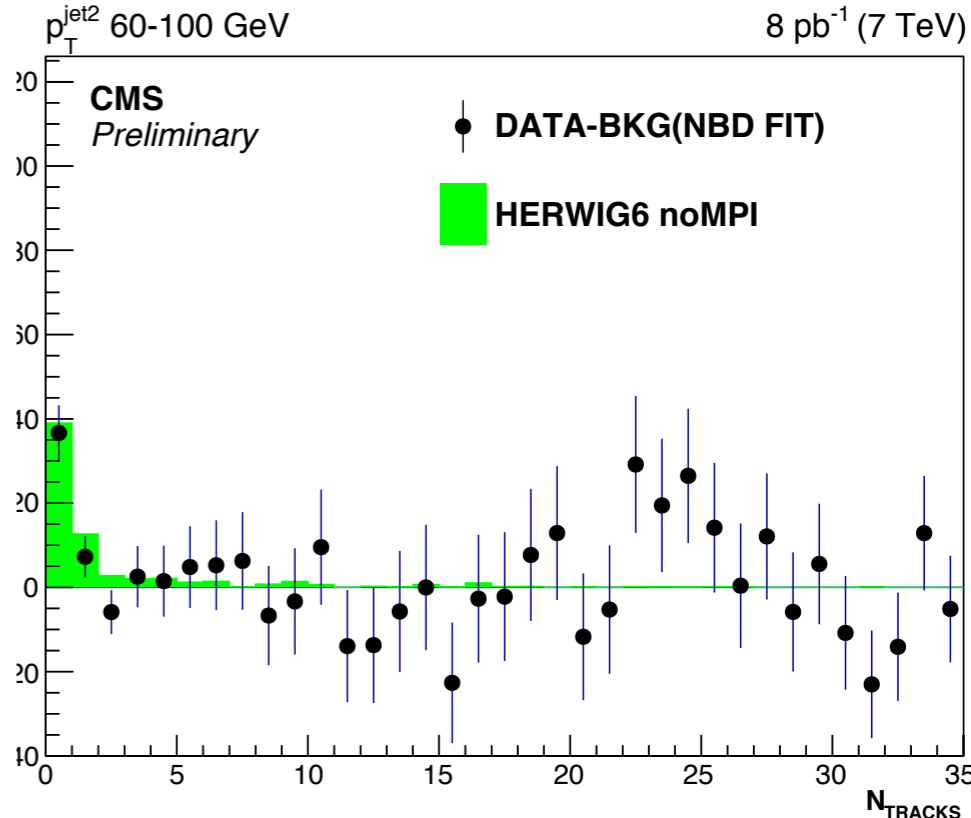
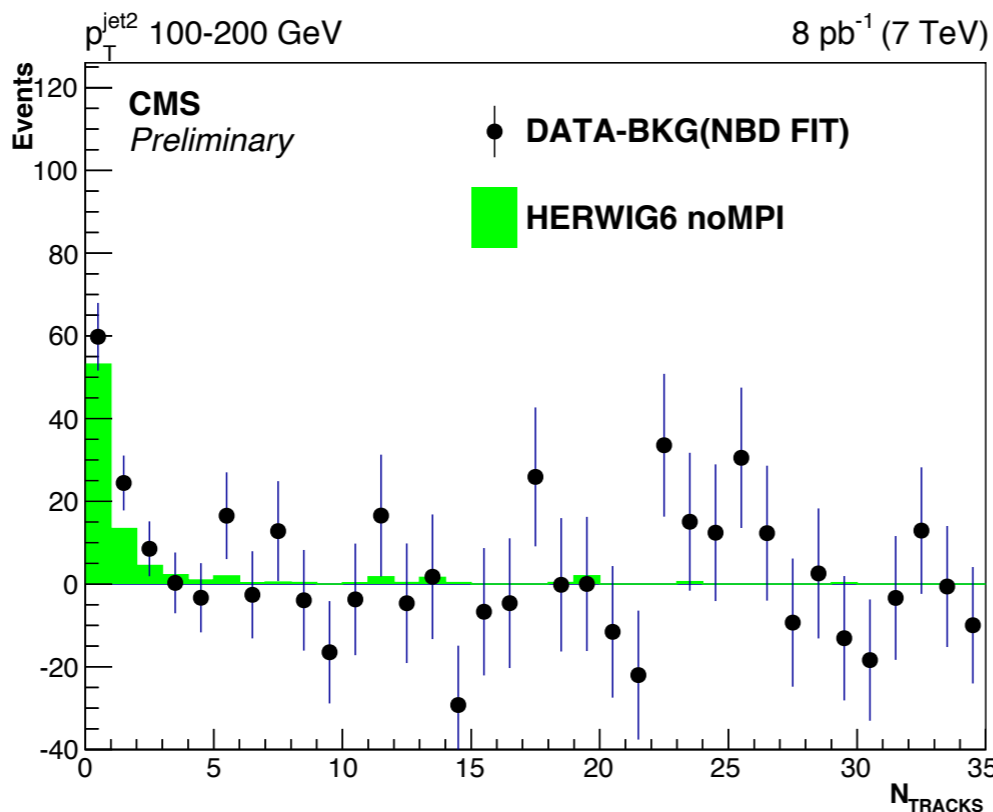
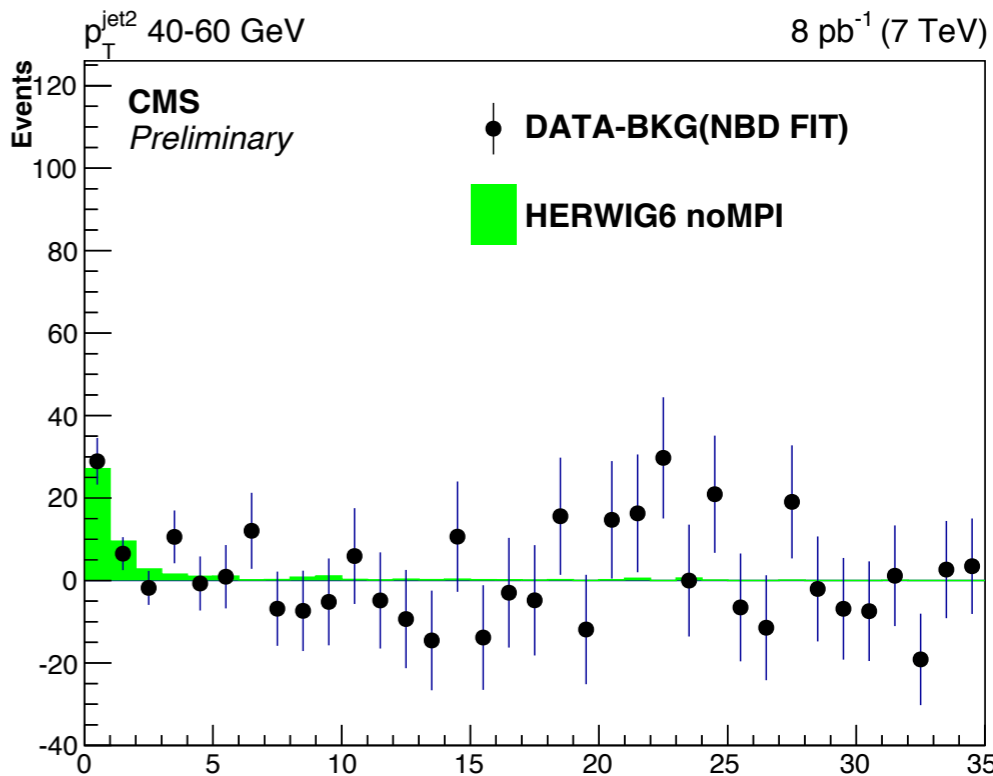
# Production of jets separated by a large rapidity gap



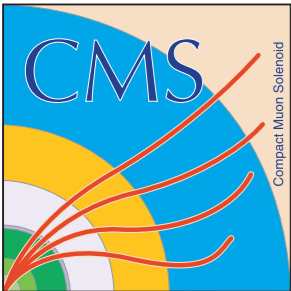
Events with two jets separated by a large rapidity gap.

Color-singlet exchange; sensitive to BFKL dynamics and rapidity gap survival probability.

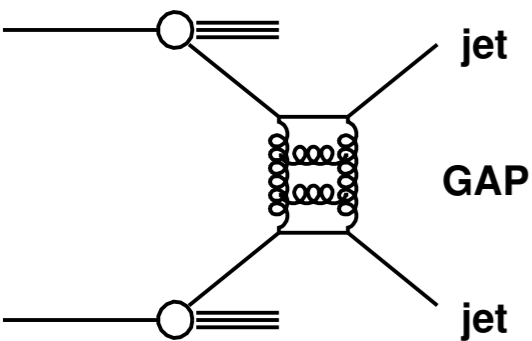
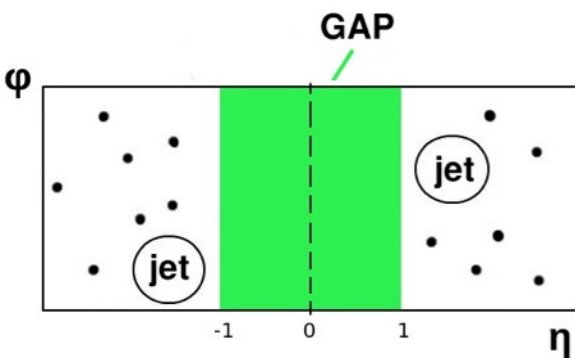
HERWIG6: hard color-singlet exchange (LL Mueller-Tang model) + UE.



CMS FSQ-12-001



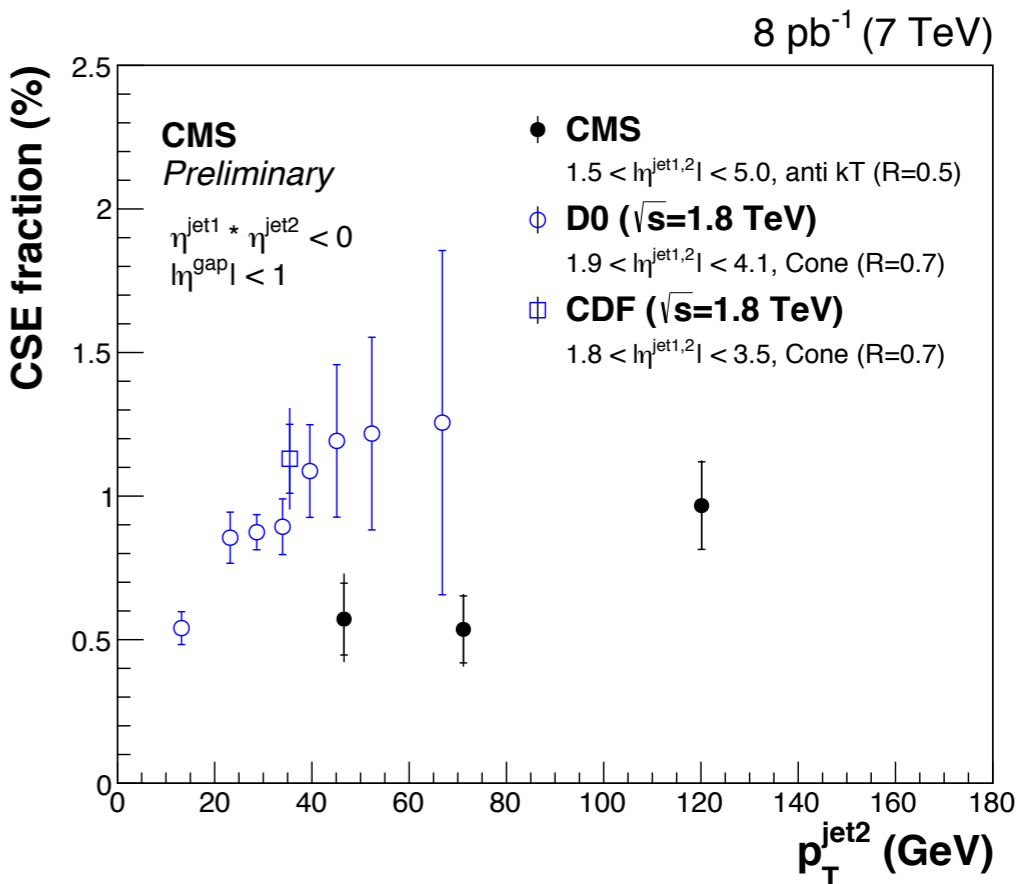
# Production of jets separated by a large rapidity gap



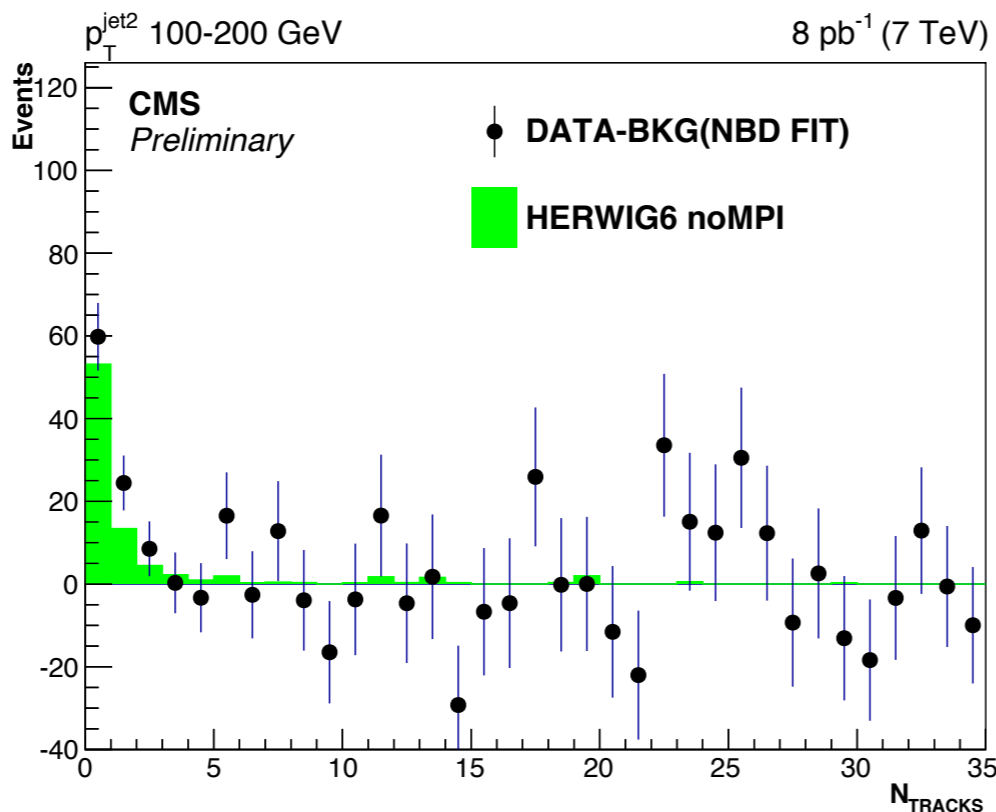
Events with two jets separated by a large rapidity gap.

Color-singlet exchange; sensitive to BFKL dynamics and rapidity gap survival probability.

HERWIG6: hard color-singlet exchange (LL Mueller-Tang model) + UE.



CMS FSQ-12-001



Extraction of color-singlet exchange fraction from first two bins of  $N_{\text{tracks}}$  distribution.

Three lower-energy jet  $p_T$  bins. Increase of fraction with jet  $p_T$ .

Decrease with center-of-mass energy (comparison to Tevatron results).

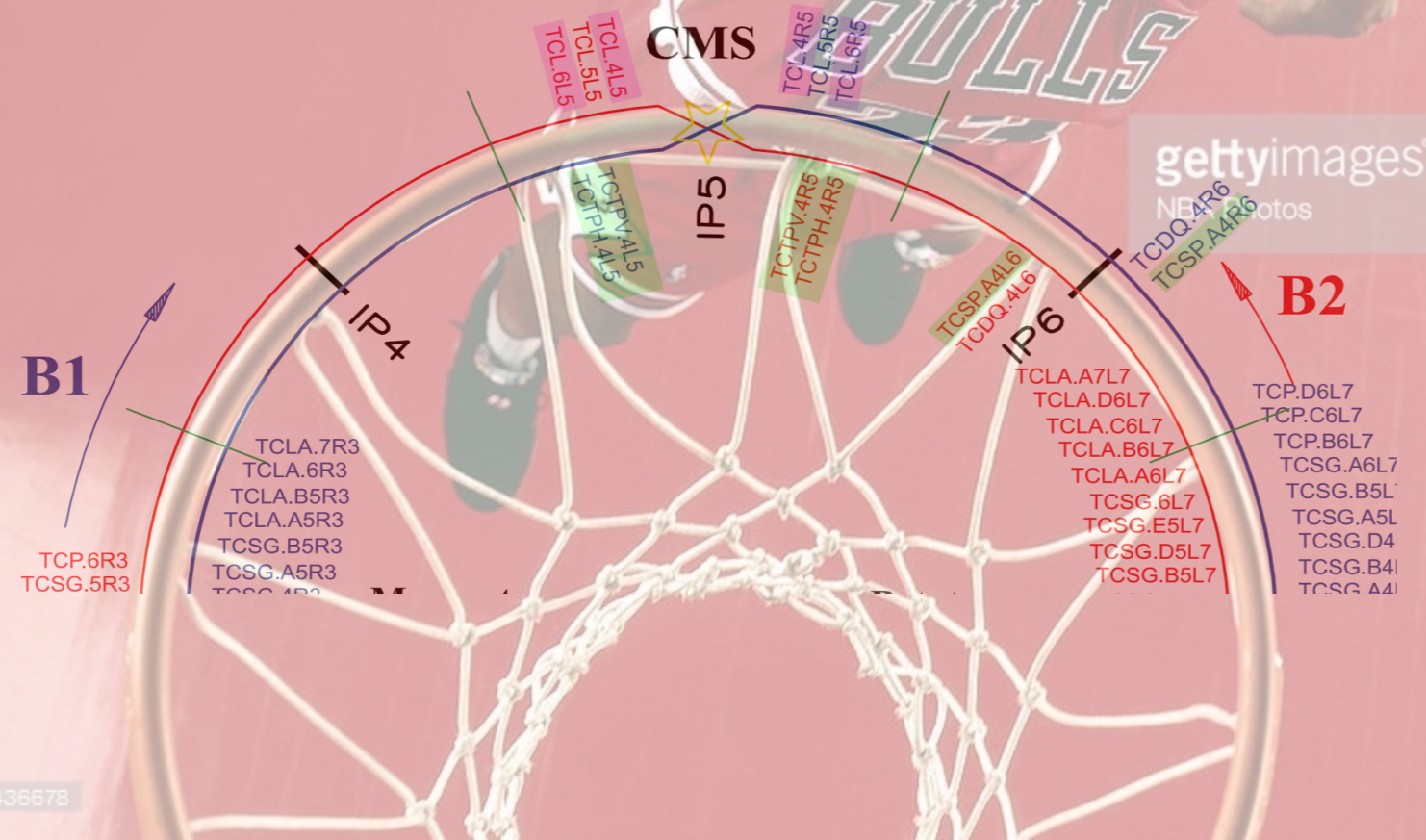
# Outline

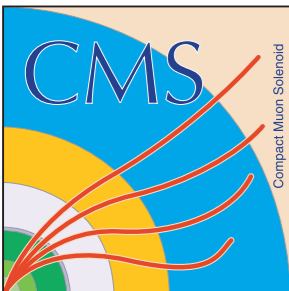
Total, inelastic & diffractive cross section measurements at the LHC

Hard diffraction

High- $\beta^*$ /Low pile-up running with proton tagging

CT-PPS and AFP: proton spectrometers at high-luminosity





# Outlook: CMS & TOTEM extended forward detectors

July 2012: ( $\beta^* = 90$  m, 8 TeV)

Common CMS-TOTEM data taking at low pile-up with around  $50 \text{ nb}^{-1}$  collected.

October 2015: ( $\beta^* = 90$  m, 13 TeV)

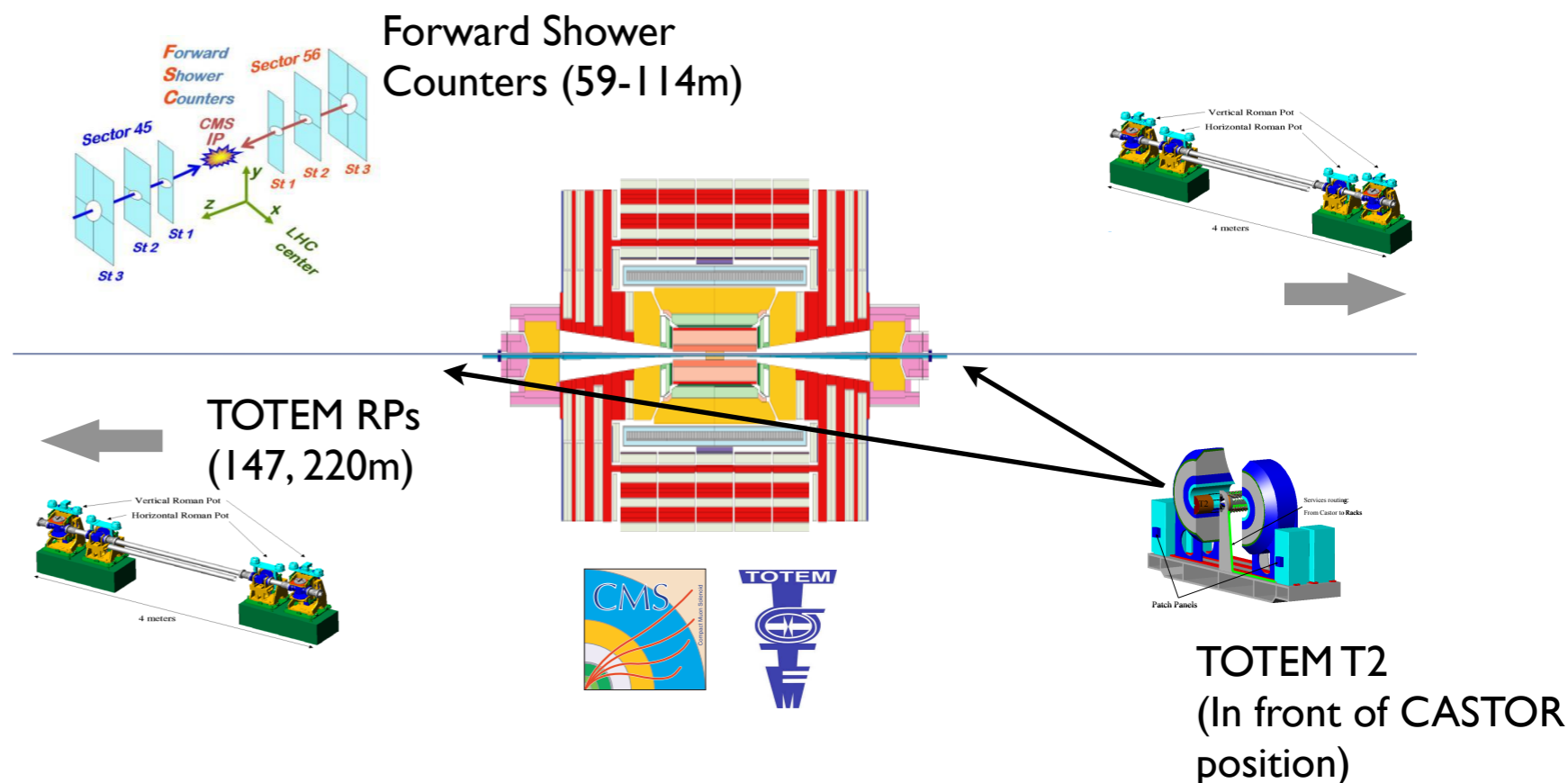
$\sim 400 \text{ nb}^{-1}$  recorded (CMS/TOTEM) from around  $700 \text{ nb}^{-1}$ .

$\langle N_{\text{Int}}/Bx \rangle$  less than  $\sim 0.10$ .

TOTEM Roman Pots (RPs) to detect protons scattered from diffractive processes.

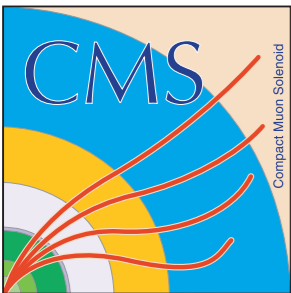
TOTEM T2 tracking stations at very forward angles

In 2012 Run also: Forward Shower Counters (FSC) covering  $|\eta| \sim 6-8$ .

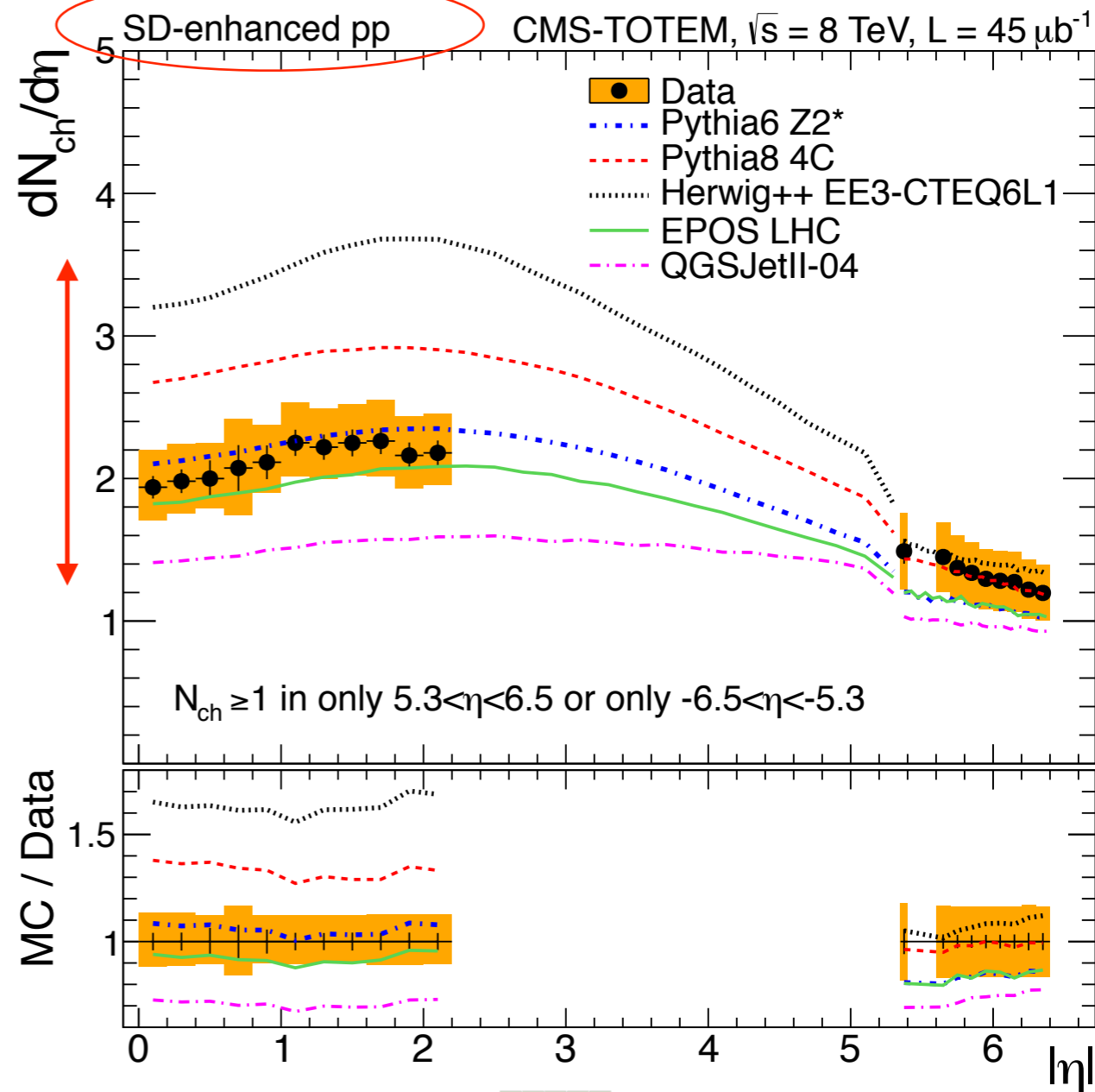
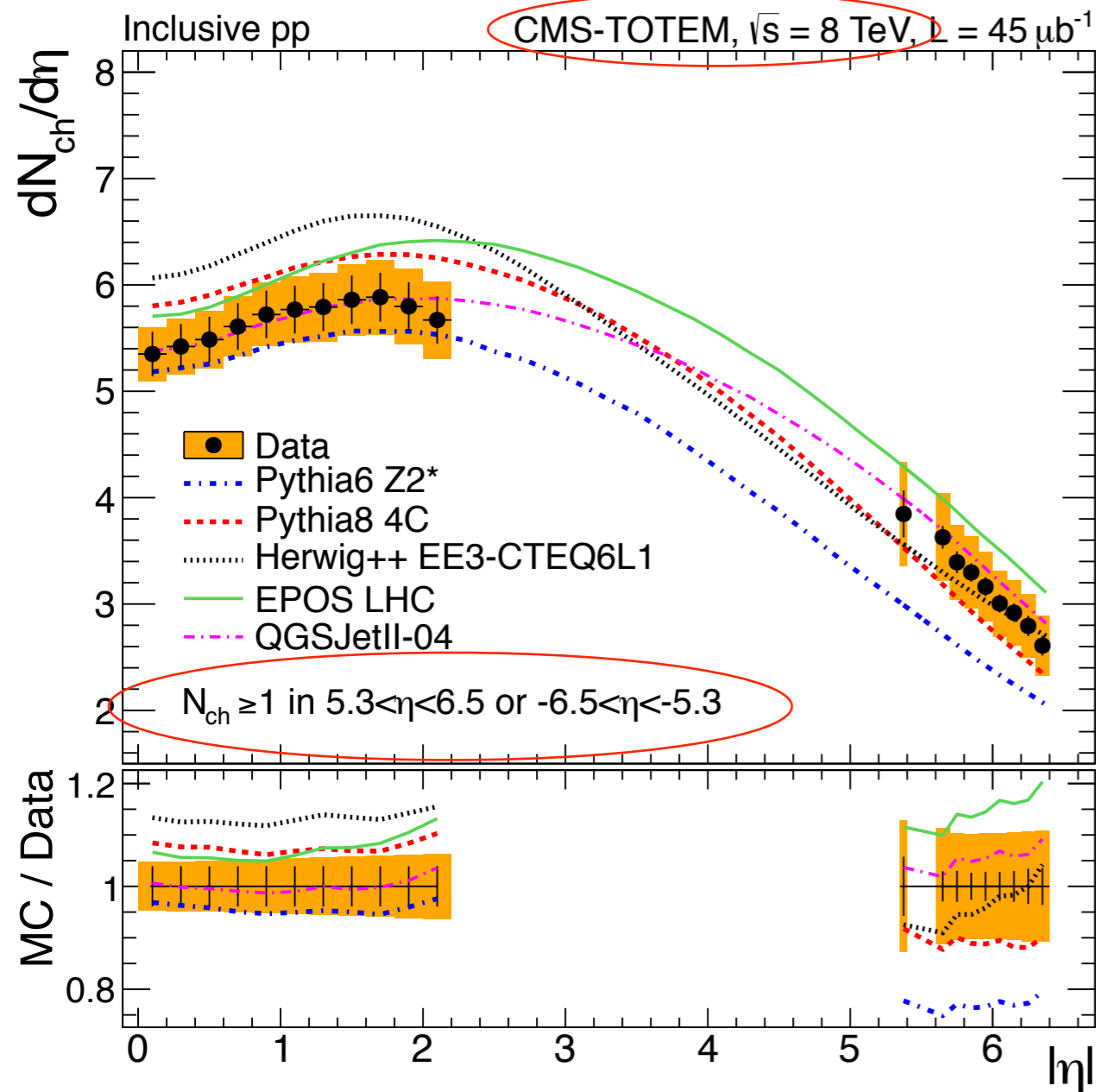


Forward proton spectrometer associated with complete central coverage

ATLAS (ALFA) operational during high- $\beta^*$  running.

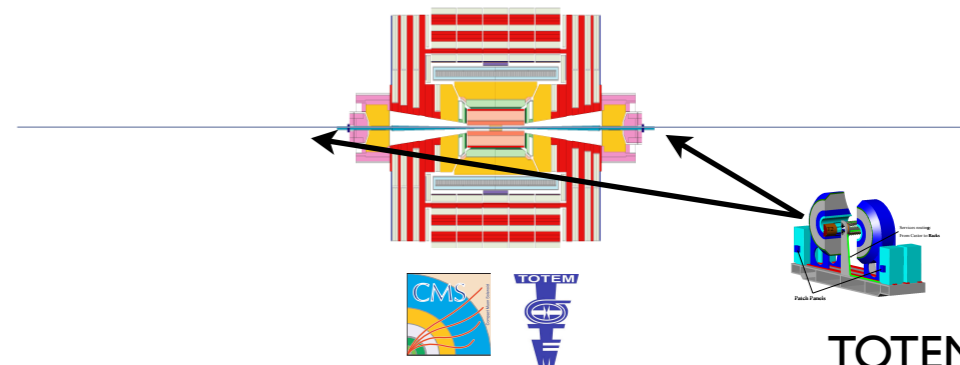


# $dN_{ch}/d\eta$ in central + forward regions

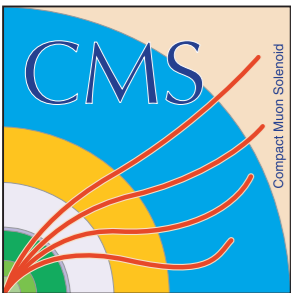


CMS FSQ-12-026

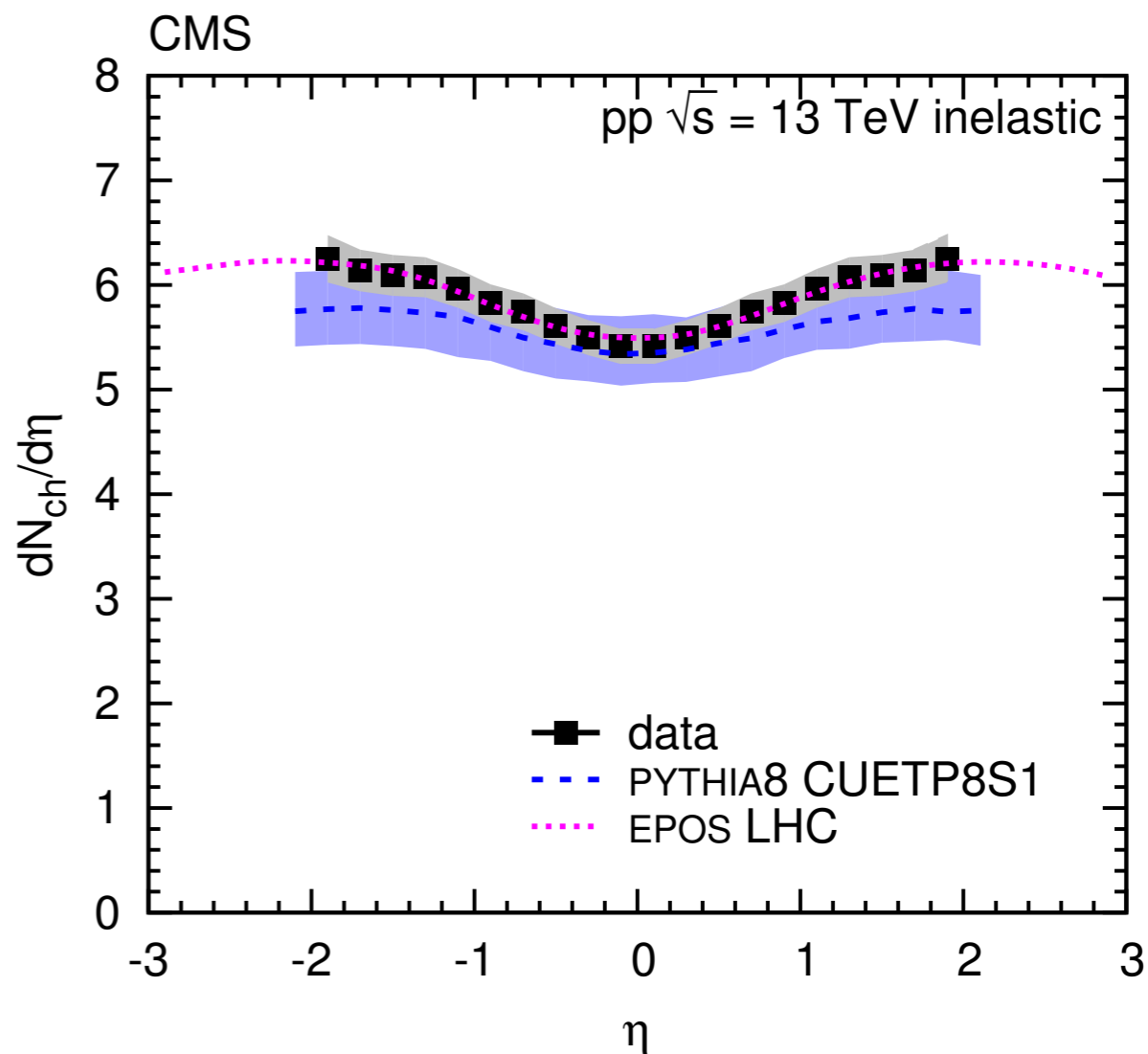
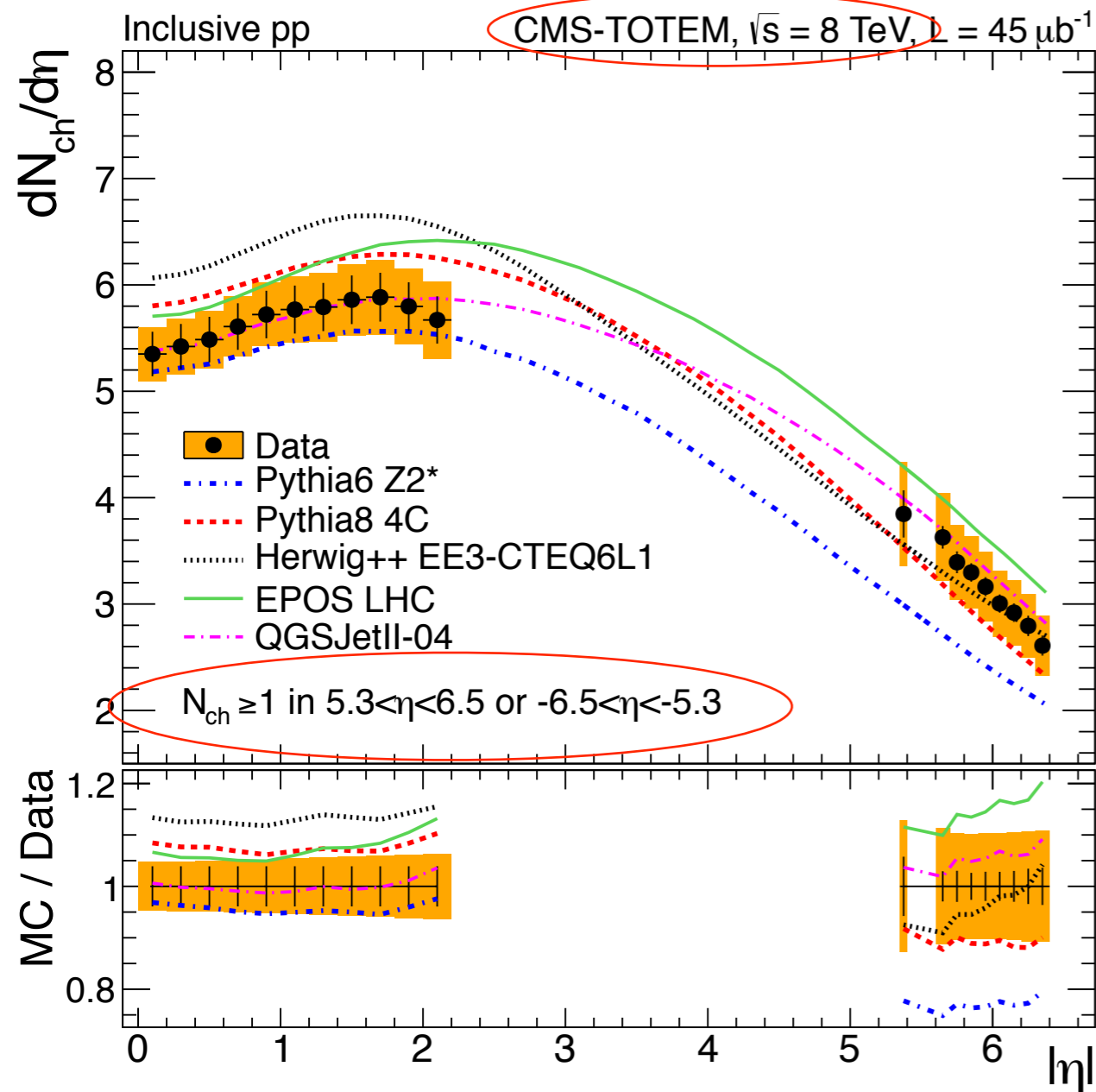
*Eur. Phys. J. C* 74 (2014) 3053



TOTEM T2



# $dN_{ch}/d\eta$ in central + forward regions

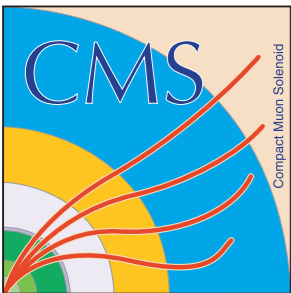


[CMS FSQ-15-001](#)

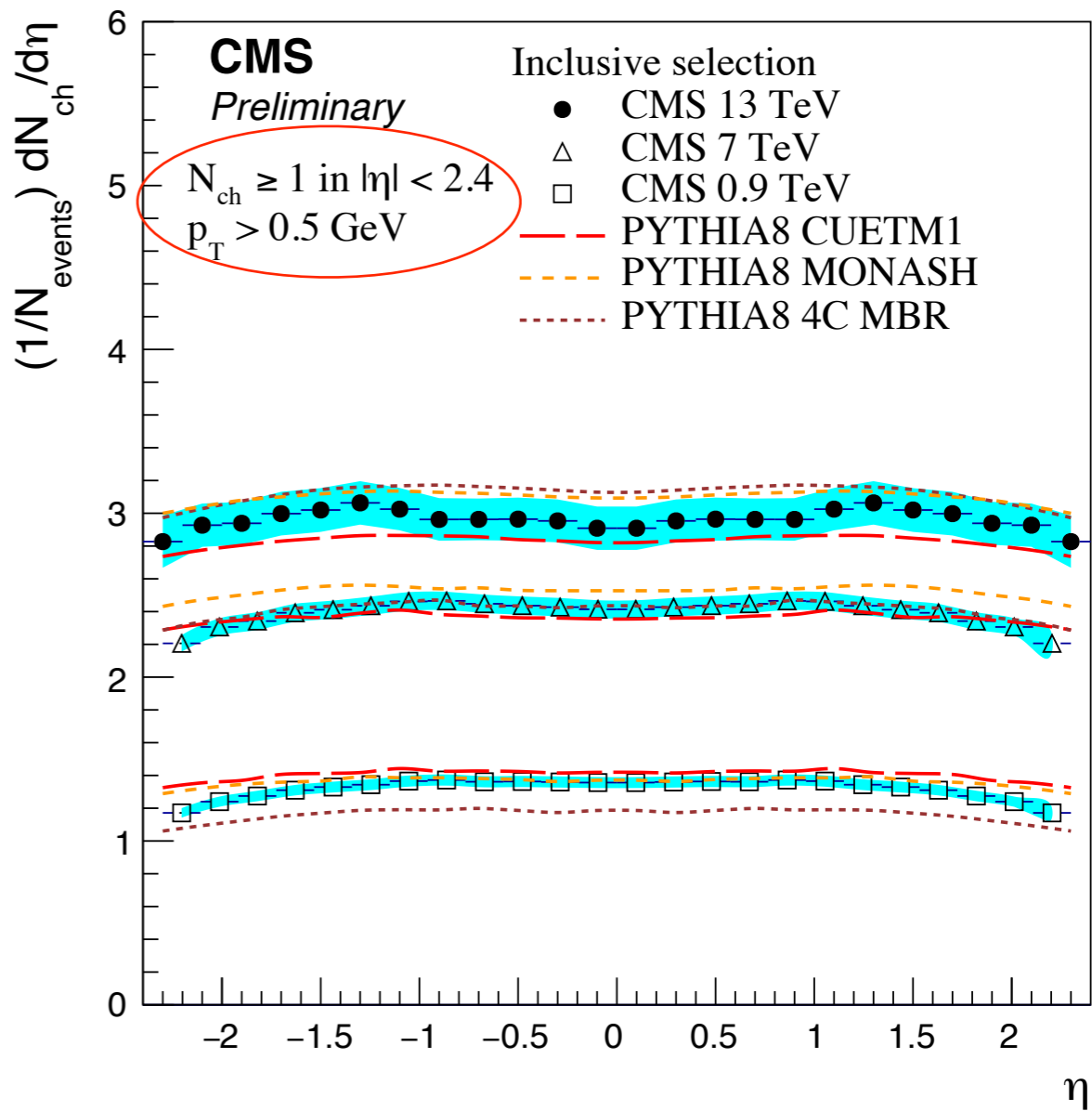
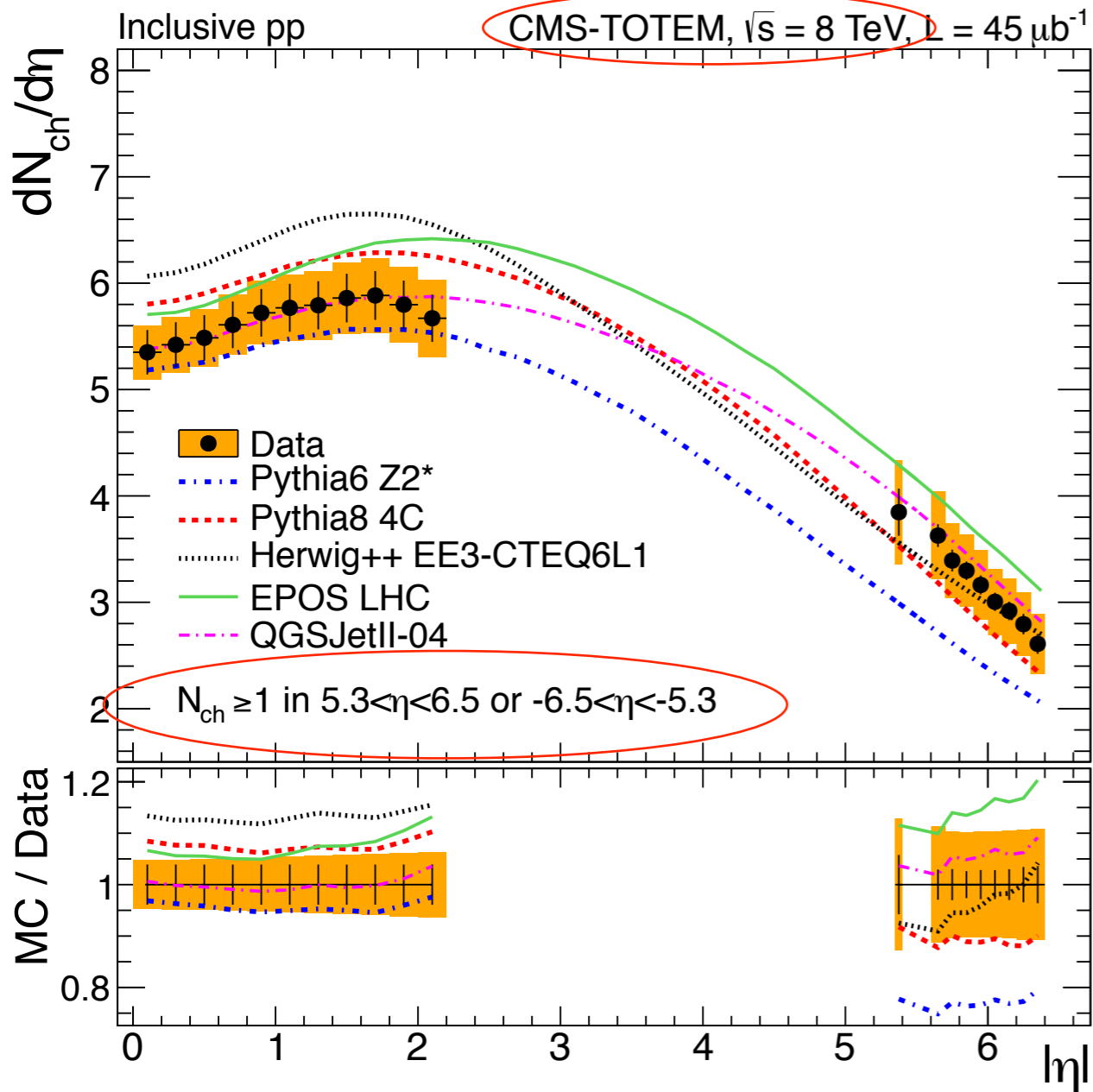
[Phys. Lett. B 751 \(2015\) 143](#)

[CMS FSQ-12-026](#)

[Eur. Phys. J. C 74 \(2014\) 3053](#)



# $dN_{ch}/d\eta$ in central + forward regions

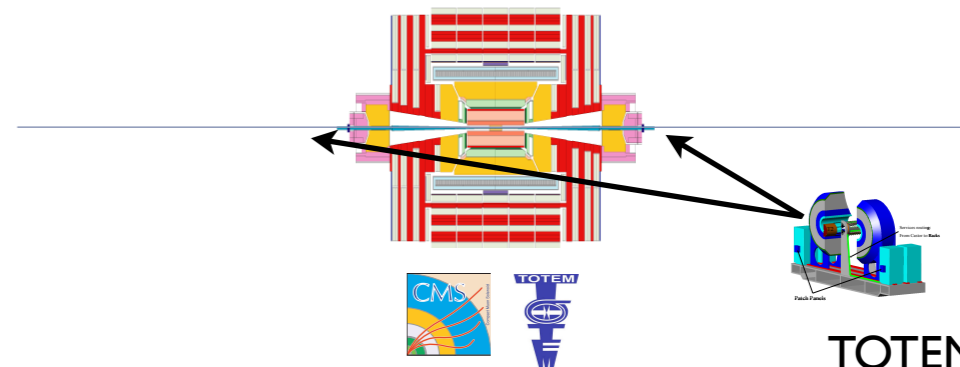
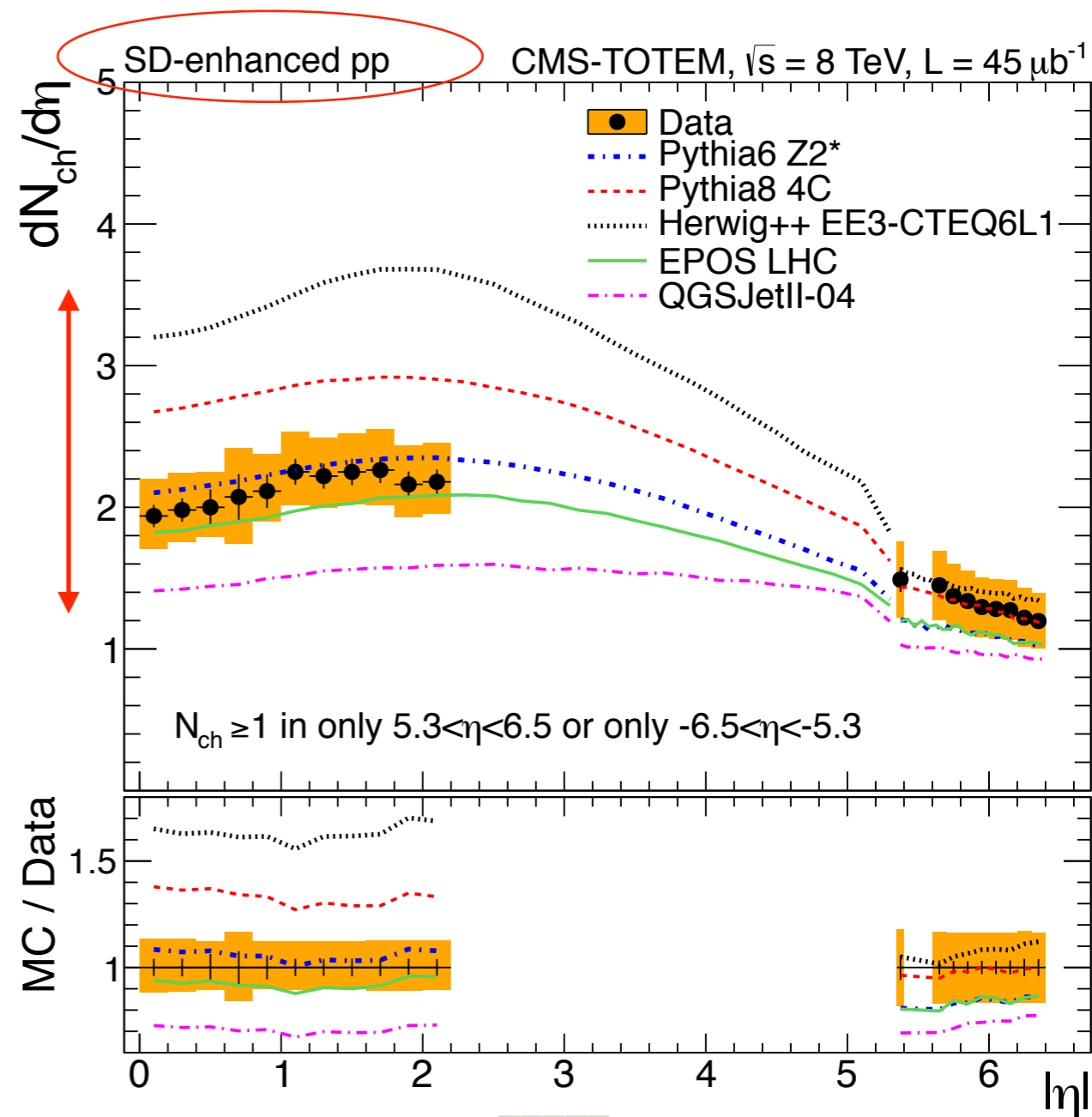
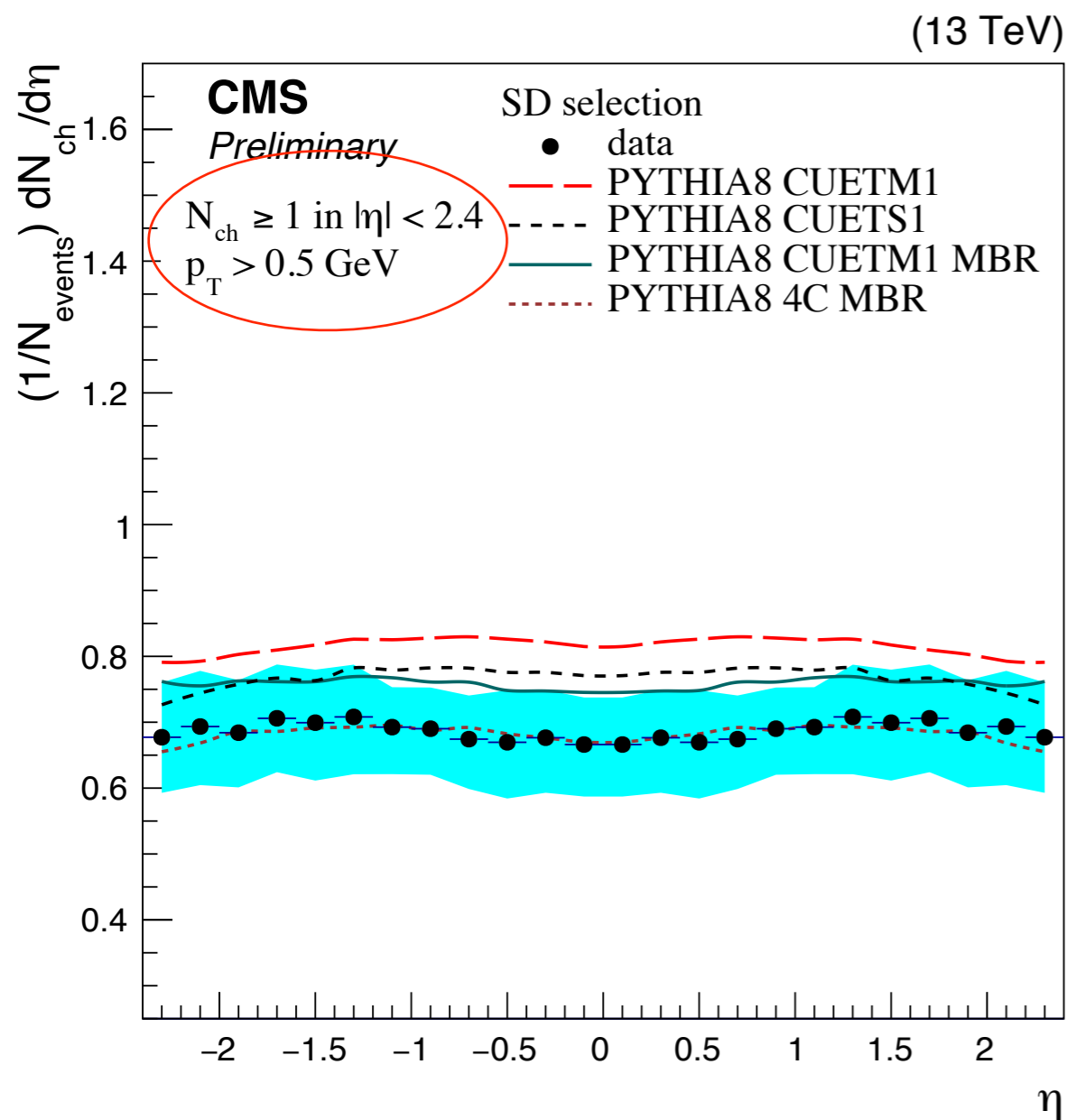


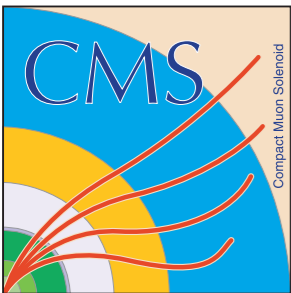
[CMS FSQ-12-026](#)

[Eur. Phys. J. C 74 \(2014\) 3053](#)

[CMS FSQ-15-008](#)

# $dN_{ch}/d\eta$ in central + forward regions





# Example: central dijet event candidate with two leading protons (2012 Run)

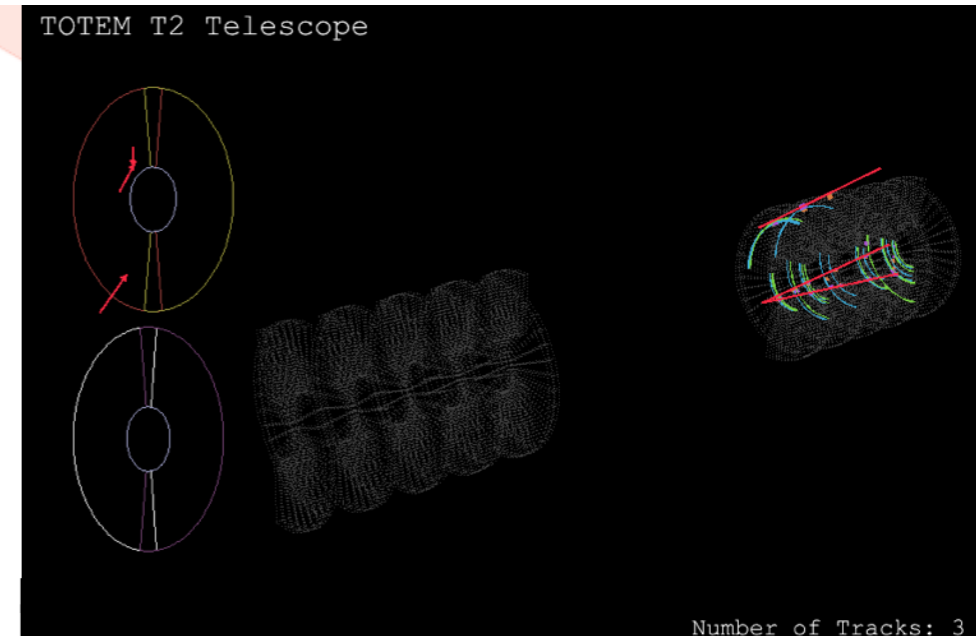
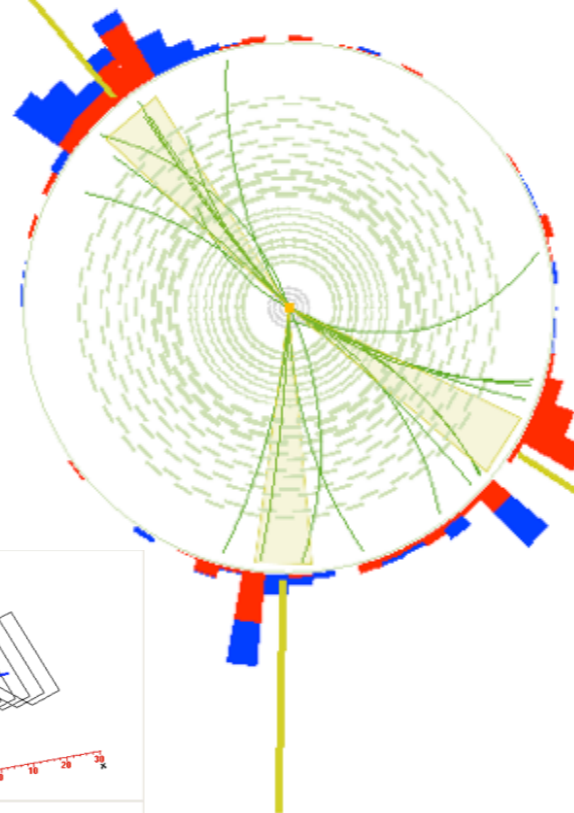
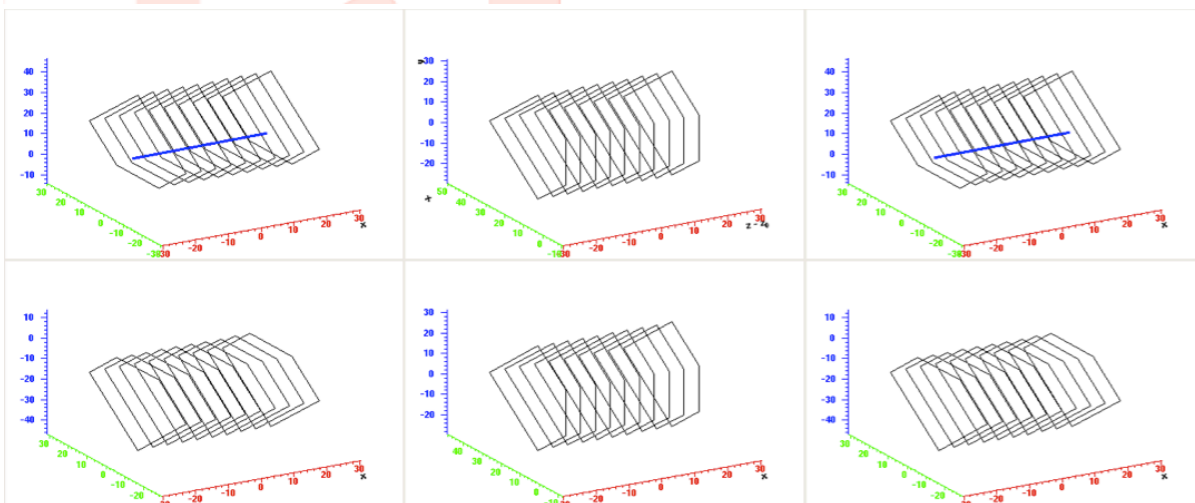
TOTEM T2



CMS Experiment at LHC, CERN  
Data recorded: Thu Jul 12 22:40:03 2012 BRST  
Run/Event: 198903 / 3478279  
Lumi section: 166  
Orbit/Crossing: 43375975 / 1789

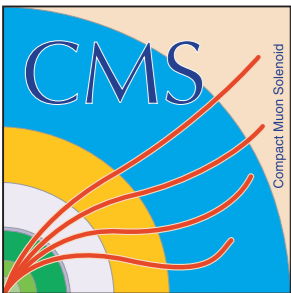
[CMS DP-2013-004](#)  
[CMS DP-2013-006](#)

TOTEM Roman Pot stations - Sector 4-5



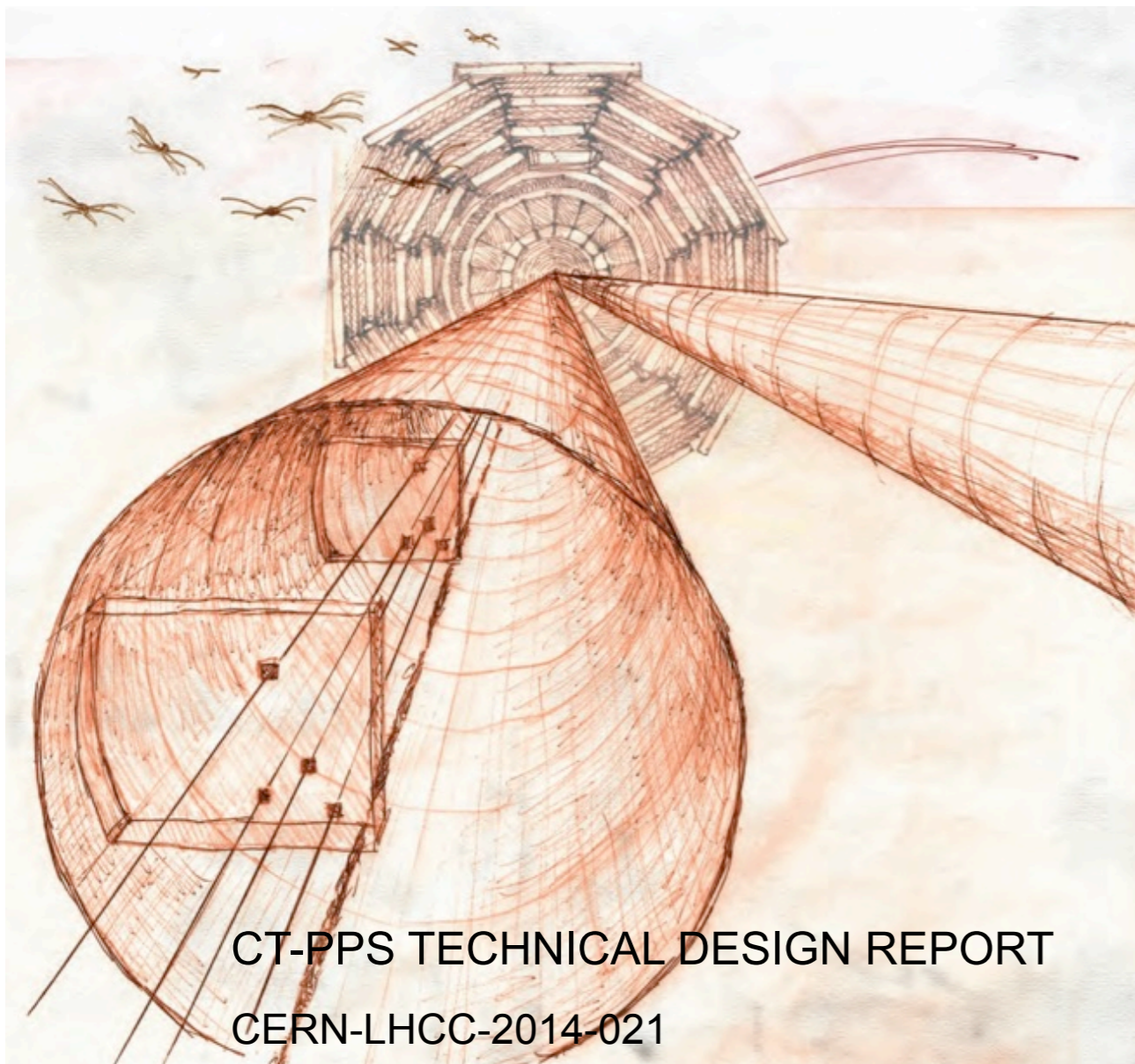
Leading three jets  $E_T = 65, 45, 27$  GeV  
proton  $\Delta p/p = -0.01$  (z+)  
proton  $\Delta p/p = -0.1$  (z-)  
 $M(pp, \text{TOTEM}) = 244$  GeV  
 $M(\text{CMS}) = 219$  GeV  
 $\Sigma p_T(\text{CMS}) = 3.4$  GeV  
FSC empty in both sides

ECAL/HCAL  $E_T > 200$  MeV  
Track  $p_T > 1$  GeV



# Outlook: The CT-PPS Project

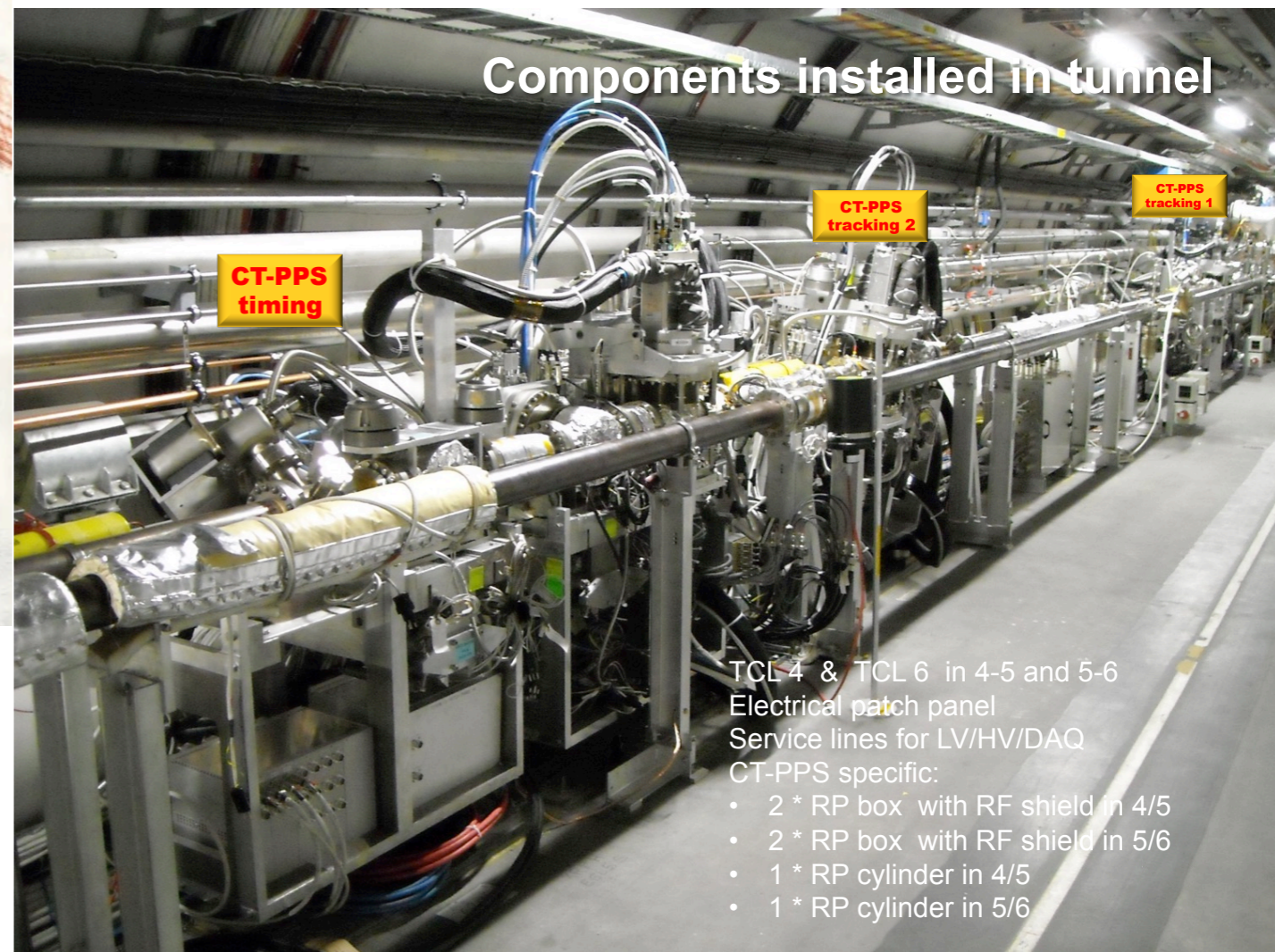
## CMS-TOTEM Precision Proton Spectrometer



CT-PPS TECHNICAL DESIGN REPORT

CERN-LHCC-2014-021

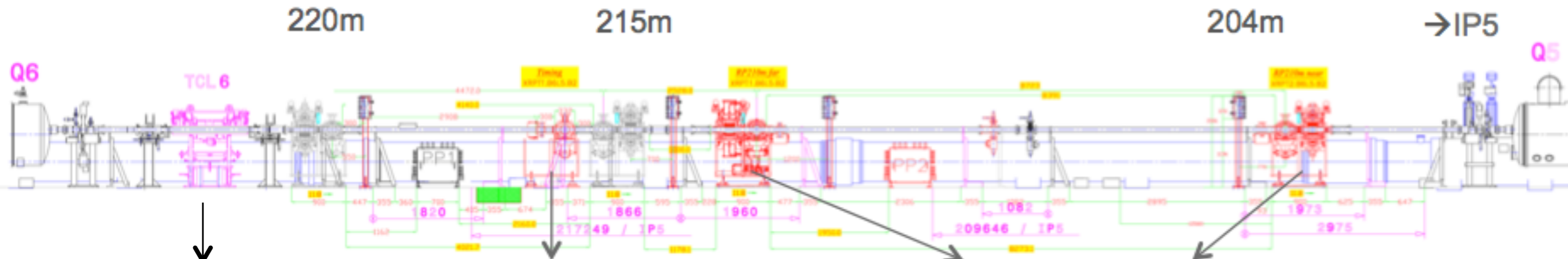
[CERN-LHCC-2014-021](#)



Components installed in tunnel

- TCL 4 & TCL 6 in 4-5 and 5-6  
Electrical patch panel  
Service lines for LV/HV/DAQ  
CT-PPS specific:
- 2 \* RP box with RF shield in 4/5
  - 2 \* RP box with RF shield in 5/6
  - 1 \* RP cylinder in 4/5
  - 1 \* RP cylinder in 5/6

# Forward proton detectors



New collimator TCL6  
to protect magnet Q6

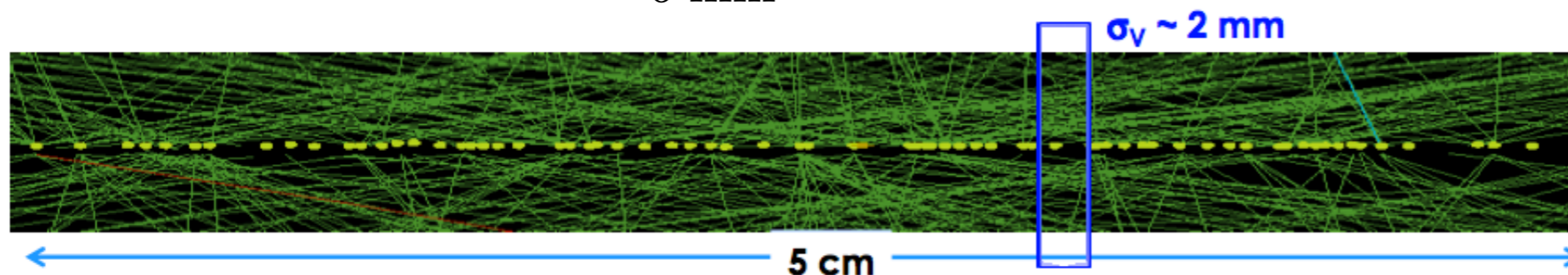
2 new horizontal  
cylindrical RPs (1 in LS1)

2 horizontal box-shaped RPs

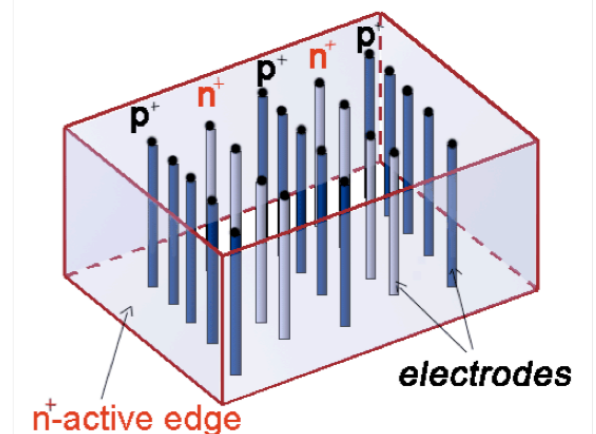
Timing detectors:  
Measures the time-of-flight of  
scattered protons

Tracking detectors:  
Measures the displacement of the  
scattered protons w.r.t. the beam

$$\sigma_{z_{vtx}} = \frac{c}{2} \sqrt{2\sigma_{\Delta t}^2} \quad \begin{matrix} \sigma_{\Delta t} \approx 10\text{ps} & 2\text{ mm} \\ \sigma_{\Delta t} \approx 30\text{ps} & 6\text{ mm} \end{matrix}$$



“3D” pixel sensors with  
columnar electrodes

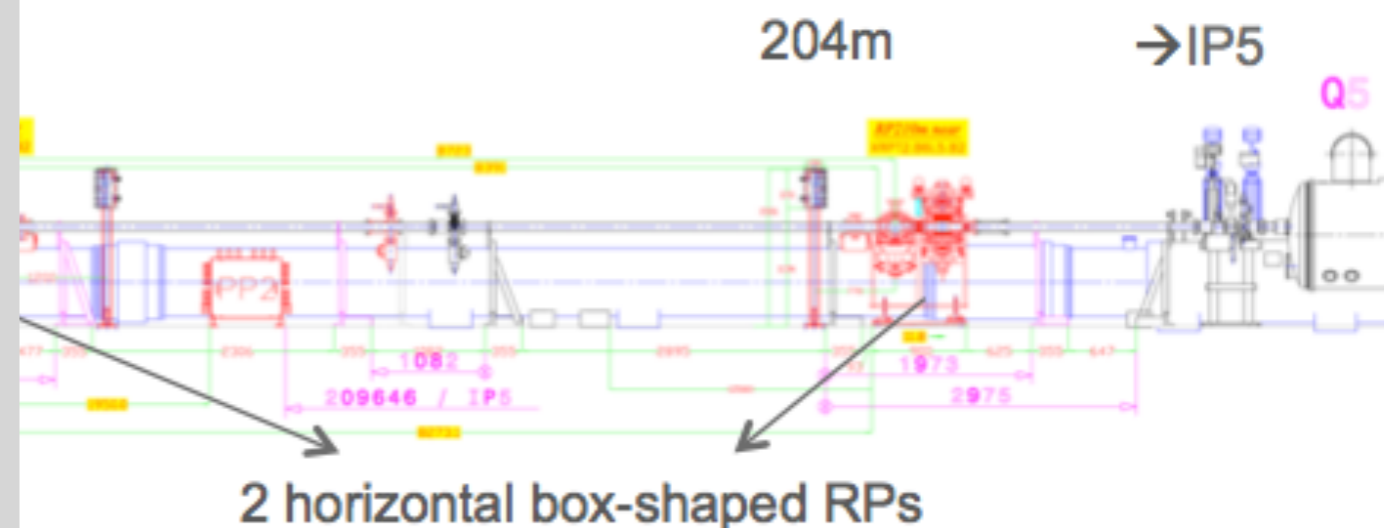


# Forward proton detectors

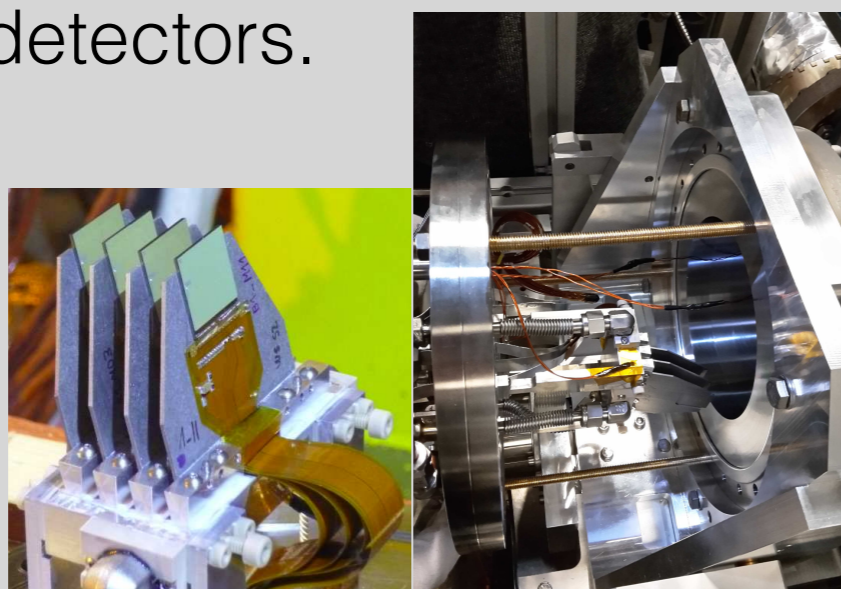
ATLAS: AFP (ATLAS Forward Proton)  
Similar strategy concerning RPs and sensors.

First arm under commissioning  
(2016/2017).

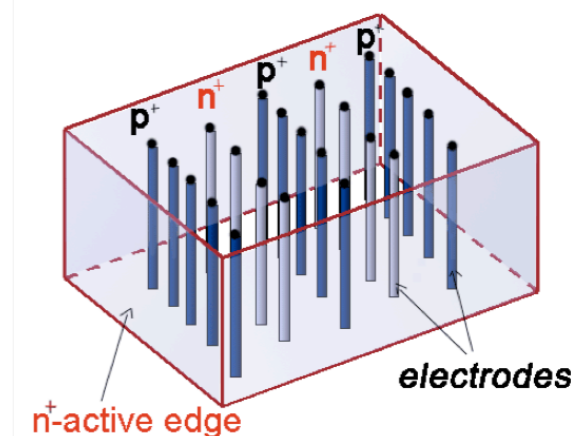
Later installation of second arm and  
time-of-flight detectors.



Tracking detectors:  
Measures the displacement of the  
scattered protons w.r.t. the beam

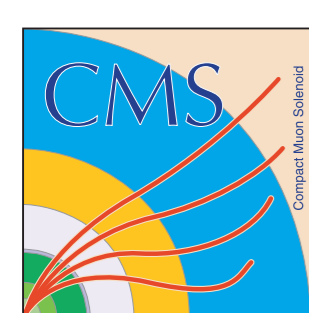


“3D” pixel sensors with  
columnar electrodes



Material taken from M. Trzebinski - LHC  
Forward Physics WG - March 2016

ICHEP2016 - Chicago - August 3-10 2016



# Forward proton detectors



ATLAS: AFP (ATLAS Forward Proton)  
Similar strategy concerning RPs and sensors.

First arm under commissioning  
(2016/2017).

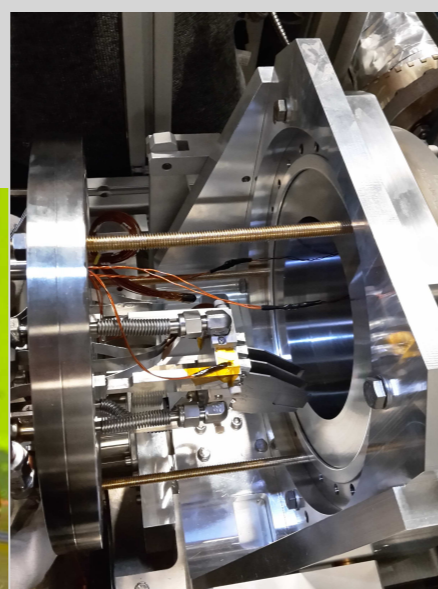
Later installation of second arm and  
time-of-flight detectors.

CT-PPS status:

First phase of operation during 2016  
using TOTEM silicon strip detectors.

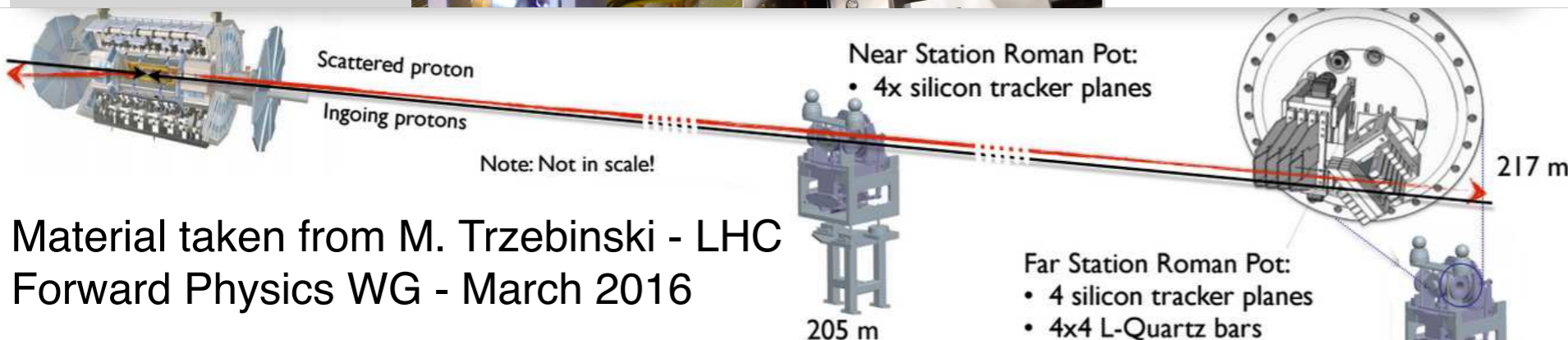
Several fb<sup>-1</sup> of data already collected.

Diamond (high resolution time-of-flight)  
detectors installed in cylindrical RP  
and under commissioning.

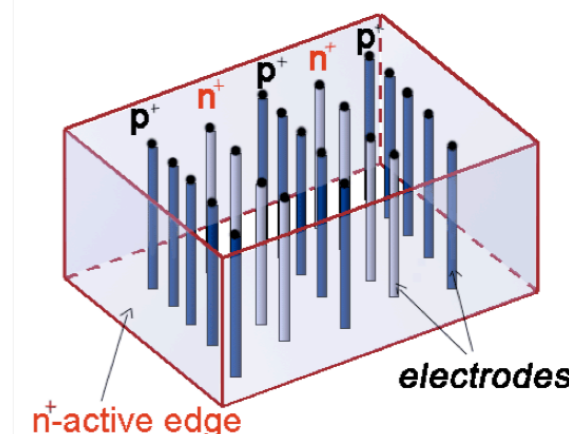


Tracking detectors:

Measures the displacement of the  
scattered protons w.r.t. the beam

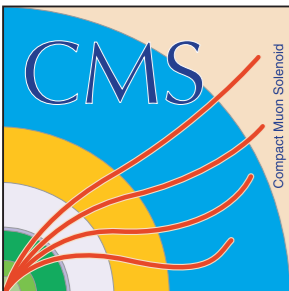


“3D” pixel sensors with  
columnar electrodes



Material taken from M. Trzebinski - LHC  
Forward Physics WG - March 2016

ICHEP2016 - Chicago - August 3-10 2016



# Summary & Outlook



Detailed measurements of total and (in)elastic cross sections across LHC centre-of-mass energies.

Direct measurements of diffractive cross sections (fiducial and extrapolated).

Hard-diffractive processes observed at the LHC (CMS and ATLAS) from LRG method. Rapidity gap survival probability MC-based extraction.

Study of BFKL dynamics from observation of dijets with a large rapidity gap.

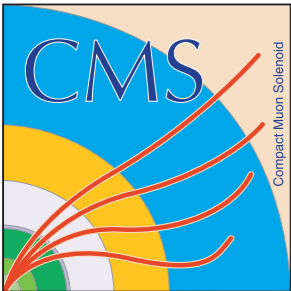
ATLAS RP system and common CMS-TOTEM data taking during special low pile-up and high- $\beta^*$  Runs at 8 and 13 TeV: studies of diffractive processes with full proton kinematics.

ATLAS AFP and CT-PPS will enhance the physics reach at the LHC.

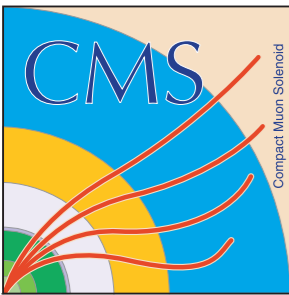
Operation of Roman Pots at high luminosity. Timing detectors with high precision. Tracking detectors with 3D pixel sensors.

Sensitivity to anomalous gauge couplings and search for new resonances.





# Extra slides



# $dN/d\eta$ of charged hadrons at 13 TeV

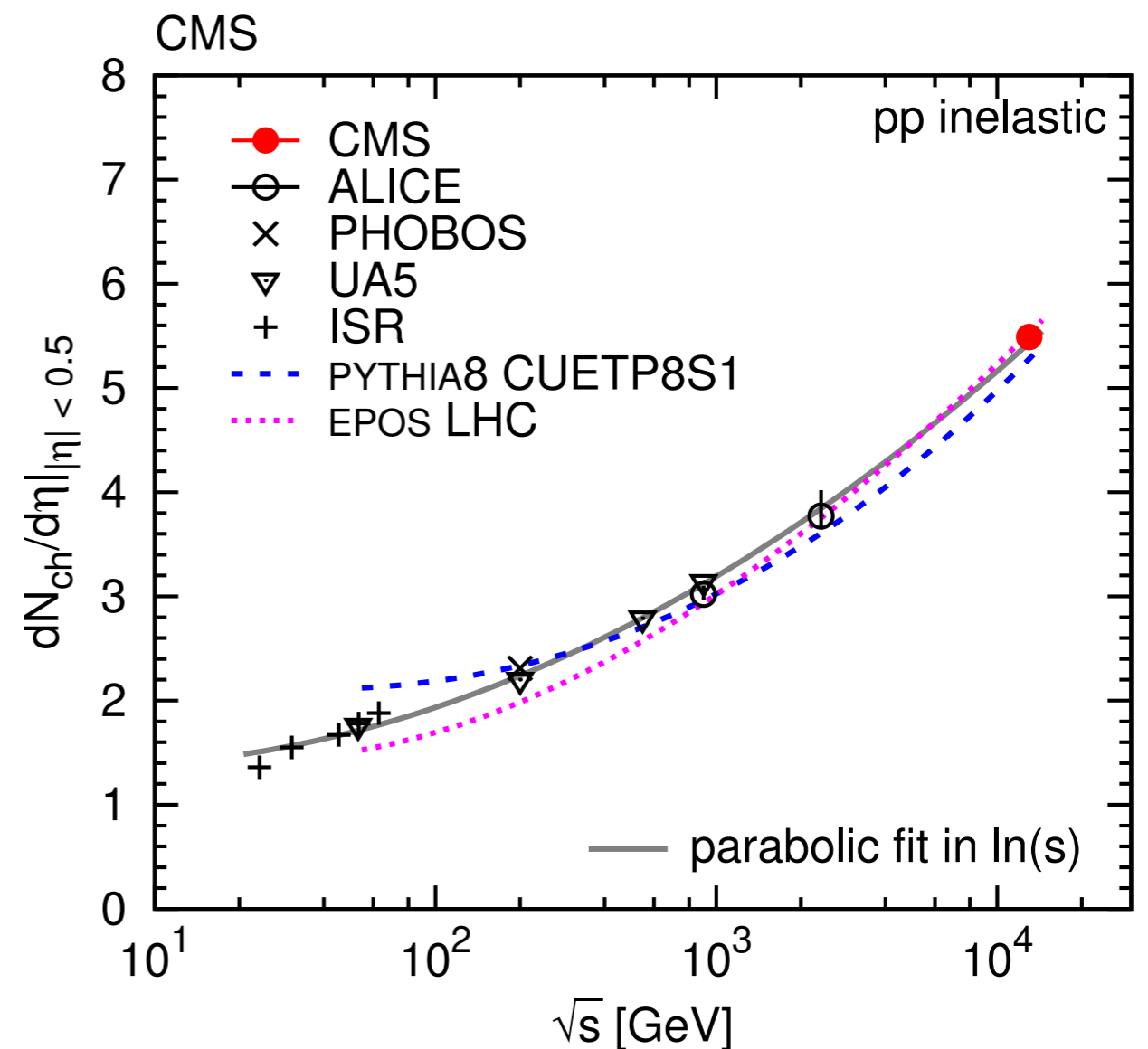
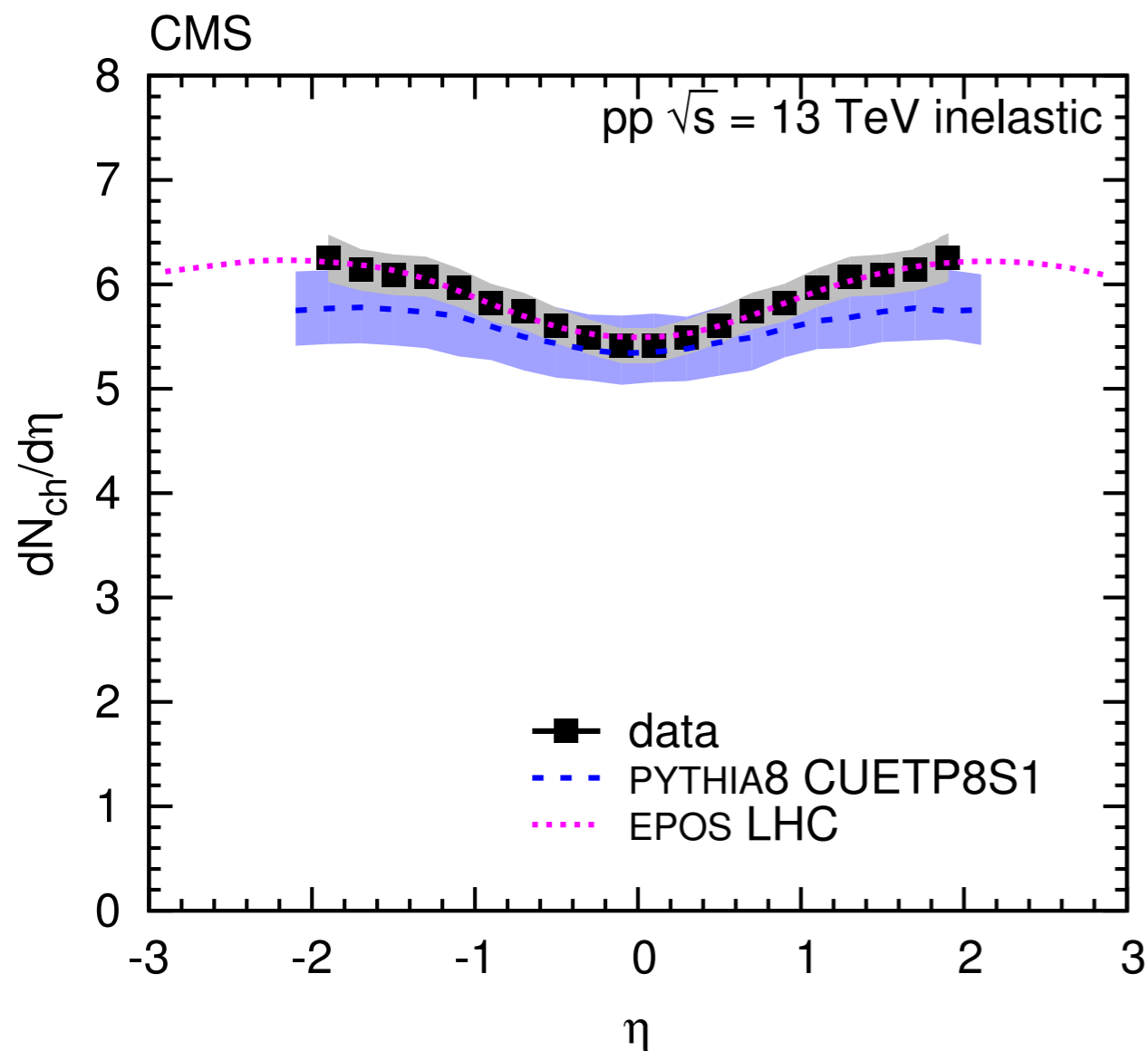
Charged hadron pseudorapidity density in inelastic pp collisions at 13 TeV;

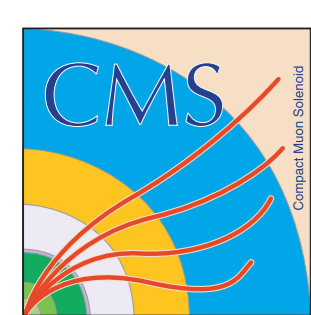
Central value:  $5.49 \pm 0.01$  (stat.)  $\pm 0.17$  (syst.);

First LHC paper at 13 TeV.

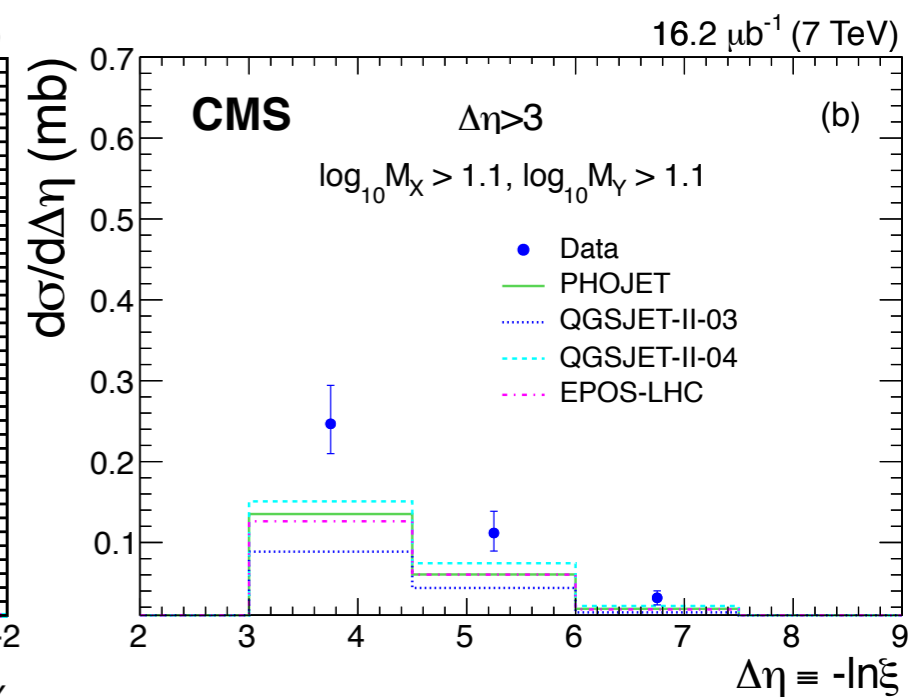
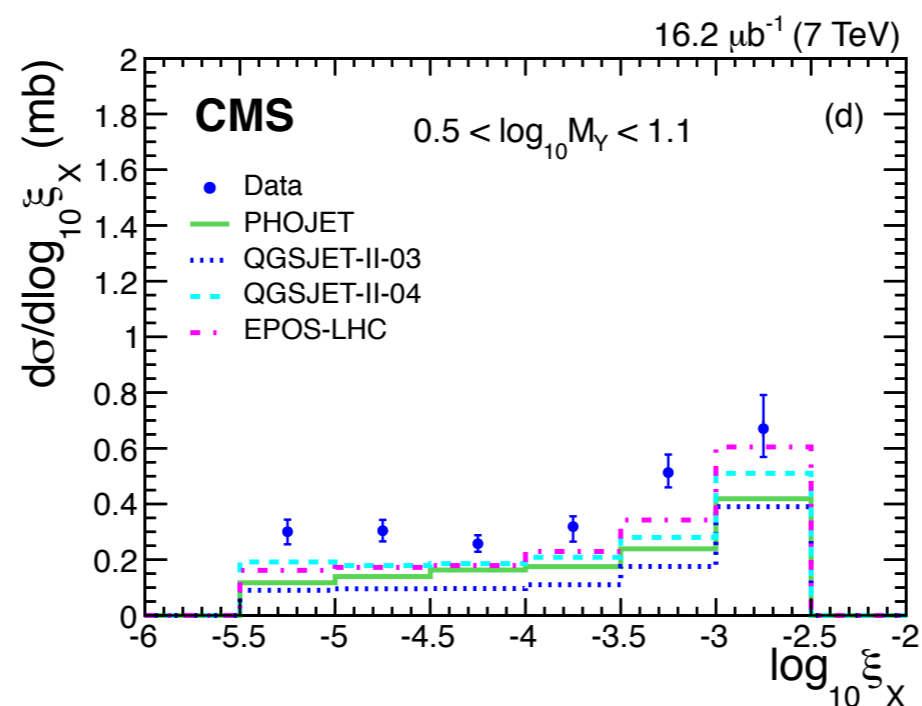
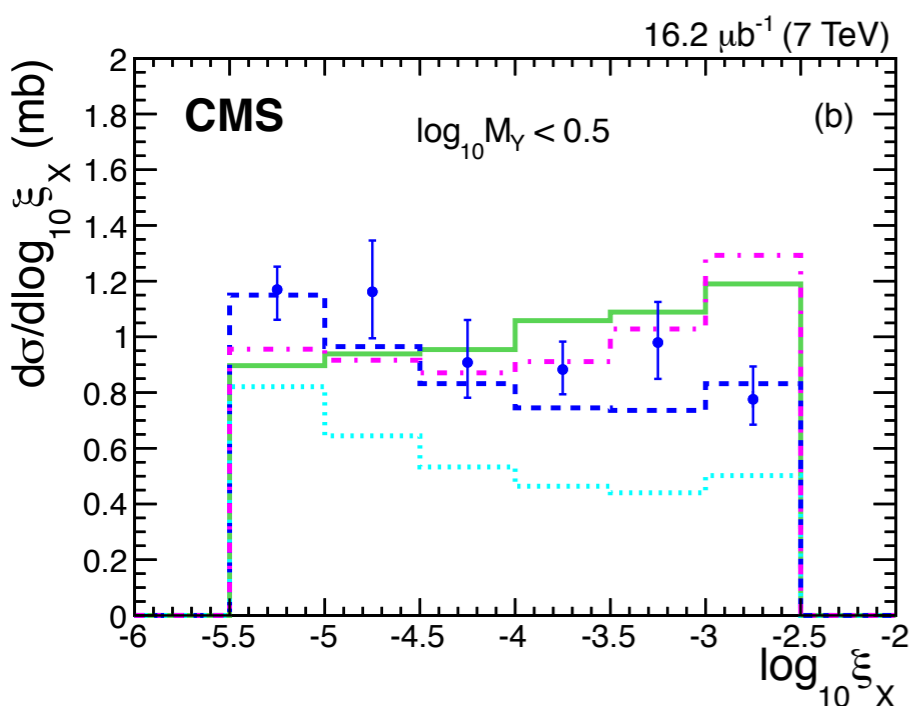
[CMS FSQ-15-001](#)

[Phys. Lett. B 751 \(2015\) 143](#)





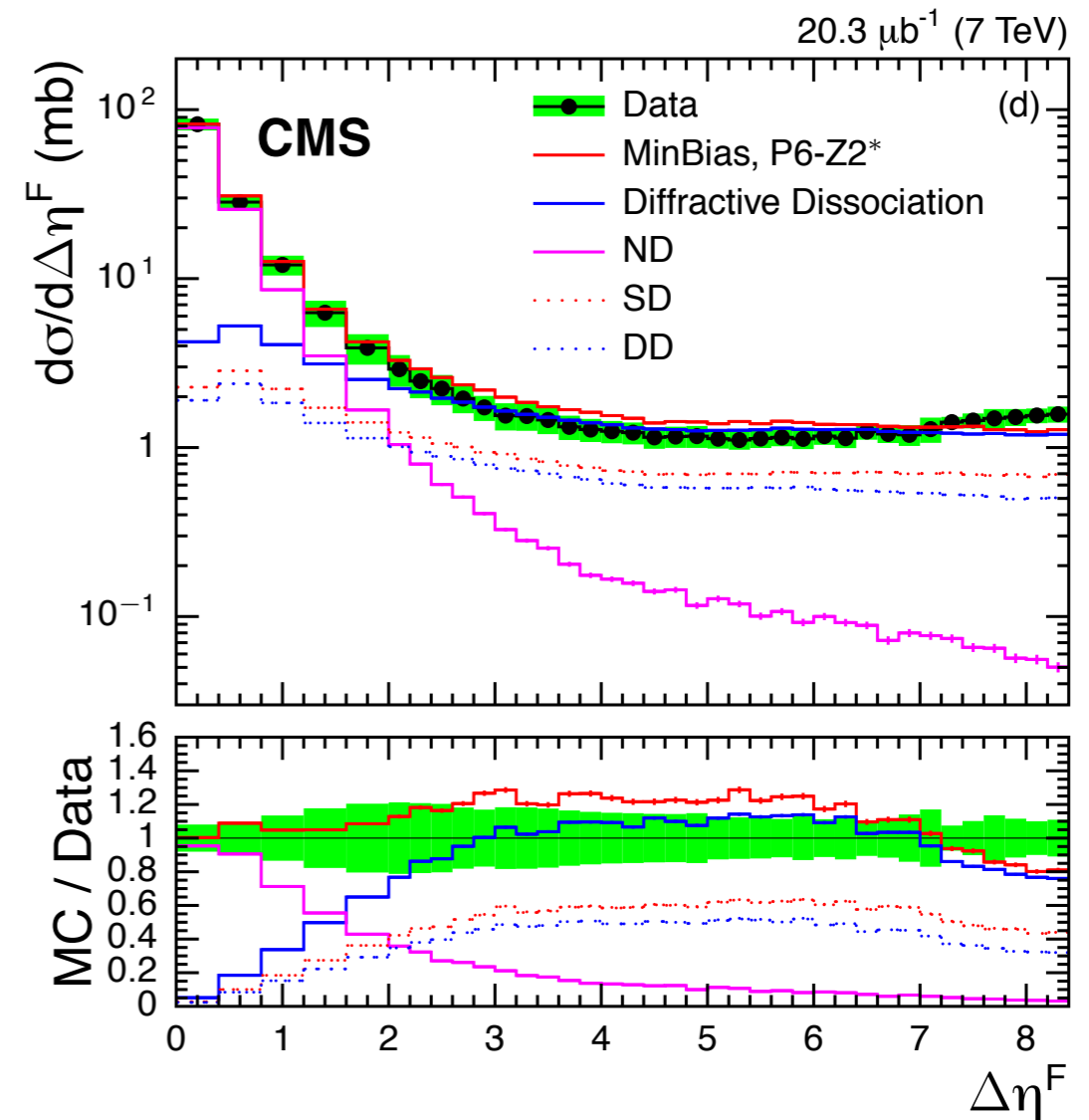
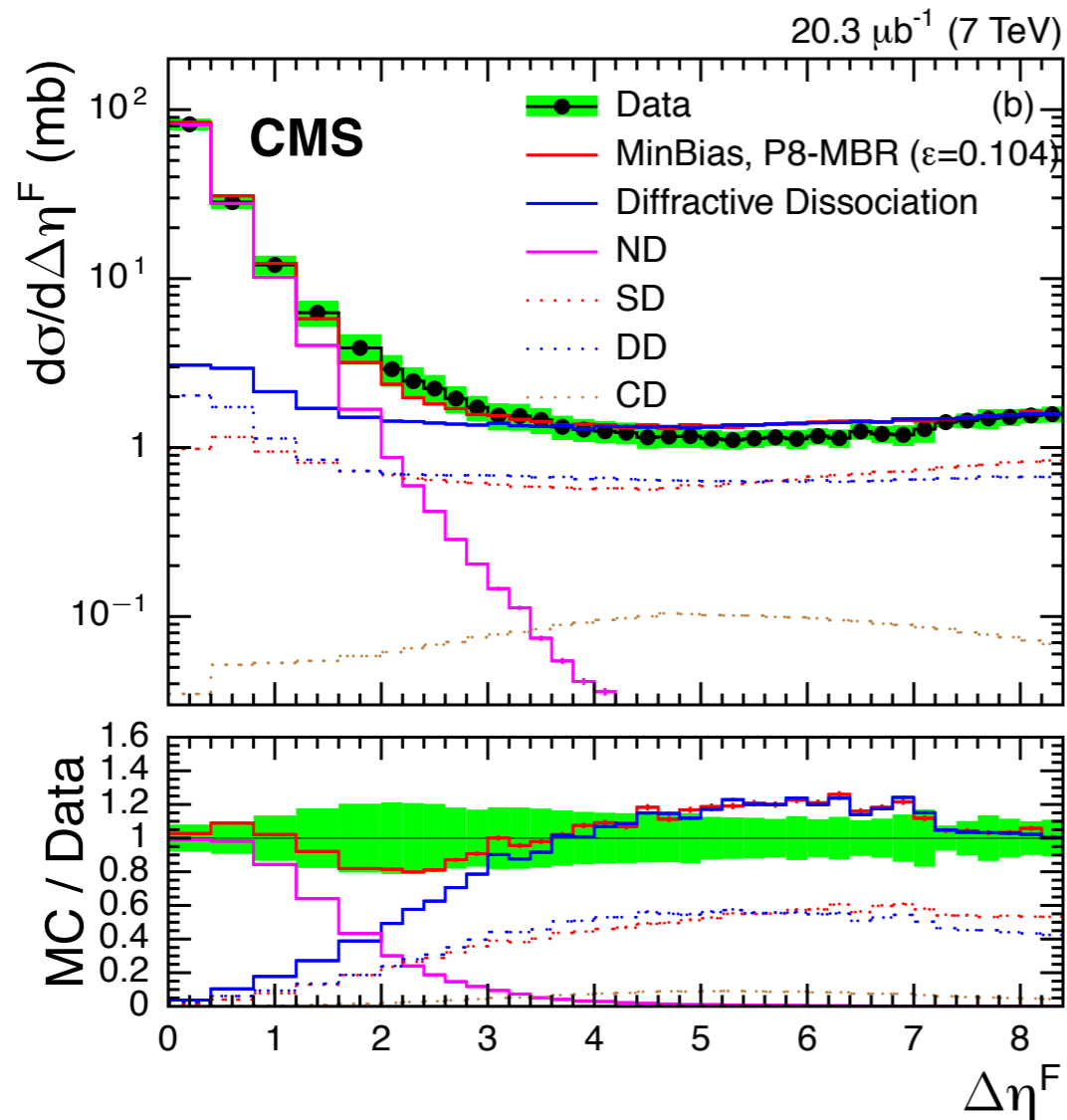
# Diffractive cross sections



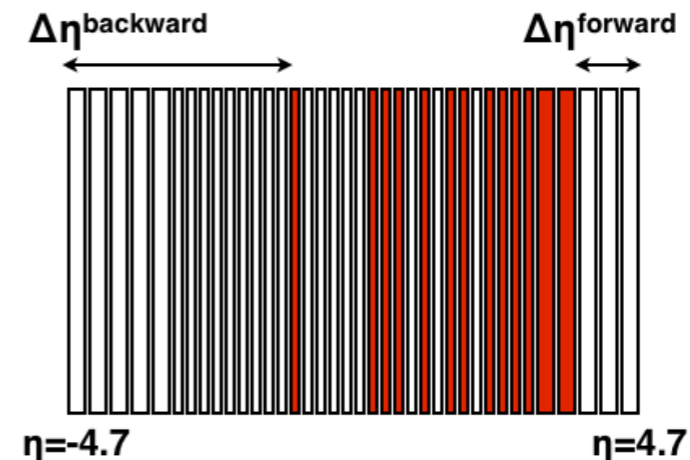
[CMS FSQ-12-005](#)

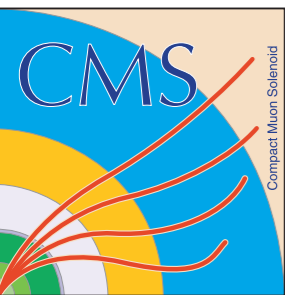
[Phys. Rev. D 92 \(2015\) 012003](#)

# Forward pseudorapidity gap cross section



Forward pseudorapidity gap cross section from backward/forward edge of detector (up to HF only).  
Hadron level definition directly related to that at detector level.

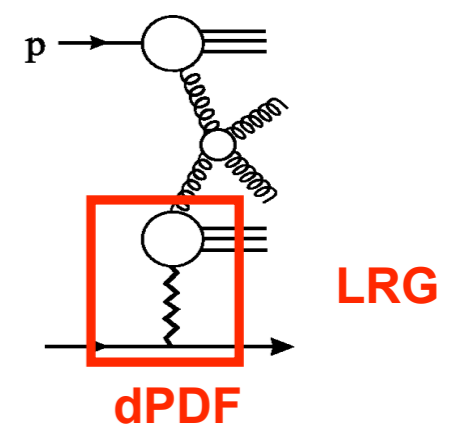
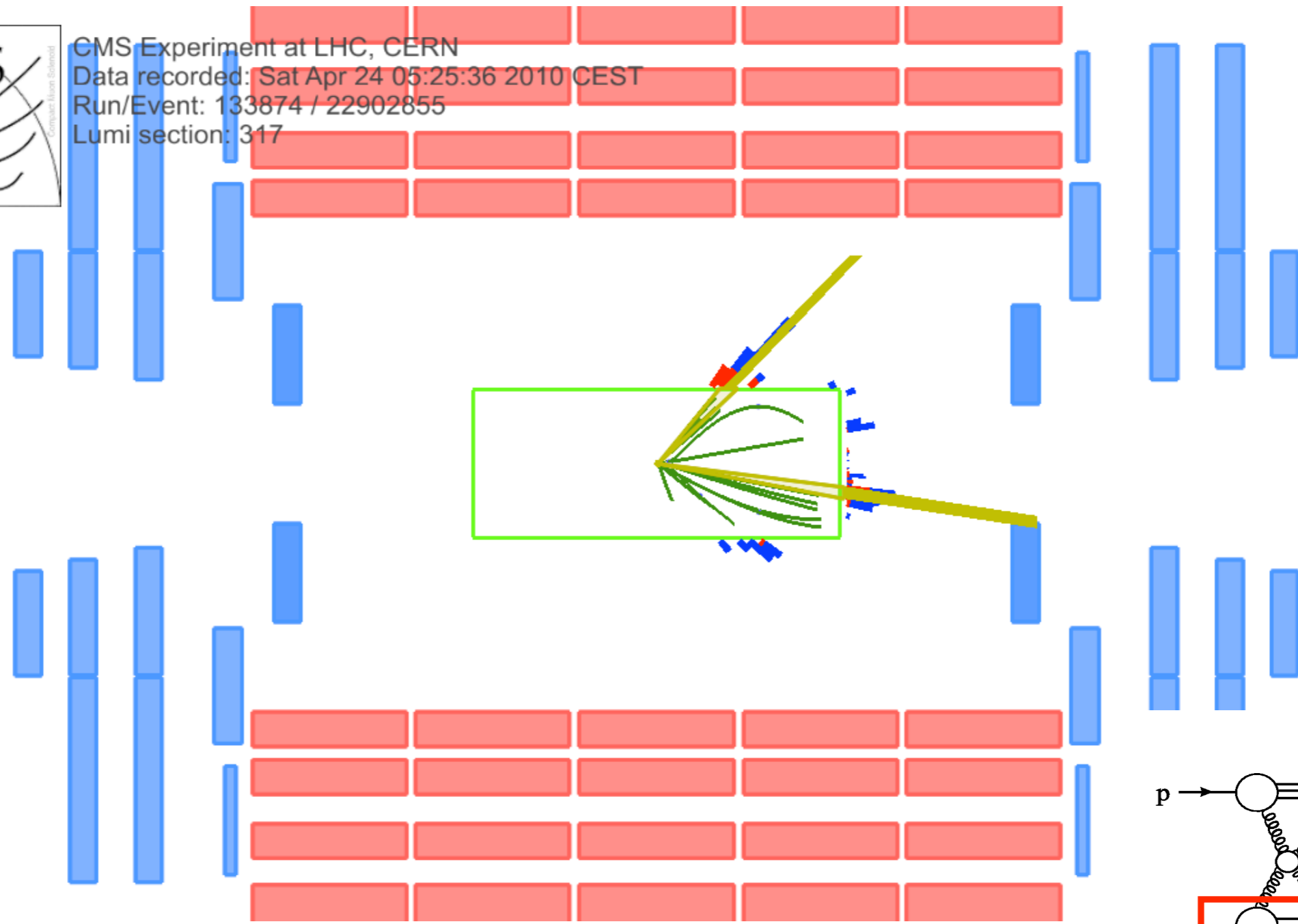




# Diffractive dijet candidate



CMS Experiment at LHC, CERN  
Data recorded: Sat Apr 24 05:25:36 2010 CEST  
Run/Event: 133874 / 22902855  
Lumi section: 317





# Dijet production

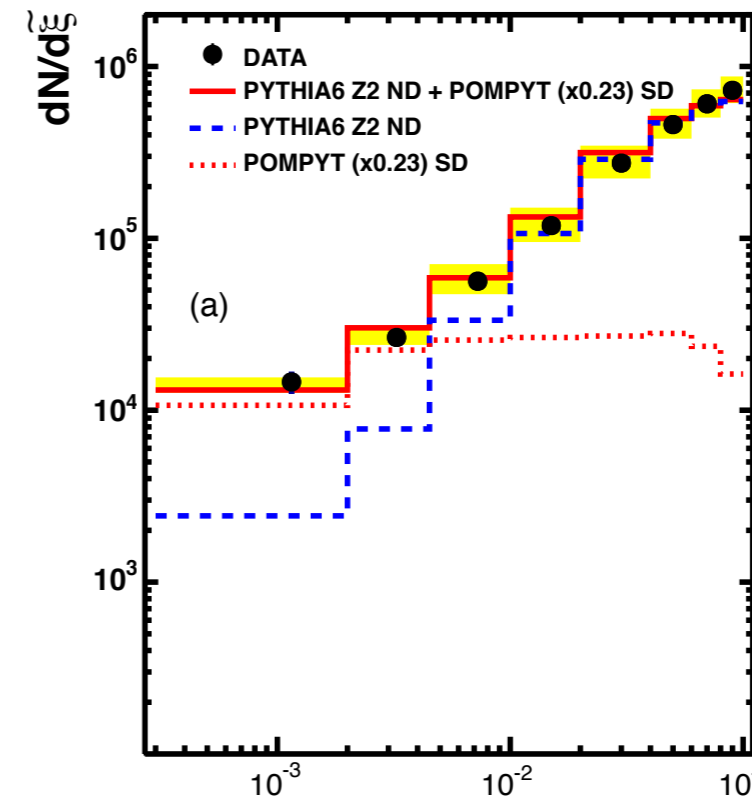
Distributions are obtained as a function of  $\xi^+$  and  $\xi^-$ , and averaged

A combination of PYTHIA6 (Tune Z2) and POMPYT is used to describe the data, where their relative contributions are obtained from a fit to the  $\xi$  distribution

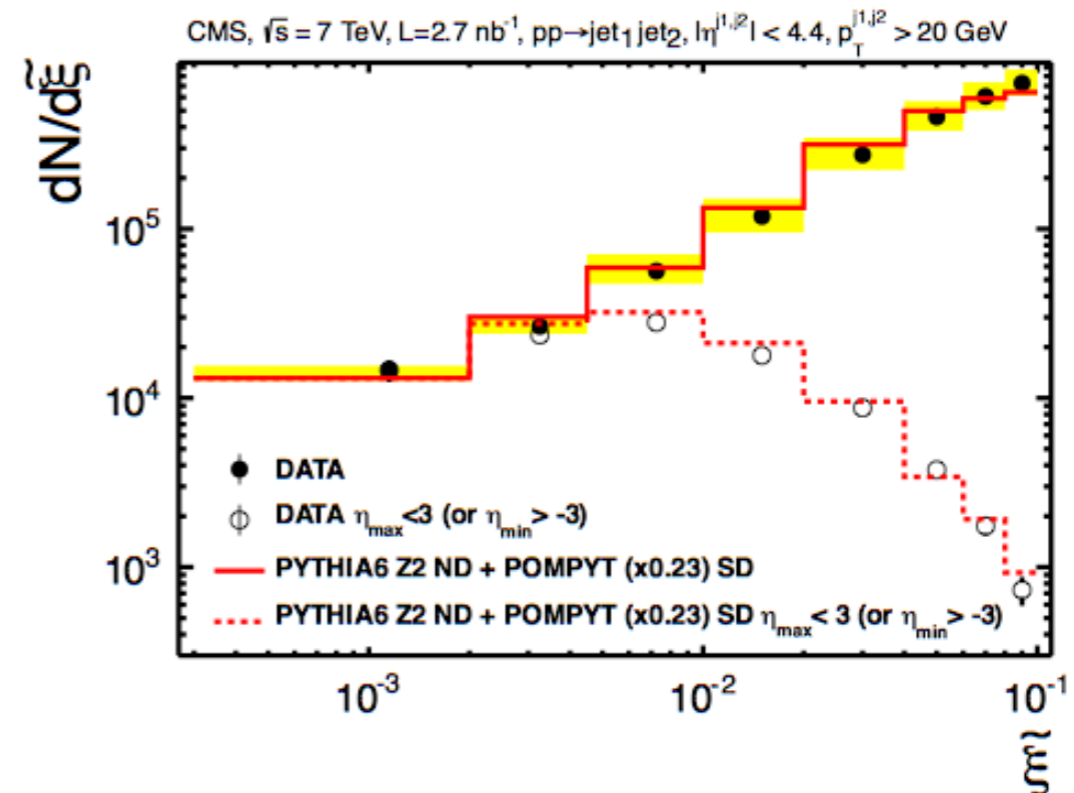
Note that different MC tunes would imply considerable variations in relative yields

Suppression of events with high  $\xi$  values after  $\eta_{\max} < 3$  (or  $\eta_{\min} > -3$ ) selection, while low- $\xi$  region is mostly unaffected

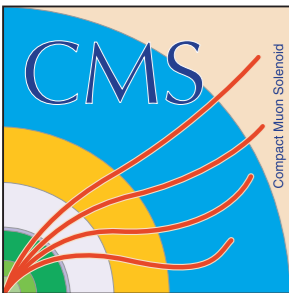
Results in three  $\xi$  bins: (0.0003,0.002); (0.002,0.0045); (0.0045,0.01)



$$\tilde{\xi}^{\pm} = C \frac{\sum (E \pm p_z)}{\sqrt{s}}$$



CMS FWD-10-004  
Phys. Rev. D 87 (2013) 012006



# Dijet cross section

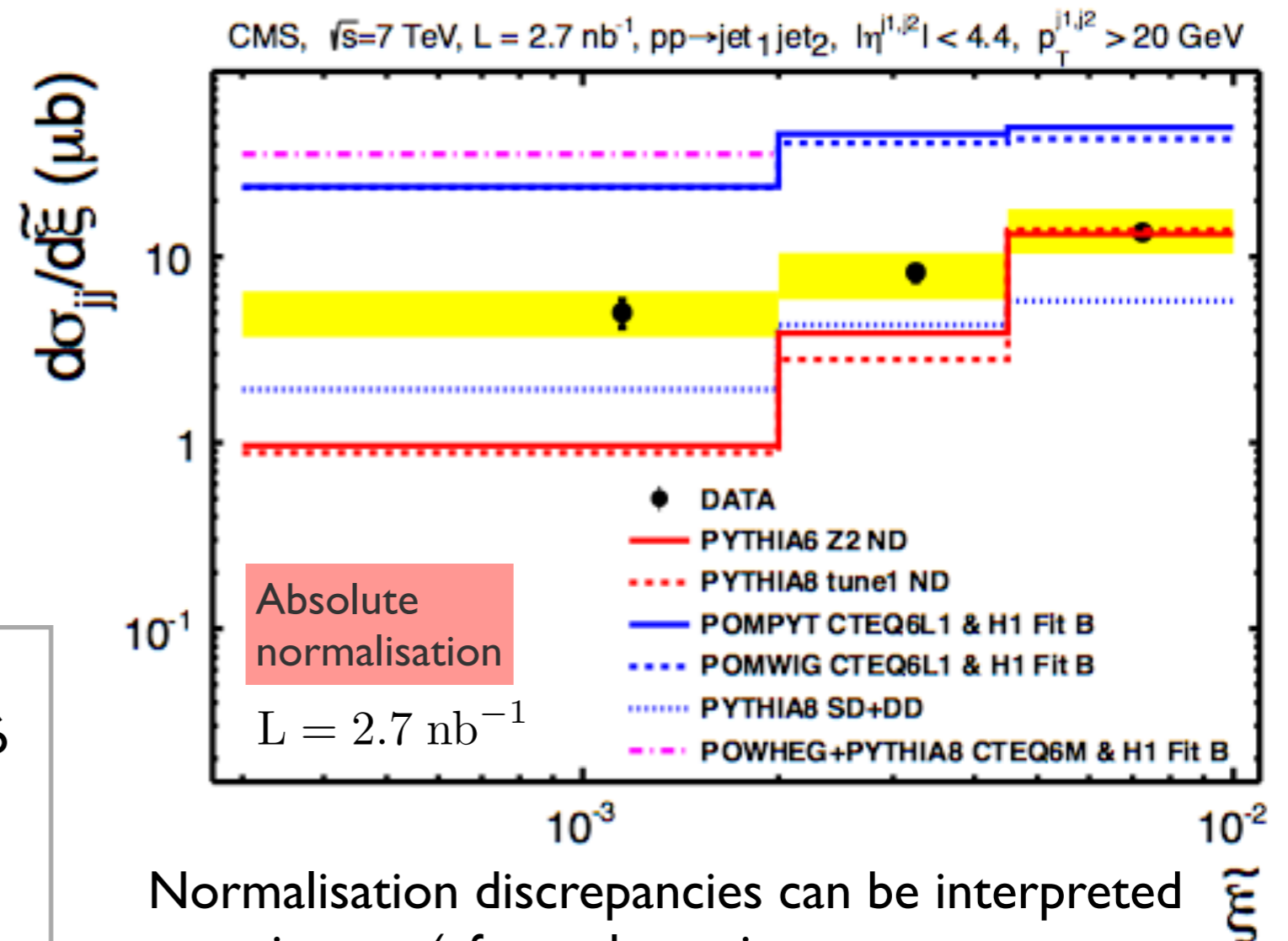
$$\frac{d\sigma_{jj}}{d\tilde{\xi}} = \frac{N_{jj}^i}{L \cdot \epsilon \cdot A^i \cdot \Delta\tilde{\xi}^i}$$

$$A_{MC}^i = \frac{N^i(\tilde{\xi}_{Rec})}{N^i(\tilde{\xi}_{Gen})}$$

Excess of events in low- $\xi$  region with respect to non-diffractive MC's PYTHIA6 and PYTHIA8

POMPYT and POMWIG (LO) diffractive MC's as well as the NLO calculation from POWHEG, using diffractive PDFs, are a factor  $\sim 5$  above the data in lowest  $\xi$  bin

PYTHIA8 diffractive cross sections are considerably lower due to different pomeron flux parametrisation

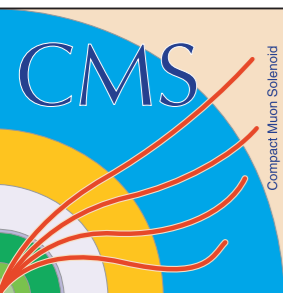


Normalisation discrepancies can be interpreted as estimates (after subtracting proton dissociation) of rapidity gap survival probability:

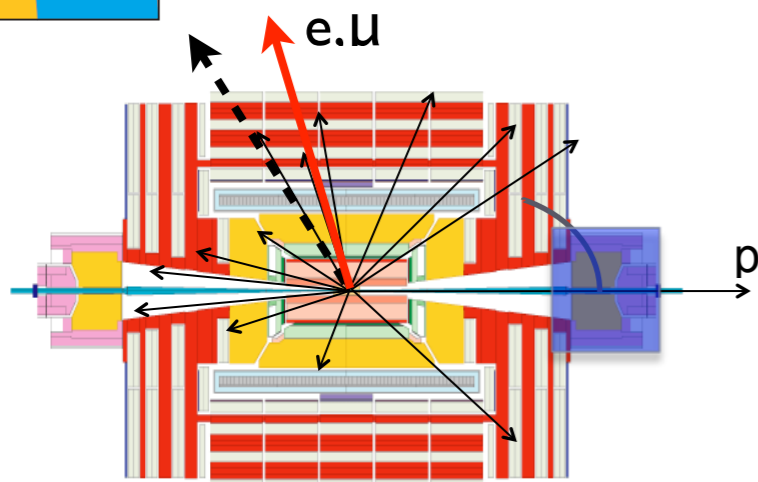
$$S_{\text{data/MC}}^{2(*)} = 0.12 \pm 0.05 \text{ (LO MC)}$$

$$S_{\text{data/MC}}^{2(*)} = 0.08 \pm 0.04 \text{ (NLO MC)}$$

(\*) MC based subtraction of proton dissociation

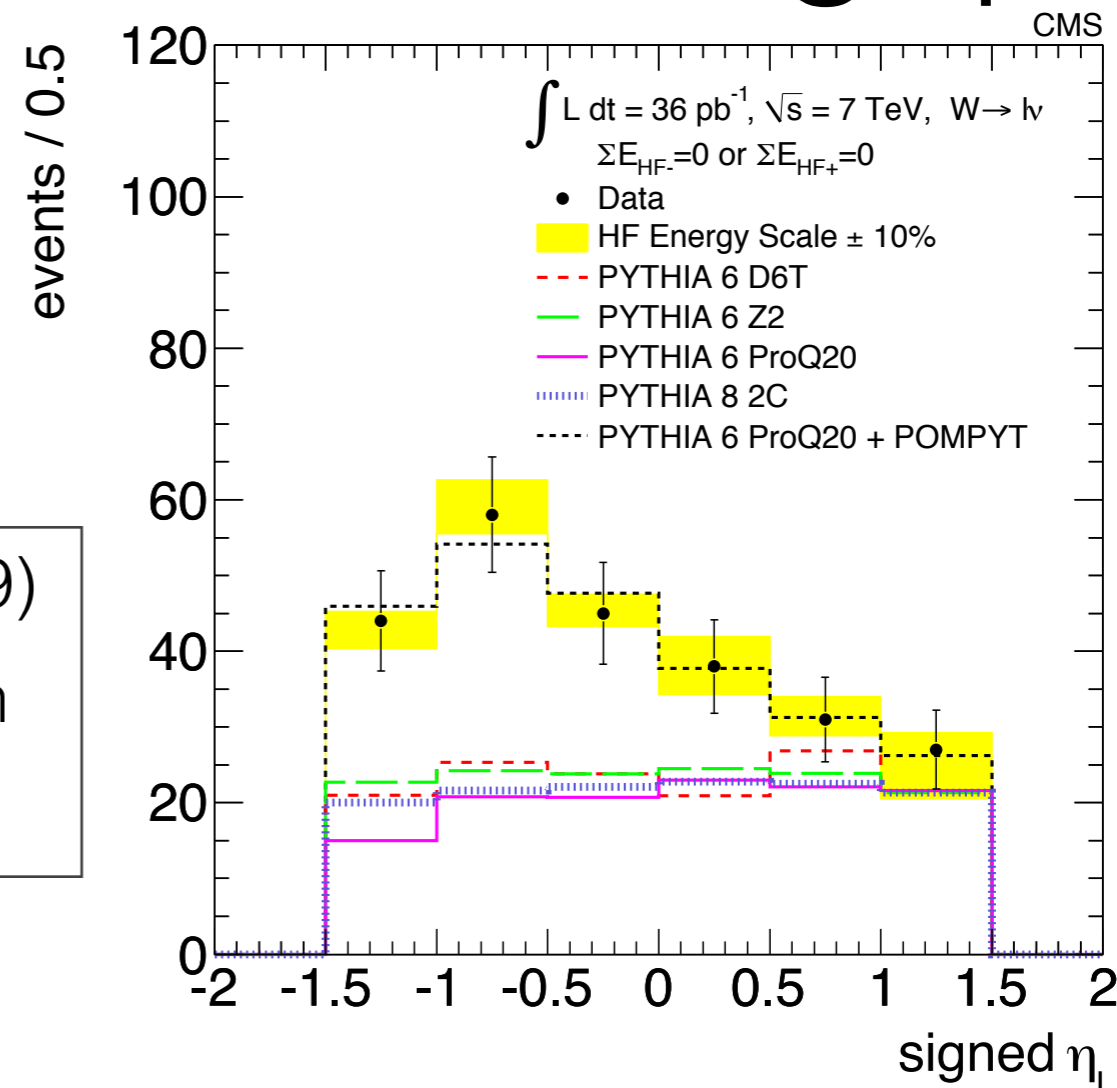
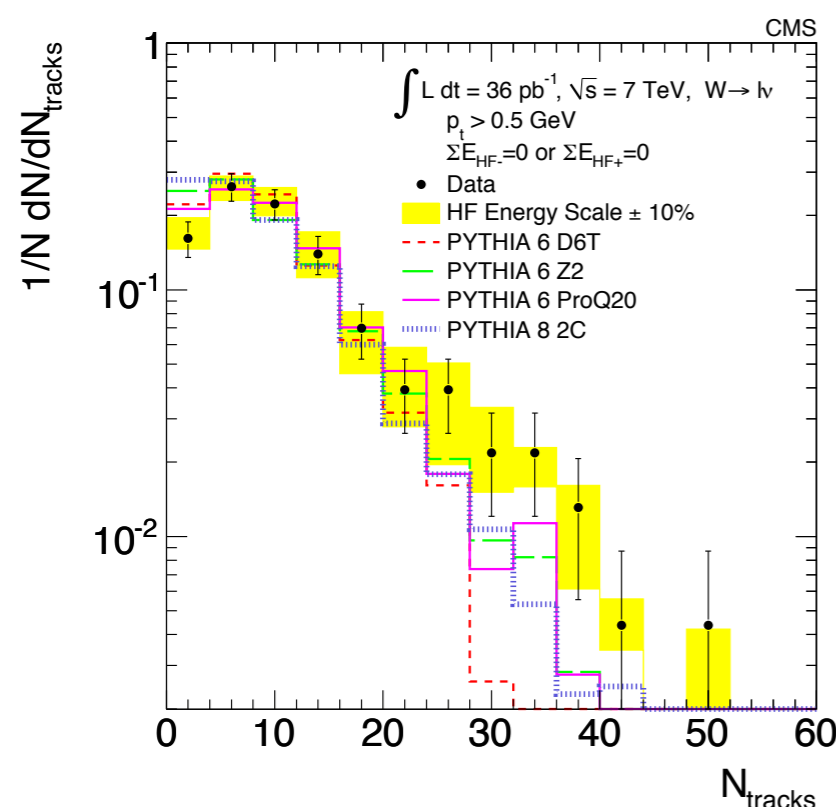


# $W \rightarrow e\nu(\mu\nu)$ events with a gap



Forward gap selection in HF ( $3 < |\eta| < 4.9$ )

Signed  $\eta_{\text{lepton}}$  distribution ( $\eta_{\text{lepton}} < 0$  when  $e, \mu$  opposite to the pseudorapidity gap)



Normalised to fit of  
PYTHIA6 + POMPYT

Flat for non-diffractive, asymmetric for diffractive events

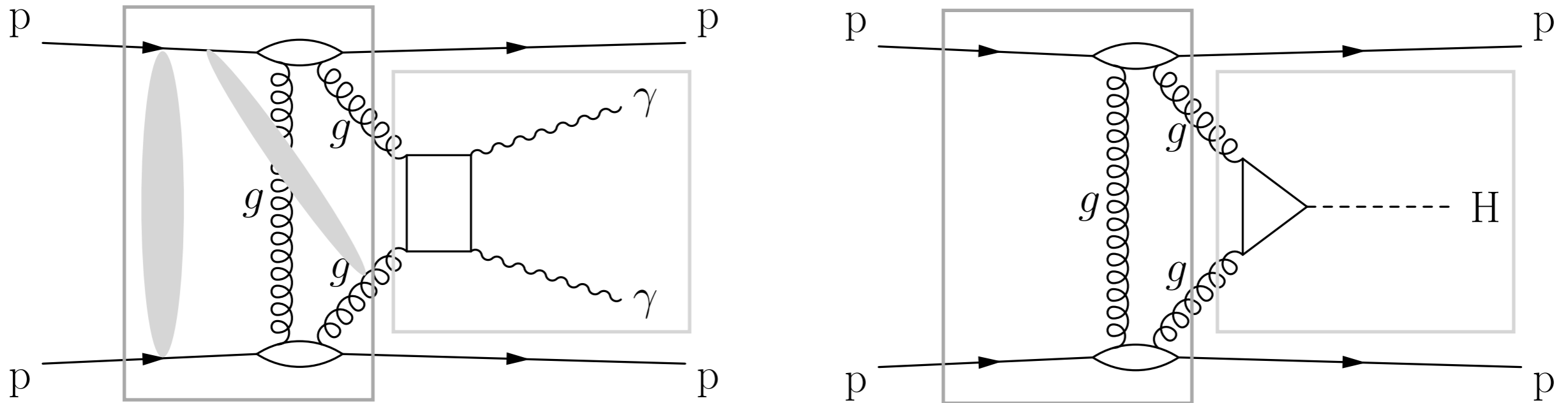
Evidence of diffractive W production in the data

Fit for PYTHIA (ND) + POMPYT (SD):

$$f_{\text{SD}} = 50.0 \pm 9.3(\text{stat.}) \pm 5.2(\text{syst.}) \%$$

( $\eta$ -gap sample)

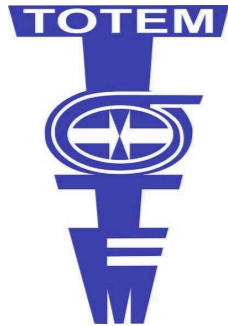
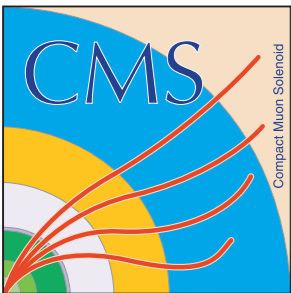
# “Central Exclusive” production



Exclusive channel through exchange of color singlet, lowest order given by gluon-gluon fusion, plus *screening* low- $Q^2$  gluon

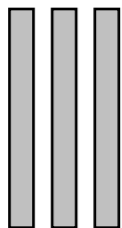
Protons remain intact as in QED process, or dissociate in a low mass system, and are separated from the central system ( $\gamma\gamma$ , H, etc.) by rapidity gaps

Main theoretical uncertainties common among different final states. Higher cross section channels, such as  $\gamma\gamma$  or dijets, can test predictions for central exclusive production of new states.



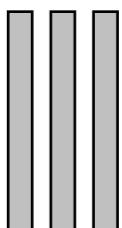
# CMS-TOTEM central dijet events

Forward Shower  
Counters



59 - 114 m

Forward Shower  
Counters



P

P

P

P

220 m

TOTEM T2

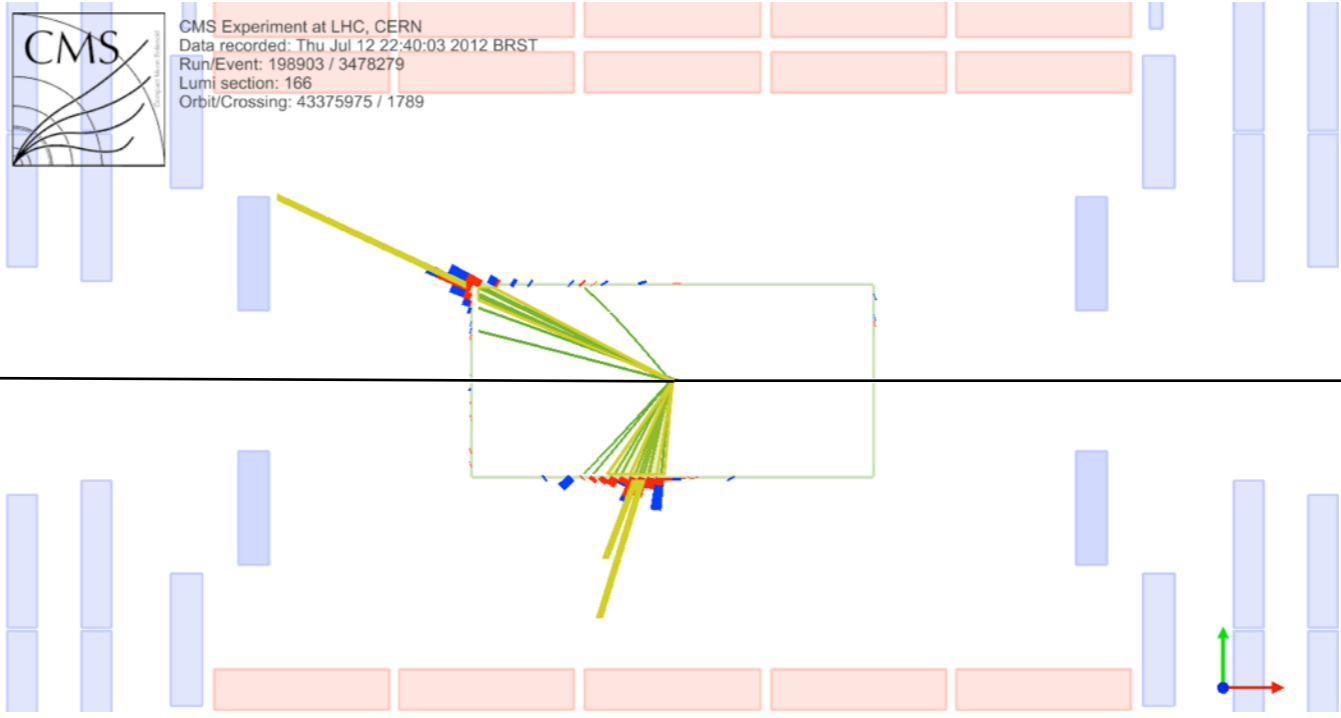


TOTEM T2

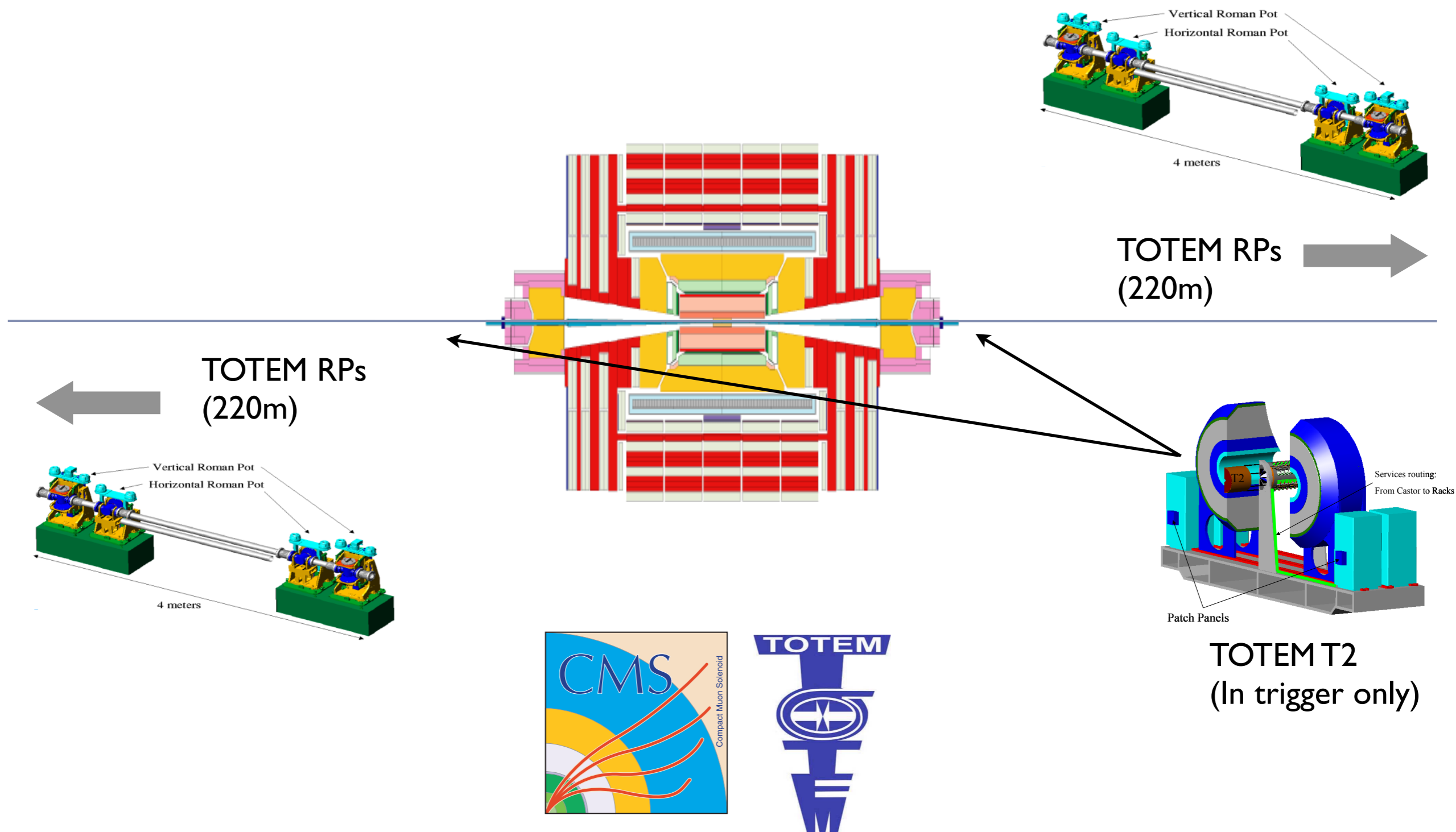


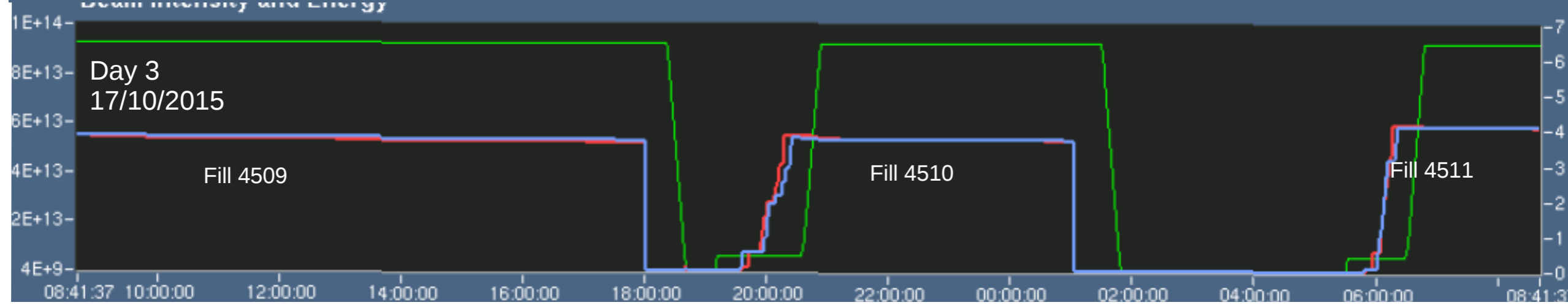
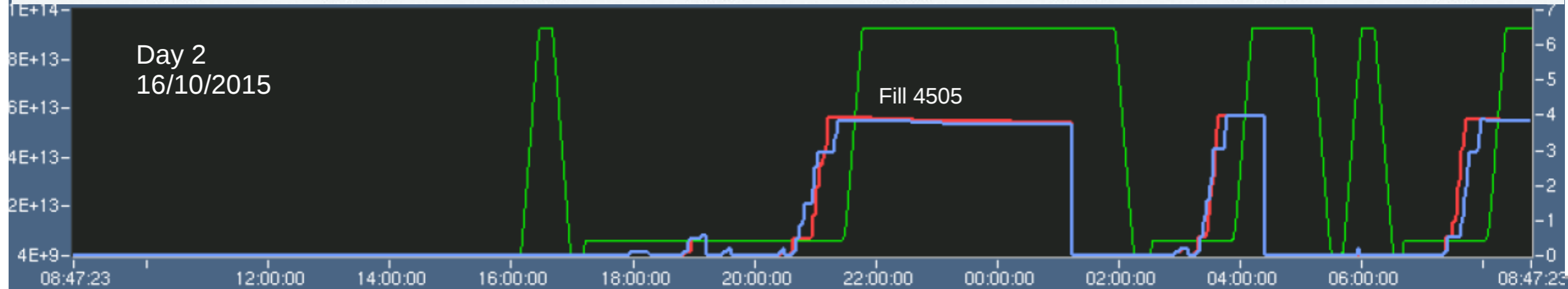
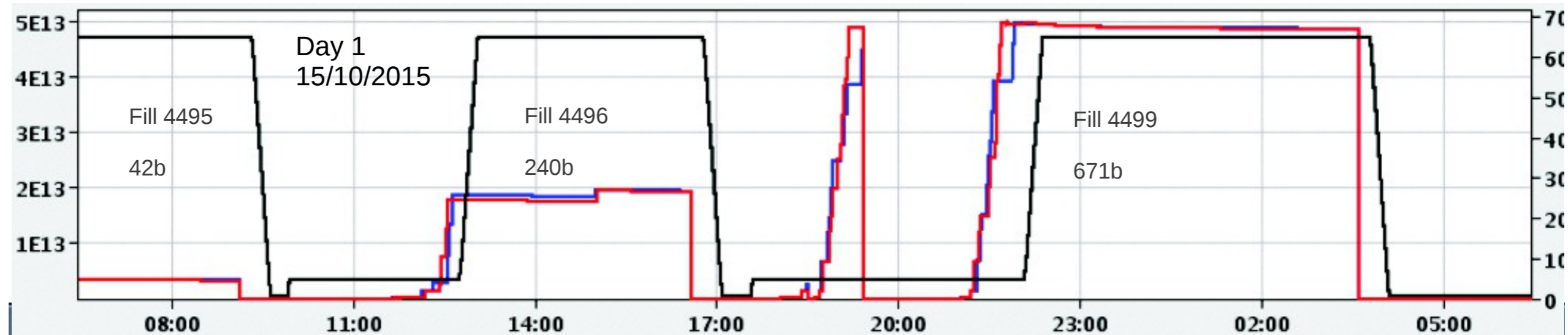
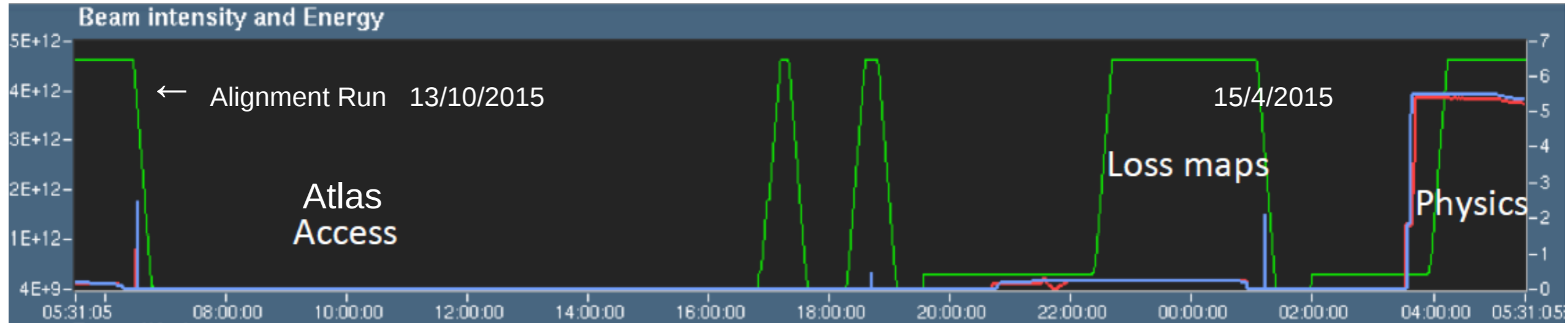
TOTEM  
Roman Pots

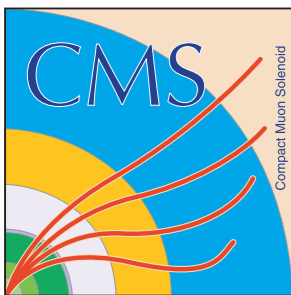
TOTEM  
Roman Pots



# CMS-TOTEM detectors



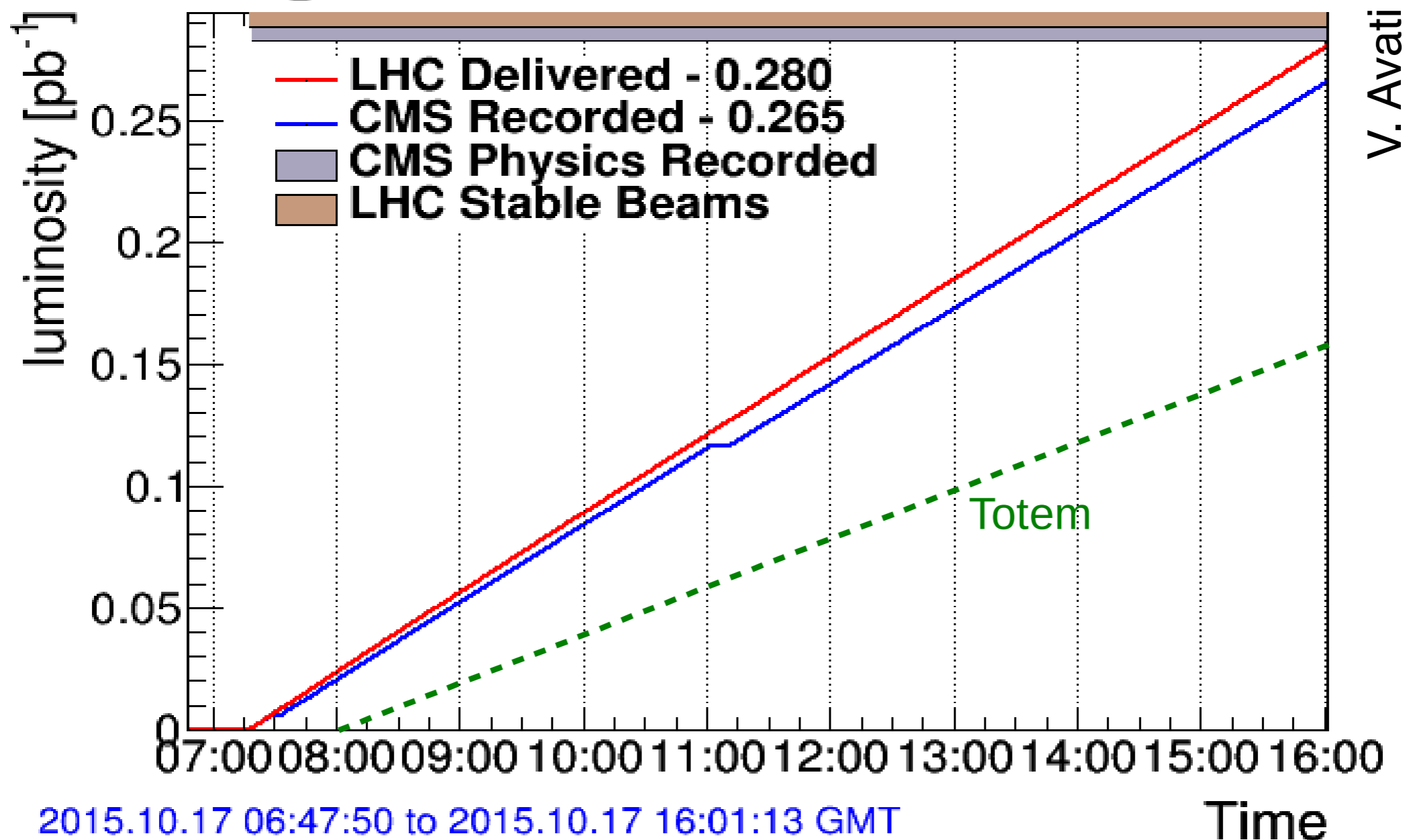




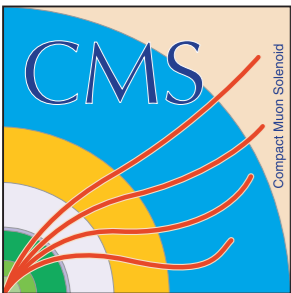
# Recorded data (2015 high- $\beta^*$ )

CMS overall recorded  $\sim 0.7 \text{ pb}^{-1}$   
TOTEM overall recorded  $\sim 0.4 \text{ pb}^{-1}$   
 $\langle N_{\text{Int}}/Bx \rangle$  less than  $\sim 0.10$

## CMS: Fill 4509 Luminosity



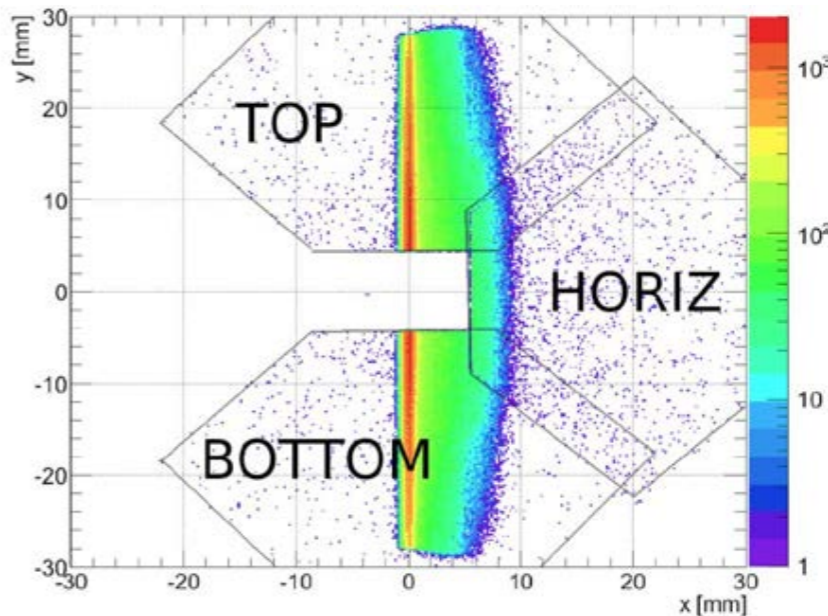
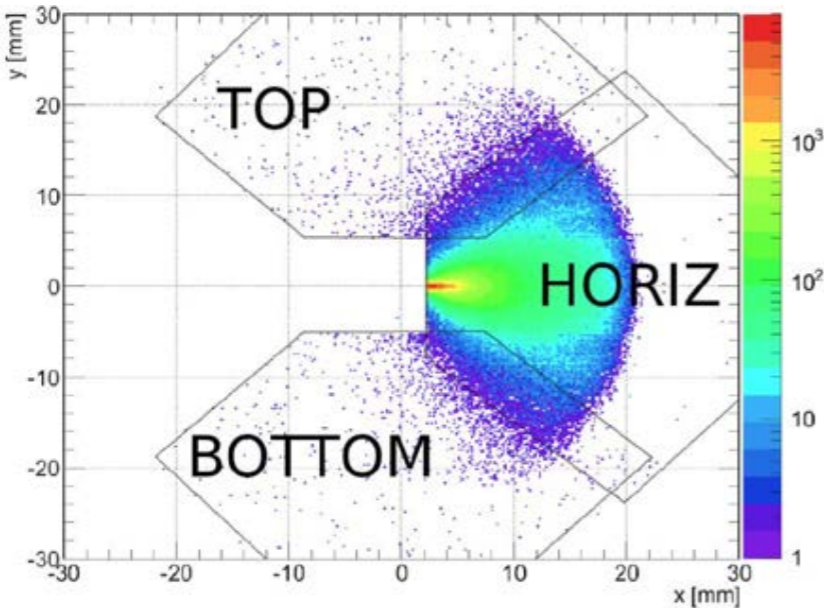
ATLAS (ALFA) operational during high- $\beta^*$  running.



# Detector acceptance vs $\beta^*$

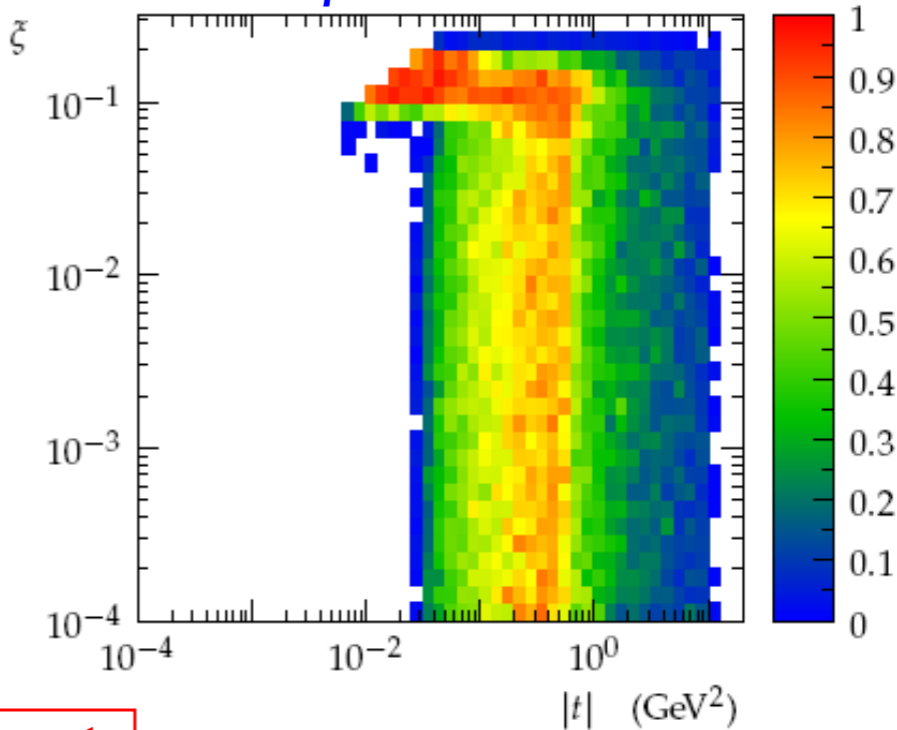
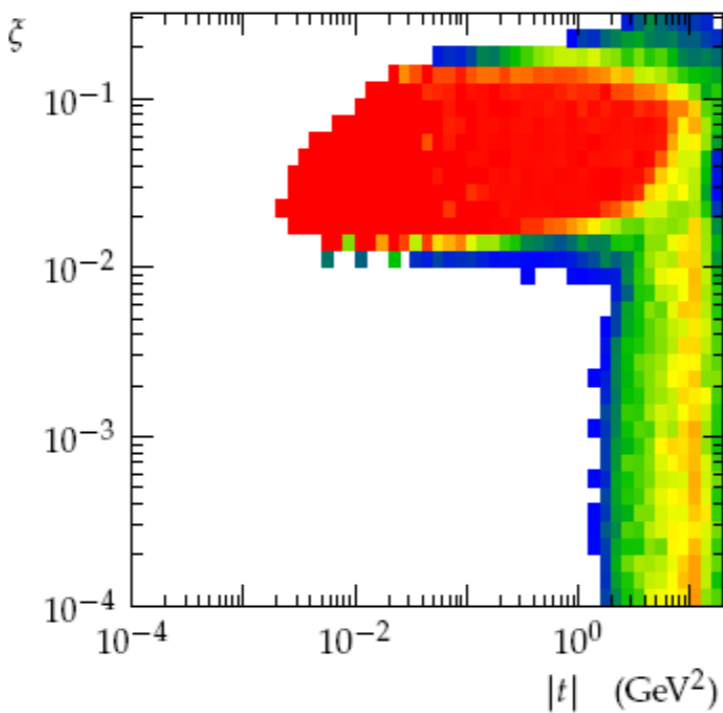
$\beta^* = 0.55$  m (low  $\beta^*$  = standard at LHC)

$\beta^* = 90$  m (special development for RP runs)



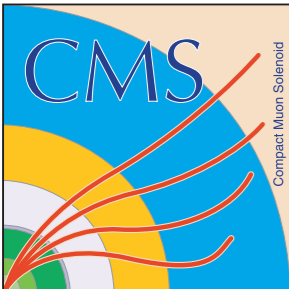
$\beta^* = 0.55$  m

$\beta^* = 90$  m



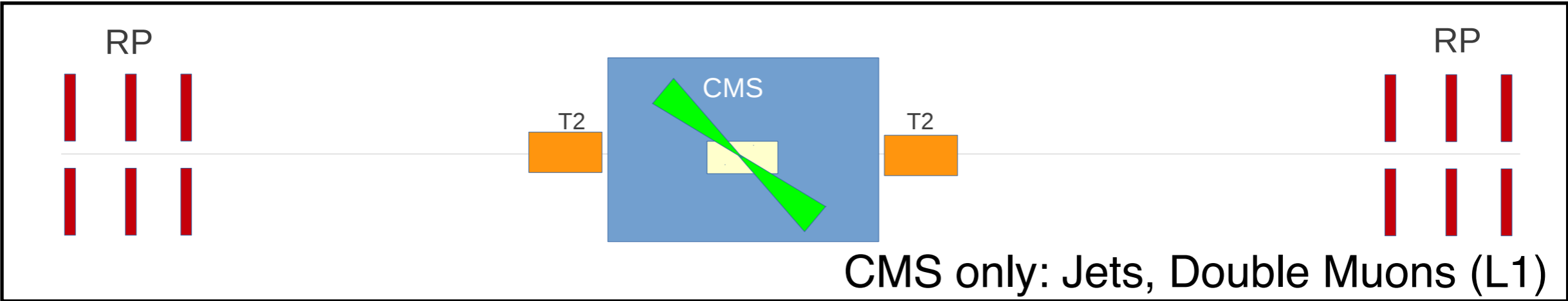
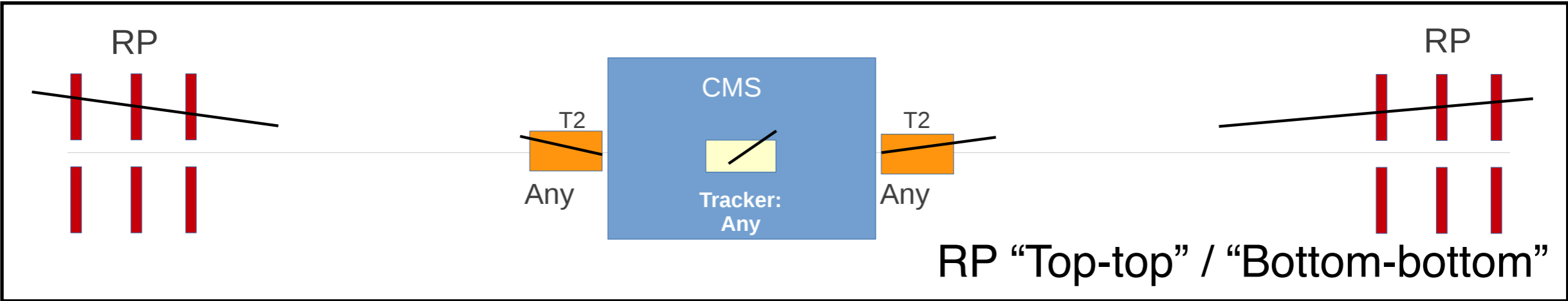
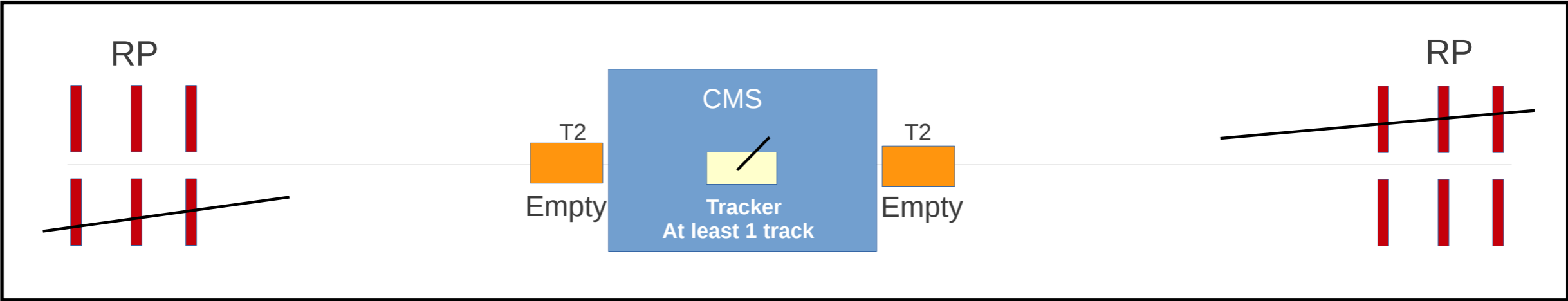
$$\mathcal{L} \propto \frac{1}{\beta^*}$$

M. Deile, 2015



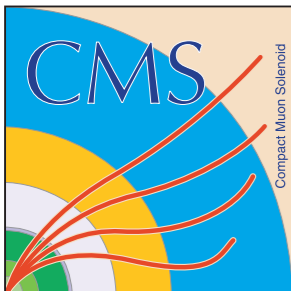
# CMS + TOTEM triggers: Summary

In CMS: RP + T2 veto (L1) + Track (HLT)

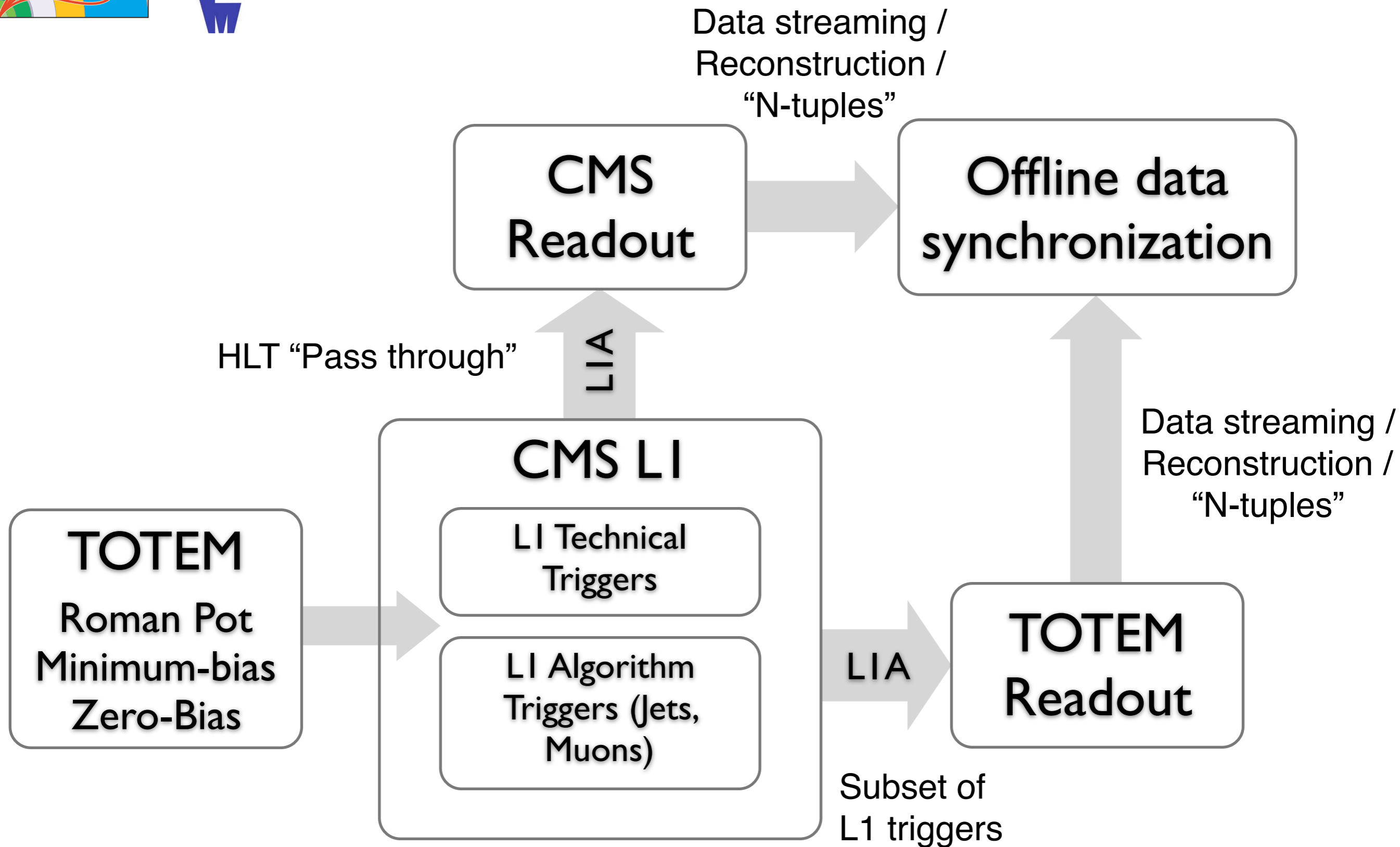


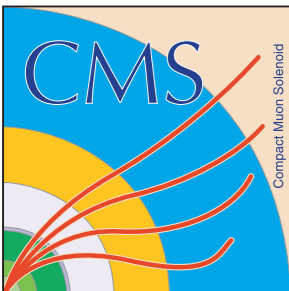
V. Avati

CMS HLT up to ~ 10 kHz

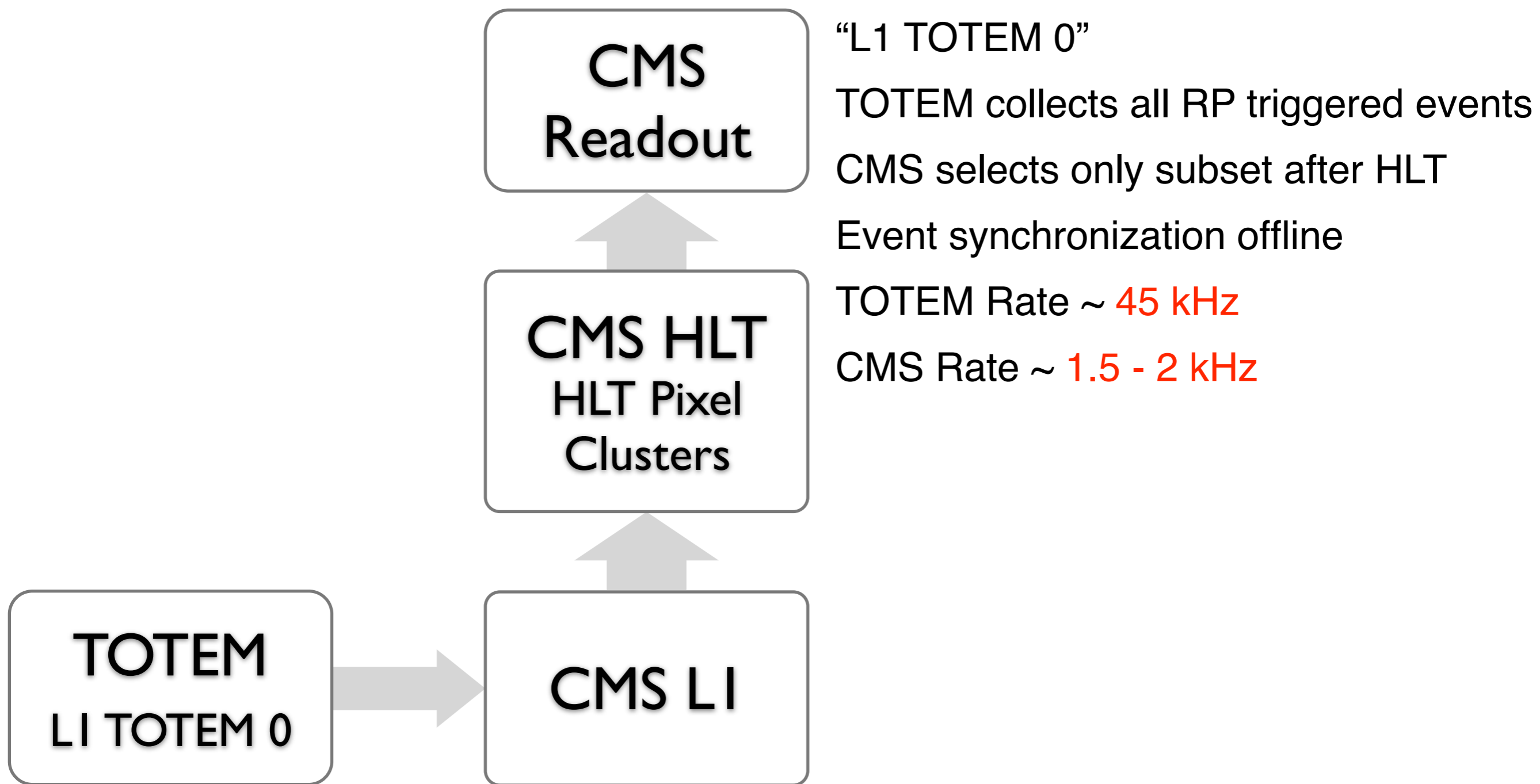


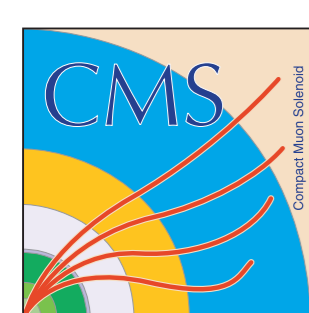
# CMS-TOTEM common data taking





# CMS-TOTEM common data taking: Low mass states + 2 protons





# Physics performance: Central Exclusive Production

Central Exclusive Production as main Physics motivation:

- i) photon-photon fusion
- ii) gluon-gluon fusion in colour-singlet,  $J^{PC} = 0^{++}$ , state

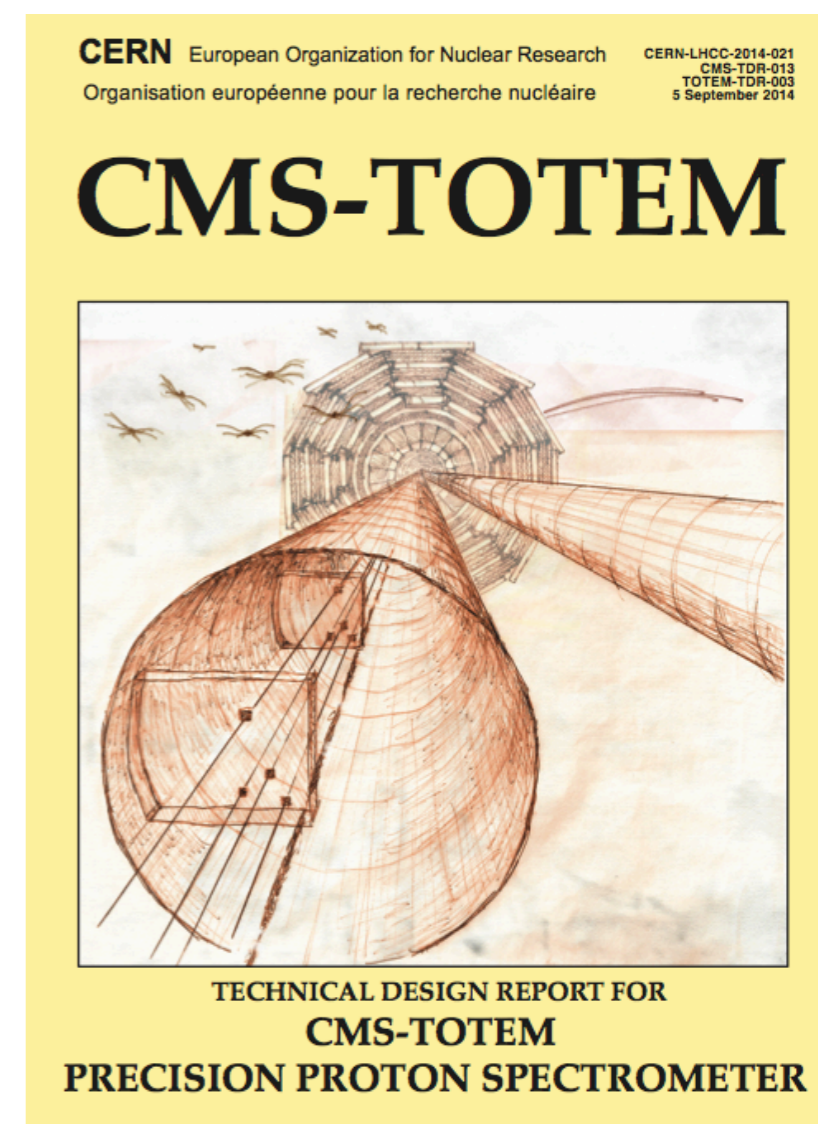
High- $p_T$  system X detected by the CMS detectors at central pseudorapidity with high-energy, very low angle scattered protons detected by CT-PPS;

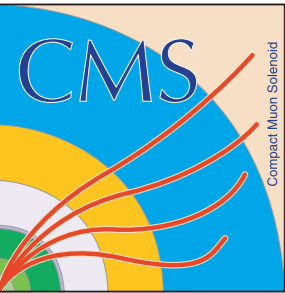
The two outgoing protons must balance perfectly the system X momentum, hence creating strong kinematical constraints;

Its mass  $M_X$  is obtained from the momentum loss of the two protons, allowing to study invisible final states with difficult reconstruction in CMS;

The Physics potential includes the study of gauge boson production by photon-photon fusion and anomalous  $\gamma\gamma WW$ ,  $\gamma\gamma ZZ$  and  $\gamma\gamma\gamma\gamma$  couplings, search for new BSM resonances and the study of QCD in a new domain.

Full simulation studies carried out for two benchmark channels:  
Exclusive WW production and Exclusive dijet production.





# Anomalous quartic couplings

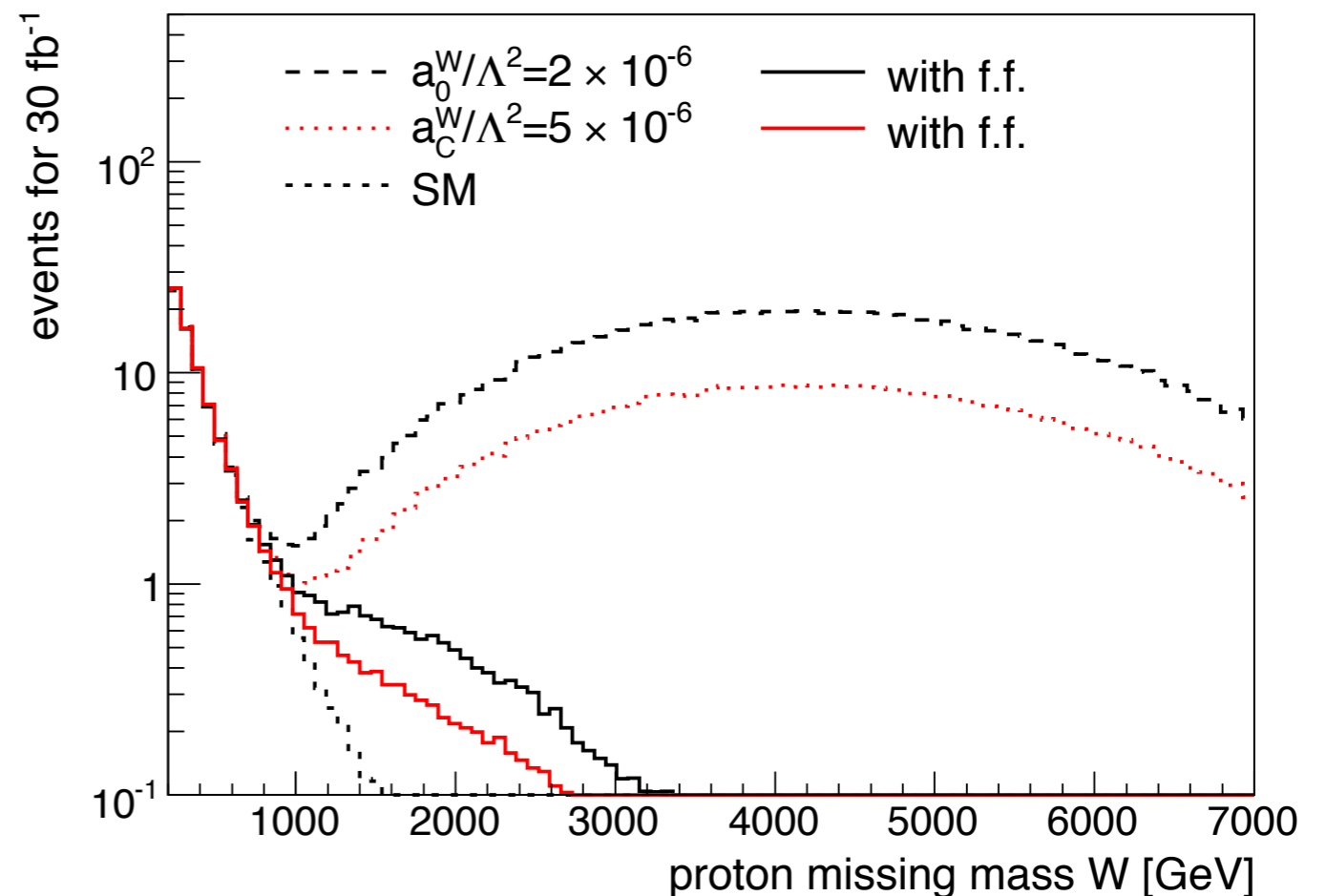
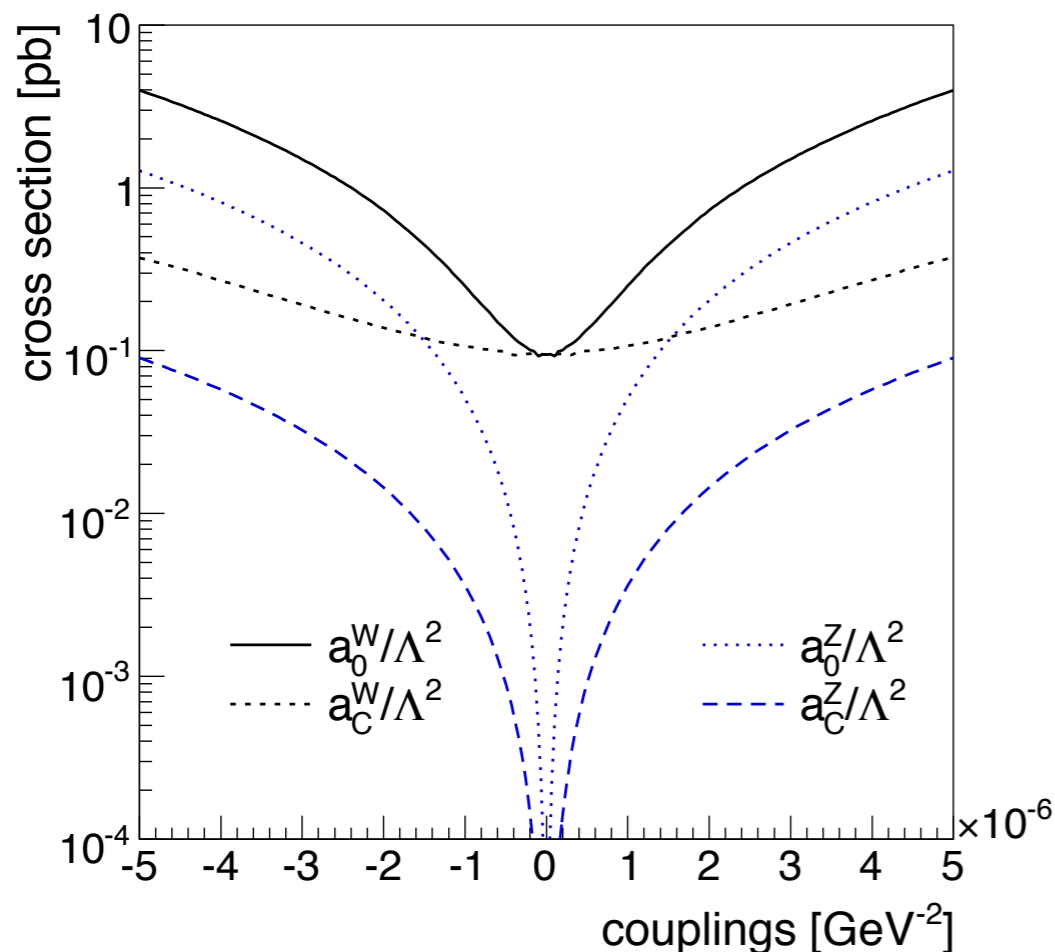
Effective Lagrangian with quartic anomalous operators  
 $\gamma\gamma WW$  and  $\gamma\gamma ZZ$ :

$$\mathcal{L}_6^0 = \frac{-e^2}{8} \frac{a_0^W}{\Lambda^2} F_{\mu\nu} F^{\mu\nu} W^{+\alpha} W_{\alpha}^{-} - \frac{e^2}{16 \cos^2 \theta_W} \frac{a_0^Z}{\Lambda^2} F_{\mu\nu} F^{\mu\nu} Z^{\alpha} Z_{\alpha}$$

$$\mathcal{L}_6^C = \frac{-e^2}{16} \frac{a_C^W}{\Lambda^2} F_{\mu\alpha} F^{\mu\beta} (W^{+\alpha} W_{\beta}^{-} + W^{-\alpha} W_{\beta}^{+}) - \frac{e^2}{16 \cos^2 \theta_W} \frac{a_C^Z}{\Lambda^2} F_{\mu\alpha} F^{\mu\beta} Z^{\alpha} Z_{\beta}$$

Ansatz coupling form factors introduced to avoid violating unitarity at high energies:

$$a \rightarrow \frac{a}{(1 + W_{\gamma\gamma}^2 / \Lambda^2)^n}$$



E. Chapon, C. Royon, O. Kepka (2009)